REPORT NO.
UCB/EERC-80/03
JANUARY 1980

EARTHQUAKE ENGINEERING RESEARCH CENTER

OPTIMUM INELASTIC DESIGN OF SEISMIC-RESISTANT REINFORCED CONCRETE FRAME STRUCTURES

by

STAN W. ZAGAJESKI
VITELMO V. BERTERO

Report to Sponsor:
National Science Foundation

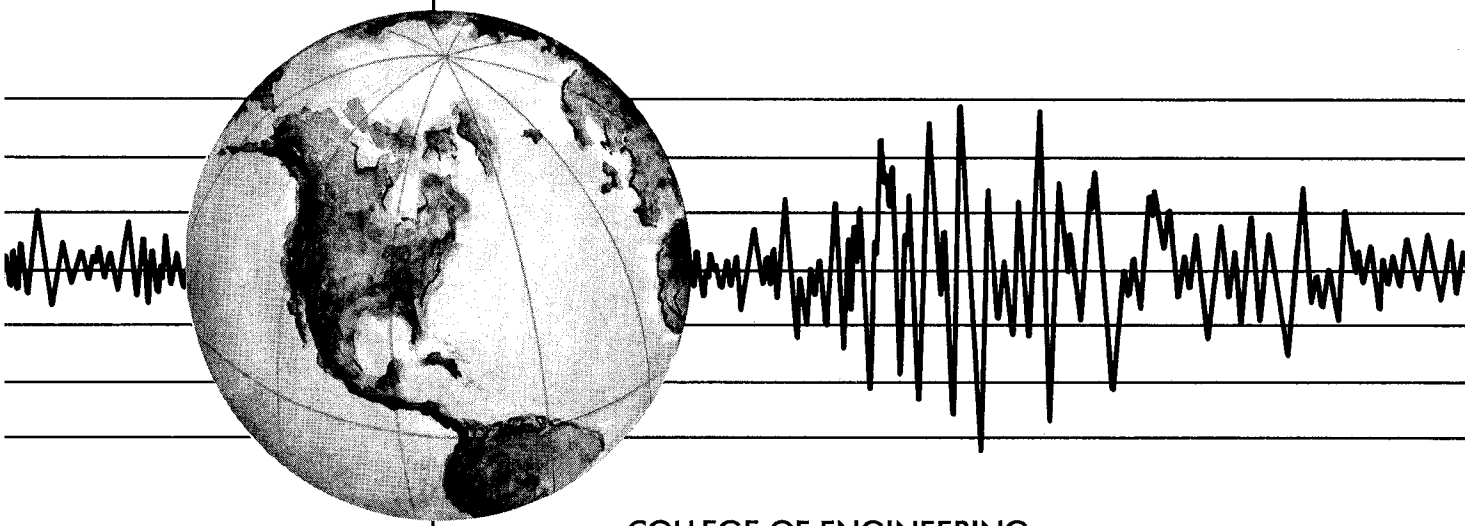

COLLEGE OF ENGINEERING

UNIVERSITY OF CALIFORNIA · Berkeley, California

BIBLIOGRAPHIC DATA SHEET	1. Report No. NSF/RA-800020	2.	3. Recipient's Accession No. PB 80 164635
4. Title and Subtitle: Optimum Inelastic Design of Seismic-Resistant Reinforced Concrete Frame Structures			5. Report Date: January 1980 6.
7. Author(s): S. W. Zagajeski and V. V. Bertero			8. Performing Organization Rept. No. UCB/EERC-80/03
9. Performing Organization Name and Address: Earthquake Engineering Research Center, University of California, Richmond Field Station, 47th and Hoffman Blvd., Richmond, California 94804			10. Project/Task/Work Unit No. 11. Contract/Grant No. ENV76-01419
12. Sponsoring Organization Name and Address: National Science Foundation, 1800 G Street, N.W., Washington, D. C. 20550			13. Type of Report & Period Covered 14.

15. Supplementary Notes

16. Abstracts

The design of seismic-resistant reinforced concrete, moment-resisting frame structures is discussed and an inelastic optimum design procedure described. This procedure is based on the philosophy of comprehensive design and employs a computer aided iterative technique in a series of five steps. Each step contains two phases, in each of which a weak-girder, strong-column design criterion is imposed. The discussion of the proposed inelastic design procedure concentrates on the preliminary design phase which comprises three steps--preliminary analysis, preliminary design, and analysis of the preliminary design.

Seismic design story shears are found by a spectral modal analysis technique which includes an approximation to the P-Δ effect. A nonlinear optimization technique (the cutting-plane method) is employed at each story to find the beam design moment capacities which minimize a function proportional to the volume of flexural reinforcement. Design constraints are imposed to ensure that a safe, serviceable, and practical design results. Actual member design is found employing computer design aids.

In the final step, the preliminary design is analyzed to evaluate its acceptability. Acceptability is determined by comparing the results of a series of linear elastic and non-linear analyses with established design criteria and assumptions made in formulating the design problem.

The proposed inelastic design procedure has been used to obtain a series of designs of a ten-story, three-bay frame. The designs differ with respect to the design constraints imposed in the formulation of the optimization problem and with respect to beam steel content. Different sets of practical design constraints were formulated to study the effect on beam moment redistribution of (a) the ratio of the positive and negative moment design capacity at a given design section and (b) eliminating bar curtailment at interior beam-column joints.

Two additional designs were found following UBC seismic design force provisions and considering code-allowed negative moment redistribution.

The proposed inelastic seismic design procedure is shown to be very versatile, and it allows realistic consideration of complex design excitations such as an earthquake ground motion. Automated features of the procedure free the designer from much of the computational effort associated with reinforced concrete frame design.

18. Availability Statement: Release Unlimited	19. Security Class (This Report) UNCLASSIFIED	21. No. of Pages
	20. Security Class (This Page) UNCLASSIFIED	22. Price

BIBLIOGRAPHIC DATA SHEET	1. Report No. NSF/RA-800020	2.	3. Recipient's Accession No.
4. Title and Subtitle: Optimum Inelastic Design of Seismic-Resistant Reinforced Concrete Frame Structures			5. Report Date 6.
7. Author(s)			8. Performing Organization Rept. No.
9. Performing Organization Name and Address			10. Project/Task/Work Unit No. 11. Contract/Grant No.
12. Sponsoring Organization Name and Address			13. Type of Report & Period Covered 14.

15. Supplementary Notes

16. Abstracts (Continued)

The design results obtained indicate that, in seismic-resistant design, the volume of flexural reinforcement is virtually insensitive to different distributions of beam design capacities. In addition, basing the optimum design problem on an objective function proportional to the volume of flexural reinforcement tends to maximize negative design capacities and minimize positive capacities.

17c. COSATI Field/Group

18. Availability Statement	19. Security Class (This Report) UNCLASSIFIED	21. No. of Pages
	20. Security Class (This Page UNCLASSIFIED	22. Price

OPTIMUM INELASTIC DESIGN OF SEISMIC-RESISTANT REINFORCED CONCRETE FRAME STRUCTURES

by

Stan W. Zagajeski

Assistant Professor of Civil Engineering
Colorado State University, Fort Collins

Vitelmo V. Bertero

Professor of Civil Engineering
University of California, Berkeley

Report to Sponsor:
National Science Foundation

Report No. UCB/EERC-80/03
Earthquake Engineering Research Center
College of Engineering
University of California
Berkeley, California

January 1980

ABSTRACT

The design of seismic-resistant reinforced concrete, moment-resisting frame structures is discussed. After a review of seismic design procedures proposed by the Uniform Building Code (UBC) and the Applied Technology Council (ATC), an inelastic optimum design procedure is described. This procedure is based on the philosophy of comprehensive design and employs a computer aided iterative technique in a series of five steps. The five steps are divided into preliminary and final phases. In both phases, a weak-girder, strong-column design criterion is imposed. The discussion of the proposed inelastic design procedure concentrates on the preliminary design phase which comprises three steps--preliminary analysis, preliminary design, and analysis of the preliminary design.

The objective of the preliminary analysis is to establish design criteria and determine design forces. Seismic design story shears are found by a spectral modal analysis technique which includes an approximation to the P-Δ effect.

The objective of the preliminary design step is to find member sizes and reinforcement. A nonlinear optimization technique (the cutting-plane method) is employed at each story to find the beam design moment capacities which minimize a function proportional to the volume of flexural reinforcement. Design constraints are imposed to ensure that a safe, serviceable, and practical design results. Actual member design is found employing computer design aids.

In the final step, the preliminary design is analyzed to evaluate its acceptability. Acceptability is determined by comparing the results of a series of linear elastic and nonlinear analyses with established design criteria and assumptions made in formulating the design problem. If the design is acceptable, the final design phase is entered, and final member detailing

is carried out. If not, the steps of the preliminary design phase are repeated until the design is deemed acceptable.

The proposed inelastic design procedure has been used to obtain a series of designs of a ten-story, three-bay frame. The designs differ with respect to the design constraints imposed in the formulation of the optimization problem and with respect to beam steel content. Different sets of practical design constraints were formulated to study the effect on beam moment redistribution of (a) the ratio of the positive and negative moment design capacity at a given design section and (b) eliminating bar curtailment at interior beam-column joints. In all, four complete designs have been obtained.

Two additional designs were found following UBC seismic design force provisions and considering code-allowed negative moment redistribution.

The proposed inelastic seismic design procedure is shown to be very versatile, and it allows realistic consideration of complex design excitations such as an earthquake ground motion. Automated features of the procedure free the designer from much of the computational effort associated with reinforced concrete frame design. Consequently, several alternative designs can be formulated, analyzed, and evaluated in a relatively short time.

The design results obtained indicate that, in seismic-resistant design, the volume of flexural reinforcement is virtually insensitive to different distributions of beam design capacities. In addition, basing the optimum design problem on an objective function proportional to the volume of flexural reinforcement tends to maximize negative design capacities and minimize positive capacities. In seismic-resistant construction, it is desirable to have a negative moment redistribution that results in a decrease of the negative moment in order to relieve steel congestion at beam-column joints.

A comparison of designs based on spectral seismic design forces and those based on the UBC forces indicates that required material volume does increase in the case of spectral design forces. However, the resulting increase in stiffness and strength improves the overall performance of the structure.

ACKNOWLEDGMENTS

Financial support for this investigation was provided by the National Science Foundation under NSF/RANN Grant No. ENV76-01419, "Structural Design Implications of Recent Seismic Research Results," Professor V. V. Bertero, Principal Investigator. The computer facilities of the University of California and Colorado State University were used during the course of this investigation.

The authors would like to thank Professor J. Axley for his advice regarding the formulation of the nonlinear programming solution algorithm employed in this research.

Finally, the authors would like to acknowledge the editorial assistance of M. C. Randall and E. L. Matthews, and the technical illustrations by D. Ullman.

TABLE OF CONTENTS

LIST OF TABLES

LIST OF FIGURES

1. INTRODUCTION

1.1 General

Seismic-resistant design confronts the structural designer with a number of challenging problems. For any given site, large uncertainties exist in predicting the dynamic characteristics and frequency of occurrence of future earthquake motions. Although the likelihood is small that a given structure located in a region of high seismicity--for example, the West Coast of the United States--will experience a severe ground motion, the structure will more than likely experience frequent minor earthquake ground shakings during its service life. These characteristics of seismic events complicate the designer's task of defining design earthquake excitations at each possible design limit state and of selecting the limit state which controls the preliminary design.

At present, the general philosophy of seismic-resistant design for other than essential facilities is based on the philosophy of comprehensive design [1]. Different design limit states are considered for earthquake ground motions of different severity and frequency of occurrence. However, difficulties are encountered in selecting design excitations. An earthquake ground motion may be considered the single realization of a set of random parameters (magnitude, focal depth, attenuation characteristics, frequency content, duration, etc.) [2]. Real ground motion records are limited in number and, because of their random nature, recurrence is unlikely. As a result, basing design on previously recorded real ground motions may be unsatisfactory. For example, Jennings et al [3] have noted that current available accelerograms lack definitive data of severe ground shaking in the vicinity of the causative fault.

The problem of defining design excitations is further complicated by the fact that the inertial forces caused by an earthquake ground motion depend on the dynamic characteristics of the whole soil-structure system as well as on the characteristics of the ground motion. Consequently, the selection of a design earthquake depends on the mass, damping, stiffness, and strength of the structure being designed.

A review of how current seismic-resistant design procedures deal with the above problems is presented in the following section.

1.2 Current Seismic Design Procedures

In current practice, design earthquakes are typically defined by acceleration response spectra from which seismic design base shears are computed. Such design spectra typically depend on the seismic activity of the site, soil conditions, fundamental period of vibration, and the type of lateral force resisting system. For example, the 1976 Uniform Building Code (UBC) [4] seismic-force provisions define the design base shear as

$$V = ZIKCSW \tag{1.1}$$

where

Z = Numerical coefficient dependent on the seismic zone (seismic activity)

I = Occupancy Importance Factor

K = Numerical coefficient dependent on type of lateral force-resisting system

C = Numerical coefficient specified as $1/(15\sqrt{T}) \leq 0.12$

T = Structure's fundamental period of vibration

S = Numerical coefficient for site-structure resonance

and

W = Total weight of the structure.

Recently, the Applied Technology Council (ATC) [5] has suggested the following expression for the design base shear:

$$V = \frac{1.2\ A_v S}{RT^{2/3}} W \leq \beta \frac{A_a}{R} W \qquad (1.2)$$

where

A_v = Seismic coefficient representing the Effective Peak Velocity-Related Acceleration

A_a = Seismic coefficient representing the Effective Peak Acceleration

R = Seismic response modification coefficient which is related to the framing system

S = Seismic coefficient of the site soil profile characteristics

T = The fundamental period of the building

β = Coefficient which depends on site soil profile characteristics

and

W = Total gravity load of the building.

The above ATC proposal is recommended only for regular buildings, i.e.,

> "Buildings which have an approximately symmetrical geometry configuration and which have the building mass and seismic resisting system nearly coincident. . . ."

For irregular buildings, a modal analysis technique is proposed in conjunction with design response spectra defined by equation (1.2).

The UBC and ATC design earthquakes will be compared by considering the design of the ten-story, three-bay frame illustrated in Fig. 1. The first step in the design process is to define the building site. For this example, the building is to be constructed in Oakland, California. Based on seismic maps, Z in equation (1.1) would be 1.0 (zone 4), and both A_v and A_a in equation (1.2) would be 0.4 (area 1).

Next, it is supposed that an office building consisting of a reinforced concrete ductile moment-resisting frame structural system is to be constructed. As a result, K in equation (1.1) is 0.67, R in equation (1.2) is 7, and I in equation (1.1) is 1.

Using empirical relationships to define the structure's fundamental period, it is found that: T in equation (1.1) is T = 0.1N = 1 sec (UBC 12-3B) where N is the number of stories; and T in equation (1.2) is $T = 0.025h_n^{3/4} =$ .91 sec (ATC 4-4) where h_n is the total height of the structure.

Finally, it is assumed the soil conditions are such that the site effects, as defined by the UBC or ATC, are negligible. Consequently, S in both equations (1.1) and (1.2) is set to one.

Substituting the above values into equation (1.1), we find that

$$V_{UBC} = (1.0)(1.0)(0.67)\ \frac{1}{15}\ (1.0)\ W = .046\ W;$$

and, substituting into (1.2), we find that

$$V_{ATC} = \frac{1.2\ (0.4)(1.0)}{7(.91)^{2/3}}\ W \leq 2.5\ \frac{0.4}{7}\ W = .073\ W.$$

However, V_{UBC} is at service level conditions and must be factored to make it equivalent to V_{ATC}.

$$V^u_{UBC} = 1.4\ V_{UBC} = .063\ W$$

A comparison of V_{ATC} and V^u_{UBC} indicates that the UBC design base shear is 86 percent of that specified by the ATC.

Once the design base shear has been determined, it must be distributed through the height of the structure. UBC suggests

$$F_x = \frac{(V - F_t)\ w_x h_x}{\sum_{i=1}^{n} w_i h_i} \qquad (1.3)$$

where

h_i, h_x = Height above the base to level i or x

w_i, w_x = That portion of W which is assigned to level i or x

n = Number of stories

F_x = Lateral force at level x

F_t = That portion of V considered at the top of the structure in addition to F_n defined by equation (1.3)

= 0.07 TV $\leq$ .25V for T > 0.7 secs

= 0 if T $\leq$ 0.7 secs.

Part of the base shear is concentrated at the top of the structure in order to include higher mode effects on the force distribution. It should be noted that, for highly irregular buildings, UBC recommends that the force distribution be determined considering the dynamic characteristics of the building (Section 2312[c]3).

The force distribution recommended by the ATC is

$$F_x = V \cdot \frac{w_x h_x^k}{\sum_{i=1}^{n} w_i h_i^k} \qquad (1.4)$$

where

k = A coefficient related to period

= 1 if T $\leq$ 0.5

= 2 if T > 0.5 or

= 1 + (T - 0.5)/2 if 0.5 < T < 2.5

= 2 if T $\geq$ 2.5

The coefficient, k, approximates higher mode effects on seismic force distribution.

Both the ATC and the UBC assume that, for other than essential facilities, the ultimate limit state controls design; and they also recognize that inelastic response may be significant. The effect of inelastic behavior is included in the design base shear definitions by the factors K and C in equation (1.1) and by the factor R in equation (1.2). The factors R and K are defined on the basis of the inelastic deformation characteristics of the various lateral force resisting systems.* In addition, although only elastic analysis is required in both seismic design procedures, the resulting deflections are increased by what can be referred to as a deflection amplification factor, C_d, to account for inelastic behavior. For a ductile moment-resisting frame system, the UBC defines a C_d value of 1.5 (1/K) at service-level loads and requires that the lateral story deflection or drift not exceed $0.005\ h_x$. In contrast, the ATC recommends a value of 6 for C_d at ultimate-load conditions and requires that the story drift be smaller than $0.015\ h_x$.

The fact that the UBC and the ATC drift limitations are based on different design limit states complicates a comparison of the two design requirements. Suppose, however, that a valid comparison is possible at the ultimate-load level without deflection amplification. If a characteristic structure displacement, δ, is defined as

$$\delta = \frac{V}{K_s} \tag{1.5}$$

where V is the base shear level at which deflection is computed and K_s is a characteristic structure stiffness (assumed the same for UBC and ATC), the UBC displacement, δ_{UBC}, at ultimate load (at V^u_{UBC}) is $0.86\ \delta_{ATC}$ (at V_{ATC}).

---

*It should be noted that, while the UBC (1976) permits redistribution of negative moments, ATC does not.

The UBC and ATC drift limitations, R^{UBC} and R^{ATC*}, respectively, are modified to reflect the limit state chosen for comparison by the expression

$$R_M = \frac{R}{C_d} (LF) \tag{1.6}$$

where LF is the design load factor (1.4 for UBC, 1.0 for ATC). Based on equation (1.6), $R_M^{UBC} = .005(1.4)/1.5 = 0.0047$ and $R_M^{ATC} = .015(1.0)/6 = 0.0025$.

Accounting for the different force levels ($\delta_{UBC} = 0.86\ \delta_{ATC}$), the ATC drift requirement is more than twice as stringent as the UBC requirement. Consequently, either the ATC drift limitation is conservative or the UBC requirement is unconservative. It is felt that, for a severe earthquake ground motion, the latter is true.

The increase in deflections associated with the P-Δ effect has not been included in the above discussion. Consideration of this effect in the ATC design procedure is equivalent to an increase in C_d. Consequently, R_M^{ATC} would decrease. However, since UBC does not stipulate how to account for the P- Δ effect, R_M^{UBC} remains the same; and the difference between the UBC and ATC drift limitations would increase.

The fact that structural design is based on a fictitious linear elastic limit state is a major shortcoming of the seismic design procedures reviewed above. Although special provisions to enhance local inelastic deformation capacity are stipulated by ATC and UBC in sections covering member design, neither procedure requires an estimation of local inelastic deformation demands.

---

*The term, R, has been used previously in equation (1.2) as a seismic-response modification factor. However, in previous work [6], R has been used to indicate story drift index which is defined as the ratio of interstory displacement to interstory height. Subsequent uses of R will indicate drift index.

The authors believe that such estimates are required in design for severe earthquake ground motion. Known deformation capacities can be compared to the estimated deformation demands to determine whether or not they are compatible. In addition, estimates of required inelastic deformations can be used as guidelines for member detailing.

The authors have recently proposed an inelastic seismic-resistant design procedure for multistory frame buildings expected to experience a severe earthquake ground motion during their service lives [6]. The procedure was developed specifically for ductile reinforced concrete frame structures. In the procedure, seismic design forces are obtained by a modal analysis technique from smooth inelastic design response spectra. The structural design is based on an optimum limit state design and expected inelastic deformation demands are determined from time history analyses. In the design procedure, special emphasis is placed on obtaining a preliminary design which is as close as possible to the desired final design. The design procedure is currently limited to planar behavior.

1.3 Objectives

The main objectives of this report are to present: (1) an evaluation and an improvement of the seismic-resistant design procedure proposed in Ref. 6--in particular, an improvement in the formulation and solution of the optimum inelastic design problem; (2) an investigation into the effect of different practical design constraints on the optimum design solution and on the seismic response of the resulting designs; and (3) a comparison of designs based on the proposed procedure with designs based on the UBC design procedure.

1.4 Scope

The inelastic seismic-resistant design procedure proposed in Ref. 6 is reviewed in Chapter 2. The optimization problem is reformulated as a nonlinear programming problem which is solved by the cutting plane method [7, 8]. The nonlinear programming technique is discussed in Chapter 3.

Several different designs of a ten-story, three-bay reinforced concrete frame (Fig. 1) have been obtained using the new optimization technique. The different designs were formulated to study:

(a) The effect of varying the lower bound on the positive (bottom steel) moment capacity at a given section $|M^+| \geq p|M^-|$. The values of p considered were 0.50, 0.75, and 1.00.

(b) The effect of eliminating bar curtailment at interior beam-column joints.

(c) The effect of varying the maximum flexural reinforcement ratio, ρ_{max}, allowed in beam design. Values of 0.5 ρ_b and 0.75 ρ_b were used.*

In addition, two designs based on the UBC (1976) seismic design provisions [4] are obtained. The two UBC designs differ in the value of ρ_{max} used in the beam design. The different designs are discussed and compared in Chapters 3 and 4. The conclusions drawn from these results, and recommendations for future research are presented in Chapter 5.

---

*ρ_b is the balanced failure reinforcement ratio [ACI Section 10.2 (9)].

2. INELASTIC SEISMIC-RESISTANT DESIGN PROCEDURE

2.1 General Characteristics of the Design Procedure

Recently, the authors have proposed a computer-aided iterative procedure for the seismic-resistant design of multistory reinforced concrete frame structures [6]. The procedure was developed for structures which are expected to experience a severe earthquake ground motion during their service lives. The objectives of this chapter are: (a) to review the essential features of the design procedure and (b) to point out aspects of the procedure which are explored in this report. In the discussion of the design procedure, reference is made to the design of the ten-story, three-bay frame defined in Fig. 1.

The design procedure consists of five basic steps which are divided into preliminary and final design phases (Fig. 2). In both phases, an optimum inelastic design which minimizes the volume of flexural reinforcement is found for each story. In order to limit column inelastic deformation and prevent formation of soft stories (partial sway mechanism), a weak-girder, strong-column design philosophy is followed in both design phases. Additionally, in order to prevent large concentrated inelastic deformations, transitions in strength, stiffness, and mass are made as smooth as possible through both the height and the plan area of the structure.

2.2 Preliminary Design Phase

Regardless of how sophisticated the analysis techniques employed in determining member design capacities, the final design will be only as good as the preliminary design used to define seismic forces and to carry out the analysis. In view of this fact, the objective of the preliminary design phase is to obtain a preliminary design which is as close as possible to the desired final

design. The preliminary phase entails three steps--preliminary analysis, preliminary design, and analysis of the preliminary design. To achieve the stated objective, these steps are repeated until the preliminary design is deemed acceptable with respect to established design criteria, which reflect the desired characteristics of the final design, and with respect to dynamic characteristics and ductility factors assumed in evaluating seismic design story shears.

2.2.1 Preliminary Analysis

The objective of the first step of the design procedure is to establish design loads and design criteria. On the basis of structural geometry and building function, gravity and wind loads are determined, and story masses are estimated. Design earthquakes, which are represented by smooth ground-motion spectra, are established on the basis of available seismic and geological data and soil characteristics of the building site.

Ground-motion spectra are defined by selected values of effective peak ground acceleration, velocity, and displacement. Figure 3 illustrates the spectrum for a peak ground acceleration of 0.40g, velocity of 486 mm/secs, and displacement of 366 mm [10].

Although in previous design examples [6, 11] and in the design examples presented later in this report, only one design earthquake (corresponding to a severe ground motion) has been considered, additional ground-motion spectra corresponding to different design limit states (for example, the serviceability limit state) are a possibility.

Once the design earthquakes have been established, dynamic characteristics of the structure--defined by period ratios T_1/T_i and mode shapes $\underline{\phi}_i$--are selected. T_1 is the fundamental period, and T_i is the period of the i*th* mode

of vibration. The initial selection of T_1/T_i and $\underline{\phi}_i$ may be based on previous experience with similar structures, tabulated results [12], and/or the results of analyses of a starting design. After completing one iteration of the preliminary design phase, T_1/T_i and $\underline{\phi}_i$ may be updated to reflect the characteristics of the latest preliminary design.

The final task of the preliminary analysis is the determination of seismic design story shears. Based on an assumed damping ratio, ξ, an elastic response spectrum is constructed from the ground-motion spectrum using amplification factors suggested by Newmark [10]. An inelastic response spectrum is then constructed by dividing the elastic response spectrum by appropriate functions of the assumed displacement ductility factor, μ, (Fig. 3). Assuming a value for T_1, the design story shears are evaluated on the basis of the inelastic response spectrum employing a modal analysis technique. The various modal contributions are combined by taking the square root of the sum of the squares of the modal maxima.

In determining seismic design forces, the final selection of ξ, μ, and T depends on an iterative process in which estimates of response based on a given set of ξ, μ, and T are compared to the established yielding seismic coefficient, C_y, and the design drift index for ultimate-load conditions, R_{ult} (values of C and R, service-level design criteria, are used for a service-level earthquake). These design criteria (C, C_y, R and R_{ult}) should be established on the basis of their relative effect on initial design cost and the cost of expected damage during response to the design excitations.

The story shears obtained by the modal analysis are modified to account for the P-Δ effect [6].

Although the use of a modal-analysis technique for an inelastic multi-degree-of-freedom system is correct only in the rare case that all plastic hinges associated with the assumed failure mechanism form simultaneously,

such a technique is considered a significant improvement over current code seismic-force specifications [13].

2.2.2 Preliminary Design

The problem in this step of the design procedure may be stated as follows:

Given: Gravity, wind, and seismic-design loads; critical load combinations; and mechanical characteristics of design materials.

Find: Beam and column sizes and flexural reinforcement.

The solution to this problem is found by solving an optimization problem for each story formulated on the basis of the design subassemblage in Fig. 4. The optimum design minimizes the volume of flexural reinforcement. The weak-girder, strong-column design criterion reduces the problem to one of finding the beam design moments.

The design problem may be summarized as follows:

$$M_i > 0 \qquad i = 1,N$$

which minimize the objective function,

$$C(M_i) > 0, \tag{2.1}$$

and which satisfy the design constraints

$$G_j(M_i) \geq 0 \qquad j = 1,NC \tag{2.2}$$

where N is the number of desired beam design moments and NC is the number of design constraints.

Design constraints are imposed to ensure that equilibrium is satisfied and that a serviceable and practical design results. The form of $C(M_i)$ and $G_j(M_i)$ are presented below. In previous work [6, 11], $C(M_i)$ and $G_j(M_i)$ were assumed linear, and a linear programming technique was used to solve the optimization problem.

(i) Objective function

The objective function is based on the following approximate relationship between the beam design capacity at section i, M_i, and the corresponding steel area A_{s_i} [6]:

$$M_i = A_{s_i} f_y jd \tag{2.3}$$

where f_y is the nominal steel yield stress and jd is the lever arm between the resultant internal tensile and compressive forces. Separating the contributions of the beam and column reinforcements, the objective function may be written as

$$C(M_i) = C_C(M_i) + C_B(M_i) \tag{2.4}$$

where $C_C(M_i)$ accounts for the column reinforcement and $C_B(M_i)$ accounts for the beam reinforcement.

In the authors' previous work [6, 11], both components were considered linear functions and $C(M_i)$ was expressed as

$$C(M_i) = \gamma_i M_i = \left(\gamma_i^* + \gamma_i^{**}\right) M_i \tag{2.5}$$

where

γ_i = Effective length of reinforcement corresponding to the *ith* design moment

γ_i^* = Beam contribution

and

γ_i^{**} = Column contribution.

The column term was determined on the basis of the weak-girder, strong-column design criterion. The sum of the column moments at a beam-column joint was expressed in terms of the beam moments by considering joint equilibrium. Assuming that the column reinforcement does not vary through the column height defined by the design subassemblage, γ_i^{**} may be expressed as

$$\gamma_i^{**} = \ell \cdot \sum_{k=1}^{NJ} f(M_i, h_c, \ell_b, h_b) \tag{2.6}$$

where

$\ell = h_{i-1}/2 + h_i/2$ (Fig. 4)

f = A linear function derived from joint equilibrium which depends on joint geometry and a safety factor imposed to ensure a weak-girder, strong-column design. Details of the form of f may be found in Ref. 6.

and

NJ = Total number of joints.

The beam term, γ_i^*, was obtained from reinforcement detailing corresponding to design moment envelopes. Effective reinforcement lengths were computed by considering code-allowed bar curtailment and specified bar anchorage. In order to construct moment envelopes for evaluation of γ_i^*, an initial solution M_i^o, is required. In previous work, M_i^o was defined by the results of elastic analysis. The optimum solution of the linear programming problem formulated on the basis of γ_i^* (M_i^0), (M_i^1), is strictly correct only if the solution of a new problem formulated on the basis of γ_i^* (M_i^1), M_i^2, is equal to M_1^1. In other

words, this technique to evaluate γ_i^* results in a function, $C_B(M_i)$, which is nonlinear in the design variables, M_i.

In a recent study [14], it has been found that, typically,

$$M_i^2 \neq M_i^1; \tag{2.7}$$

and the use of a linear programming technique to solve the optimization problem is questionable. In Chapter 3, a nonlinear programming technique is described which enables this nonlinearity in the objective function to be handled.

(ii) Design constraints

Three sets of linear design constraints are imposed. The constraints considered follow.

1. Equilibrium constraints

$$\theta_{ji} M_i \geq \omega_j \qquad j = 1,NEQ \tag{2.8}$$

where

θ_{ji} = Coefficient of M_i in the j*th* equilibrium constraint

ω_j = External load term in the j*th* equilibrium constraint

and

NEQ = Number of equilibrium constraints.

The equilibrium constraints are derived from the kinematic theorem of simple plastic theory. A typical θ_{ji} corresponds to the virtual plastic-hinge rotation at design section i in the j*th* subassemblage mechanism, and a typical ω_j corresponds to the virtual work done by the external loads going through the displacements associated with the j*th* mechanism.

2. Serviceability constraints

$$M_i \geq m_i \qquad i = 1,N \tag{2.9}$$

where

$m_i = \lambda_o |M_i^{SE}|$

λ_o = A coefficient greater than 1.0 which protects against yielding and excessive cracking and deformation under service load conditions

and

M_i^{SE} = The ordinate of the elastic moment envelope under service load conditions at design section i.

3. Practical constraints

$$p|M_i^-| \leq |M_i^+| \leq |M_i^-|$$

$$M_{span} \geq .25\, M_{support}$$

$$\left|M_i^-\right| \leq \left|M_i^{-UE}\right| \tag{2.10}$$

$$\left|M_i\right| \geq \left|M_{\rho_{min}}\right|$$

$$\left|M_i^-\right| \geq FAC \cdot \left|M_{i_{above}}^-\right|$$

where

p = A factor (0.5 is stipulated by the UBC) less than or equal to 1.0

M_i^{-UE} = The ordinate of the ultimate-load elastic moment envelope at design section i.

$FAC = M_i^{-UE}/M_{i_{above}}^{-UE}$

$M_{i_{above}}^{-UE}$ = M_i^{-UE} for the story above the one being designed

$M_{\rho_{min}}$ = The moment capacity corresponding to minimum reinforcement requirements ($\rho_{min} = 1380/f_y$ for f_y in MPa)

and

$M_{i_{above}}^{-}$ = The solution at section i for the story above the one being designed (the optimum design procedure is started at the roof level).

It should be noted that in the optimum design problem all M_i are positive. The notation M_i^- and M_i^+ is used to indicate that, at a typical section, two design capacities are considered, one corresponding to top steel (M_i^-) and the other corresponding to bottom steel (M_i^+).

The last practical constraint defined in equation (2.10) is imposed to attain a smooth transition in strength through the frame height and is imposed only on the negative design capacity at each support section. The constraints imposed on the positive design capacity at a given section in terms of the corresponding negative capacity, combined with the smoothness constraint imposed on the negative capacity, should ensure sufficient smoothness in the variation of positive design capacities.

The practical design constraints allow a designer to incorporate his/her practical experience into the design process. The above set of constraints may be modified and/or new constraints added in order to obtain a solution with the characteristics desired by the designer. In order to investigate the effect on design behavior of (a) the ratio of positive and negative design capacities at a given critical section, and (b) eliminating bar curtailment at interior beam-column joints, several inelastic design problems have been formulated by modifying and/or adding practical design constraints. The various practical design constraints considered, and their effects on the optimization solution, are discussed in Chapter 3. The behavior of the resulting inelastic designs is compared in Chapter 4.

Since a number of design constraints are based on the results of elastic analysis and since beam sizes are required to determine $M_{\rho_{min}}$, an initial (starting) design is required to formulate the preliminary design problem. Various methods to determine a starting design are presented in Ref. 6. Typically, member sizes found on the basis of the optimization solution are different than those used in the formulation of the design problem. As a result, the preliminary design step is repeated until the member sizes before and after optimization are the same (Fig. 5).

Once the inelastic optimum design problem has been solved for the beam-design moment capacities, beam and column sizes and flexural reinforcement are found with the aid of a digital computer. The beam sizes and flexural reinforcement required to resist the optimum beam-design moments, modified to account for column-slenderness effects and code capacity-reduction factors, are found first. Column design moments are then determined on the basis of the weak-girder, strong-column design criterion considering computed moment capacities of the designed beams. Column design axial forces are determined on the basis of gravity load and gravity load combined with seismic loading. Column cross-sections and reinforcement are then found on the basis of the critical design force combination.

Automated member design is considered an attractive feature of the design procedure. The computer relieves the designer of a tedious and time-consuming computational chore, thus freeing him/her to act creatively in the design process. In addition, this computational tool allows the designer to generate, in a relatively short period of time, several alternative designs which can be used as guidelines for the final design.

In the member design, the beam size (depth) is determined by the equation

$$\frac{M_u}{\phi} = \rho_{max}\, bd^2\, f_y \left(1 - 0.59\, \frac{\rho_{max}\, f_y}{f'_c}\right) \qquad (2.11)$$

In previous work [6, 11], ρ_{max} was the minimum of 0.025 or 0.75 ρ_b as required by UBC [4]. For the values of f'_c and f_y, used in the design examples (27.8 and 414 MPa, respectively), ρ_{max} was controlled by 0.75 ρ_b. However, in the ACI Appendix A [9] concerning seismic design, it is recommended that

$$\rho_{max} \leq 0.5\, \rho_b$$

In order to investigate the influence of ρ_{max} on the characteristics of the design, as well as on the design's response, two designs based on the same design constraints have been obtained. In one, ρ_{max} was equal to 0.5 ρ_b (1.4 percent) and, in the other, ρ_{max} was equal to 0.75 ρ_b (2.1 percent). Design results are presented and discussed in Chapters 3 and 4.

2.2.3 Analysis of the Preliminary Design

Once a preliminary design has been obtained, a series of elastic and inelastic analyses are carried out in order to determine the acceptability of the design. Elastic analyses are carried out to determine dynamic characteristics which are compared to those assumed in evaluating seismic design forces. In addition, response under service-load conditions is evaluated.

Inelastic static analyses are carried out to determine the structure's overstrength and to reveal apparent weaknesses in the design which would be indicated by large localized inelastic deformations or significant column yielding.

Finally, a series of nonlinear time-history analyses are carried out to evaluate the structure's response to representative earthquake ground motions. Response envelopes are examined to determine whether the indicated inelastic deformations are acceptable with respect to established story drift limitations and with respect to expected member deformation capacities.

On the basis of the data generated by these analyses, the designer determines the acceptability of the preliminary design. If the design is considered acceptable, the final design phase is entered; if not, the three steps defining the preliminary design phase are repeated.

2.3 Final Design Phase

The objective of the final design phase is to arrive at the optimal solution to the seismic design problem. Seismic design forces are determined utilizing characteristics of the structure found in the preliminary design phase. These forces are then used in conjunction with a more sophisticated design subassemblage to formulate the optimization problem from which the final design is obtained. Once a design has been obtained, a series of analyses is carried out to check the overall reliability of the design and to provide guidelines for detailing to ensure the degree of ductility assumed in design or indicated by analysis.

The subassemblage adopted for the final design phase is shown in Fig. 6. In this subassemblage, the column mid-height inflection point assumed in the preliminary design (Fig. 4) has been eliminated. In addition, more design parameters are involved than in the preliminary design subassemblage, which should provide a more uniform distribution of moment capacities.

3. SOLUTION OF OPTIMIZATION PROBLEM

3.1 Introduction

As discussed in the previous chapter, the preliminary design is found by solving an optimization problem formulated for each story on the basis of the subassemblage shown in Fig. 4. In summary, the design problem is:

Find the beam design moments

$$M_i > 0 \qquad i = 1,N$$

which minimize the objective function

$$C(M_i) > 0 \tag{3.1}$$

and, which satisfy the design constraints,

$$G_j(M_i) \geq 0 \qquad j = 1,NC. \tag{3.2}$$

The constraint functions, $G_j(M_i)$, are linear and may be written as

$$g_{ji} M_i \geq b_j \tag{3.2a}$$

where g_{ji} is the coefficient of i*th* design variable in the j*th* design constraint and b_j is a constant defining the j*th* design constraint. The design constraints were defined in detail in section 2.2.2 (ii).

The objective function $C(M_i)$ is proportional to the volume of flexural reinforcement. As discussed previously, if the effective length of reinforcement associated with a given design variable is determined on the basis of realistic design detailing (considering bar curtailment based on moment envelopes) the resulting objective function is nonlinear. As a result, a nonlinear programming technique is required to solve the optimization problem defined by equations (3.1) and (3.2). The technique employed here is the "cutting plane" method.

3.2 The Cutting Plane Method

The cutting plane method applies linear programming through a sequence of local linearizations to obtain the minimum of a convex function of real variables subject to convex constraints. In the method, it is assumed that the constraints confine the variables to a bounded set, S. The description of the method presented below is based on Ref. 8 and is limited to the case of linear constraints.

3.2.1 Description of the Cutting Plane Method

The cutting plane method is based on the observation that the optimization problem defined by equations (3.1) and (3.2) is equivalent to the problem of minimizing a new variable, Z, subject to the constraints

$$\begin{aligned} Z &\geq C(M_i) \\ g_{ji}\, M_i &\geq b_j \end{aligned} \tag{3.3}$$

The nonlinear constraint

$$Z \geq C(M_i)$$

is linearized by the Taylor series approximation

$$Z \geq C(M_k^t) + \nabla C_i(M_k^t)(M_i - M_i^t) \tag{3.4}$$

where

M_i^t = A known point belonging to S (how it is obtained will be discussed later).*

and

∇C_i = The gradient of $C(M_i)$

$$= \left(\frac{\partial C(M_i)}{\partial M_1}, \frac{\partial C(M_i)}{\partial M_2}, \ldots, \frac{\partial C(M_i)}{\partial M_N} \right)$$

*M_k^t and M_i^t indicate the same (M_i) point. Both k and i go from 1 to N.

Defining

$$C_t = C(M_k^t) - \nabla C_i(M_k^t)\, M_i^t, \tag{3.5}$$

we have

$$Z - \nabla C_i(M_k^t)\, M_i \geq C_t \tag{3.6}$$

The approximation for $C(M_i)$ in equation (3.4) defines the plane tangent to $C(M_i)$ at M_i^t.

Based on this linearization, the following linear programming problem results

Mimimize Z

subject to

$$g_{ji}\, M_i \geq b_j$$

$$Z - \nabla C_i(M_k^t)\, M_i \geq C_t \tag{3.7}$$

The solution of the original nonlinear problem defined by equations (3.1) and (3.2) is now found by solving the sequence of linear problems described below.

(1) Select a starting point, M_i^1 $(t = 1,\ i = 1,N)$

(2) Form the linear programming problem (equation [3.7]) and solve for M_i which is denoted M_i^{t+1}.

(3) Add the constraint, $Z - \nabla C_i(M_k^{t+1})\, M_i \geq C_{t+1}$, to the constraint set defined by equation (3.7) and set $t = t + 1$.

Steps 2 and 3 are repeated until the solution M_i^t and M_i^{t+1} are the same. Numerically, M_i^{t+1} and M_i^t are assumed the same when

$$XN \leq TOL \tag{3.8}$$

where

$$XN^2 = \frac{\sum_{i=1}^{N} \left(M_i^{t+1} - M_i^t\right)^2}{\sum_{i=1}^{N} \left(M_i^{t+1}\right)^2}$$

TOL = a convergence tolerance.

Figure 7 illustrates the process for a function of one variable. Starting with M^1, points M^2, M^3, and M^4--with minima Z_2, Z_3, and Z_4--are generated by solving the sequence of linear programming problems defined by steps 1-3, above. The constraints

$$Z - \nabla C(M^t)\, M \geq C_t \qquad t = 1,2,\ldots,$$

simply require the point (Z, M) to lie above the line tangent to the graph of C at the point M^t. A numerical example of the cutting plane algorithm is presented in Appendix A.

In order to implement the above algorithm, it is necessary to define a differentiable form for the objective function and to select a starting point in the Set S, defined by the design constraints. The form of the objective function and the selection of M_i^1 are discussed in the following sections.

3.2.2 Formulation of the Objective Function

The objective function--which is proportional to the volume of flexural reinforcement--is based on the following approximate relationship between the beam design capacity at section i, M_i, and the corresponding steel area A_{s_i}

$$M_i = A_{s_i} f_y jd \tag{3.9}$$

As discussed in Chapter 2, the objective function may be written as

$$C(M_i) = C_C(M_i) + C_B(M_i) \tag{3.10}$$

where $C_C(M_i)$ accounts for the column reinforcement and $C_B(M_i)$ accounts for the beam reinforcement.

The column term $C_C(M_i)$ is determined on the basis of the weak-girder, strong-column design criterion and is a linear function of M_i [6]. The beam term, $C_B(M_i)$, is based on equation (3.9). Since M_i is linearly related to A_{s_i}, the volume of flexural reinforcement in a given span is proportional to the area under the design moment envelope (Fig. 8). For the k*th* span

$$[C_B(M_i)]_k = -\int_0^{B_1} M_1\ (x,\ M_i)\ dx - \int_{B_2}^{L} M_2\ (x,\ M_i)\ dx + \int_{B_3}^{L} M_1\ (x,\ M_i)\ dx \tag{3.11}$$

$$+\int_0^{B_4} M_2\ (x,\ M_i)\ dx + \int_{B_4}^{B_3} M_3\ dx + XM \cdot (B_2 - B_1) + F_A\ (M_i)$$

where

$$M_i > 0 \qquad i = 1,5$$

$$M_1 = -M_1 + \frac{WLx}{2} + \frac{(M_1 + M_5)x}{L} - \frac{Wx^2}{2}$$

$$M_2 = M_2 + \frac{WLx}{2} - \frac{(M_2 + M_4)x}{L} - \frac{Wx^2}{2}$$

$$M_3 = M_3$$

$$W = 1.2\ \text{D.L.} + 1.0\ \text{L.L.}$$

$$XM = 1/4\ \text{MAX}(|M_1|, |M_4|)^*$$

*Based on ACI, A.5.5 [9] which requires at least one-fourth of the negative moment reinforcement to be continuous throughout the top of the member.

$$B_1 = x \ @ \ M_1(x, M_i) = -XM$$

$$B_2 = x \ @ \ M_2(x, M_i) = -XM$$

$$B_3 = x \ @ \ M_1(x, M_i) = M_3$$

$$B_4 = x \ @ \ M_2(x, M_i) = M_3$$

and

$F_A(M_i)$ = A linear function in M_i which accounts for anchorage of beam bars in the columns and, therefore, depends on the development length and column width.

The term, $C_B(M_i)$, for the entire design subassemblage is found by summing $[C_B(M_i)]_k$ for each span.

It should be noted that the negative sign in the first two terms is required because the indicated integration yields a negative area.*

3.2.3 Starting Point

In order to begin the cutting plane method, it is necessary to define a starting solution, M_i^1, which satisfies the design constraints $g_{ji} M_i \geq b_j$. In the current application, the starting point, M_i^1, is found by modifying the results of an ultimate load elastic analysis to ensure that the practical design constraints are satisfied.

3.3 Inelastic Optimum Designs

Five inelastic optimum design problems were formulated and solved employing the cutting plane algorithm described above. The required beam design moment capacities are summarized in Tables 1-3. In order to illustrate the degree and nature of moment redistribution obtained by the proposed inelastic design technique, the optimum beam moment capacities have been normalized with respect to beam moments obtained from elastic analysis for

*A detailed evaluation of the constraint defined by equation (3.6) is presented in Appendix A.

each design. The different formulations of the optimization problem for the designs indicated in Tables 1-3 are reviewed below.

Designs I-2.1 and I-1.4 differed by the maximum reinforcement ratio, ρ_{max}, used in beam design. In design I-2.1, ρ_{max} was equal to 0.75 ρ_b* (approximately 2.1 percent for f'_c = 27.6 MPa and f_y = 414 MPa) and ρ_{max} was equal to 0.50 ρ_b in design I-1.4 (approximately 1.4 percent). Although the same basic design constraints were used to formulate the optimization problem for both designs I-1.4 and I-2.1, the increase in beam size caused by reducing ρ_{max} from 2.1 to 1.4 percent had an effect on the optimization solution. Details of this effect are presented below.

In the formulation of the optimization problem for designs II-1.4, III-1.4, and IV-1.4, practical design constraints were modified or added to study: (a) the effect of the ratio of positive (M_i^+) to negative (M_i^-) moment capacity at a given section and; (b) the effect of eliminating bar curtailment at interior beam-column joints. In design I-1.4, which may be considered as the basic design, the absolute value of M_1^+ was subjected to the following constraint:

$$|M_i^+| \geq .5|M_i^-| \tag{3.12}$$

This reflects a design requirement stipulated in both UBC [4] and ACI [9]. In design IV-1.4, this constraint became

$$|M_i^+| \geq .75|M_i^-| \tag{3.13}$$

and, in design II-1.4, the absolute values of M_i^+ and M_i^- were constrained to be equal.

---

*The value of ρ_b used in this report is that for a singly reinforced beam.

In order to eliminate bar curtailment at interior-beam joints, the beam moment capacities on either side of an interior joint in design III-1.4 were constrained to be equal. For the design subassemblage in Fig. 4, the following constraints result:

$$M_3^- = M_4^-; \qquad M_3^+ = M_4^+. \tag{3.14}$$

With the exception of the constraints indicated above, the design constraints imposed in designs II-1.4, III-1.4, and IV-1.4 were identical to those employed in design I-1.4. In designs II-1.4 and III-1.4, equality of beam design capacities was imposed prior to solution of the optimization problem.

Negative and positive design capacities for the various designs are compared in Tables 1 and 2, respectively. In the following discussion, reference to a reduction or increase in design capacity is made with respect to the results of elastic analysis. In either Table 1 or 2, a reduction is indicated by a value less than one and, conversely, an increase is indicated by a value greater than one.

An examination of the data in Tables 1 and 2 indicates that, in the upper stories (roof to level 9), there is a typical reduction in negative design capacities M_i^- and a significant increase in positive design capacities M_i^+. This trend is attributed to the fact that gravity load controls design (strength) in the upper stories. As a result, elastic analyses yield positive moments at the beam ends which are much smaller than those required by the practical design constraints

$$\begin{aligned} |M_i^+| &\geq |M_{\rho_{min}}| \\ |M_i^+| &\geq p|M_i^-| \end{aligned} \tag{3.15}$$

*$p = 0.75$ for design IV-1.4, 1.00 for design II-1.4, and 0.50 for all other designs.

In fact, at the roof level, the elastic moments for sections 3 and 4 never become positive.

A comparison of the ratio of the positive-to-negative design capacities, which is presented in Table 3, indicates that, from the roof level to floor level 9, the positive design capacity is controlled by one of the two lower bound constraints indicated above. Consequently, it may be concluded that the positive design capacities have been minimized.

Although the positive capacities may be considered minimized, the value of the minimum constraint is larger than the moment found from elastic analyses. Consequently, the positive design sections are "overdesigned," and a reduction in negative design capacities results. Two exceptions to the above general behavior require explanation.

First, in designs I-1.4, III-1.4, and IV-1.4, M_1^- is equal to the elastic moment throughout the height of the frame. This is attributed to the interaction of the practical design constraints

$$\left|M_1^-\right| \geq \text{FAC}\left|M_1^-\right|_{\text{above}}$$

$$\left|M_1^-\right| \leq \left|M_1^{-UE}\right| \tag{3.16}$$

At the roof level in designs I-1.4, III-1.4, and IV-1.4, $\left|M_1^{-UE}\right|$ is less than $M_{\rho_{min}}$. Consequently, $\left|M_1^-\right|$ at the roof is equal to $M_{\rho_{min}}$. At story level 10, the combined effect of the two constraints in equation (3.16) is the equality

$$\left|M_1^-\right| = \left|M_1^{-UE}\right| \tag{3.17}$$

This equality remains effective throughout the height of the frame.

A second exception occurs in design III-1.4, in which M_3^- is typically greater or equal to one in the upper stories. This is a result of the combined effects of the geometry of the frame (larger central span) and of the equality constraint unique to this design [equation (3.14)].

As the effect of lateral load becomes more predominant, the nature of the inelastic moment redistribution exhibits a different character. Ignoring design II-1.4 for now, negative moment redistribution in all designs is concentrated at one design section, at M_4^- in designs I-1.4, III-1.4, and IV-1.4 and at M_1^- in design I-2.1. In addition, the positive design capacities at sections 1 and 4 are typically less than the corresponding elastic moments (Tables 1 and 2). In fact, the positive capacities at sections 1 and 4 tend toward their lower bound (Table 3).

$$\left|M_i^+\right| \geq p\left|M_i^-\right|. \tag{3.18}$$

Based on these observations, it may be concluded that the optimization solution tends to maximize the negative design capacities and minimize positive capacities.* This conclusion is consistent with the form of the beam contribution to the objective function. On examination of Fig. 8, it is evident that positive design capacities make relatively larger contributions to flexural steel volume than corresponding negative design capacities.

The tendency to maximize negative design capacities and minimize positive capacities is a major shortcoming of the proposed optimization procedure. To avoid congestion of steel at beam-column joints, a practical moment redistribution should reduce negative design capacities at beam ends and, thus, reduce the area of negative moment steel which must be passed through or developed in the beam-column joint.

*As will be discussed shortly, M_1^- tends to decrease because of the contribution of exterior column reinforcement (design I-2.1, Table 1). Consequently, in the case of long columns and short-beam spans, the exterior column steel may affect this observation.

As discussed previously, some negative moment redistribution does occur in all inelastic designs. However, it is typically concentrated at one design section. For example, negative redistribution occurs at section 1 in design I-2.1 and at section 4 in design I-1.4. Following is an explanation of why negative moment redistribution occurred at different sections in these two designs.

Redistribution at section 1 in design I-2.1 is attributed to the relative contributions of the exterior and interior column steel to the objective function. One factor which is used to evaluate the objective function coefficients associated with column reinforcement is the ratio h_b/h_c, where h_b is the beam depth at a given floor level and h_c is the column depth. This factor accounts for the effect of member depth on moment capacity (equation [3.9]).

For the designs obtained in this study, the exterior columns are smaller than the interior columns. Consequently, since h_b at a given floor level is constant, h_b/h_c was larger for exterior columns than for interior columns. For example, in design I-2.1, h_b/h_c for the exterior column varies from 1.38 at the roof to 1.17 at the second floor level. The variation for the interior column was 1.06 to 1.05. As a result, the column contribution at negative design section 1 is larger than that at negative sections 3 and 4. Consequently, the optimum solution tends to minimize M_1^-.

The above statements are also true for M_1^- in design I-1.4. However, as discussed previously,

$$\left| M_1^{-UE} \right|_{roof} < M_{\rho\ min,\ roof}$$

This fact, in combination with the interaction of the practical design constraints of equation (3.16), imposes the equality

$$\left| M_1^- \right| = \left| M_1^{-UE} \right|$$

at the remaining floor levels. Consequently, redistribution could not occur at M_1^-. It occurs at M_4^- and not M_3^- because M_4^-, being associated with the longer interior span, makes a relatively larger contribution to the volume of flexural reinforcement than M_3^-.

A comment concerning the column contribution to the objective function is warranted. As discussed in Ref. 6, the design constraint that $\left|M_1^+\right| \leq \left|M_1^-\right|$, in combination with the condition of symmetric column steel placement, causes the exterior column steel to be a function primarily of M_1^-. The designs described here, however, are not based on this condition. In this study, the exterior column steel was assumed a function of both the positive and negative capacities at section 1*. The current design problems were formulated on the basis of this condition (case 1) instead of the condition that the exterior column steel is primarily a function of M_1^- (case 2) because it was felt that the characteristics of moment redistribution resulting from case 1 are more desirable than those resulting from case 2. This may be illustrated by comparing designs which are identical with the exception of how the contribution of the exterior column steel is included in the objective function.

A comparison of design results based on case 2 with the results described in this report (case 1) indicates that the general trends are the same for both cases. In fact, the results are the same for design II-1.4. The basic difference between cases 1 and 2 is found in design capacity M_1^+.

---

* The principal component of the exterior joint equilibrium equation was divided equally between M_1^+ and M_1^-. This technique is employed because of its simplicity.

Typically, values of M_1^+ obtained in case 2 are larger than those obtained in case 1. In fact, $\left|M_1^+\right|$ was in many cases equal to $\left|M_1^-\right|$. This characteristic of the solution was expected, however. The influence of M_1^+ in the objective function for case 2 is relatively small because the contribution of column reinforcement is essentially independent of this design capacity. Consequently, $\left|M_1^+\right|$ tends toward its maximum value, $\left|M_1^-\right|$.

A difference between the two cases is also evident in the magnitude of negative moment redistribution. In all designs, the section at which moment redistribution occurred was the same for both case 1 and case 2. However, the magnitude of redistribution was typically larger in case 2. For example, in design I-1.4, a redistribution of six percent occurred at floor level 2 in case 1 (section 4, Table 1). In case 2, this redistribution was 27 percent. This increase in negative moment redistribution is related to the increase in M_1^+ discussed above. The design solution (beam design capacities) is bounded by equilibrium, serviceability, and practical design constraints. The increase in M_1^+ reduces the lower bound imposed on another capacity--in this case, M_4^-.* Consequently, M_4^- decreases.

3.4 Concluding Remarks

Although redistribution obtained by minimizing the volume of flexural reinforcement does not, in general, cause significant reduction in negative design capacities, the results for design II-1.4 demonstrate than an inelastic optimum design exhibiting significant negative moment redistribution can be obtained by imposing proper design constraints. One shortcoming of design II-1.4, however, is that moment redistribution is concentrated** at the interior

*The increase in M_1^+, in general, will affect all other variables. Consideration of a single variable is to simplify illustration.

**The magnitude of moment redistribution was typically 30 percent and 35 percent at design sections 3 and 4, respectively, while it was only 10 percent at design section 1 (Table 1).

beam-column joint which, as will be discussed later, leads to large inelastic deformation demands.

The basic problem is to find a redistribution that leads to a balance between economy, magnitude of inelastic rotation demands, and ease of construction. As discussed above, a basic feature of an optimum redistribution in seismic-resistant reinforced concrete frames is to reduce negative design capacities. One possible technique to obtain such a redistribution within the context of the proposed inelastic design procedure is to modify the practical constraint

$$\left|M_i^-\right| \leq \left|M_i^{-UE}\right| \tag{3.19}$$

so that, instead,

$$\left|M_i^-\right| \leq (1 - MR)\ \left|M_i^{-UE}\right|. \tag{3.20}$$

The factor, MR, is the magnitude of the desired negative moment redistribution.

Recently, two additional inelastic designs, A and B, have been obtained in order to evaluate this technique. Both designs are based on the member sizes found for design I-1.4.* In the formulation of design A, the constraint,

$$\left|M_i^-\right| \geq FAC\ \left|M_{i_{above}}^-\right| \tag{3.21}$$

was not imposed. With this exception, the design problem was identical to that for design I-1.4.

The formulation of the optimization problem for design B is the same as that for design A except that the upper bound constraint defined by equation (3.20) was used instead of the constraint in equation (3.19). A value of 0.2 was used for MR. This is the maximum redistribution allowed by ACI [9].

*In the objective function, the exterior column steel was a function of both M_1^- and M_1^+.

The required beam design capacities for designs A and B are compared in Table 4. The results have again been normalized with respect to elastic analysis. A comparison of the results for design A with those for design I-1.4 (Tables 1 and 2) confirms the observation that negative moment redistribution did not occur at section 1 in design I-1.4 because of the interaction of the constraints defined by equations (3.19) and (3.21).

A comparison of the results for designs A and B presented in Table 4 indicates the following:

(a) Negative moment redistribution is concentrated at section 1 in design A. In design B, however, the upper bound constraint defined by equation (3.20) causes moment redistribution to be the same at all sections.

(b) Removing the smoothness constraint defined by equation (3.21) causes rather sudden changes in negative moment redistribution at section 1 in design A. For example, at floor level 4, the redistribution is approximately 13 percent, increasing to 33 percent at level 3 and decreasing to 4 percent at level 2.

(c) Ignoring the roof and floor level 10 for now, the results for design B indicate that the constraint defined by equation (3.20) is effective in obtaining a smooth transition in strength through the height of the structure in design B. The beam-design capacities for design B have the same smoothness characteristics as the results of elastic analysis.

(d) The results for both designs are similar at the roof and floor level 10. With the exception of roof section 1, significant negative moment redistribution occurs at all sections. This behavior is attributed to the importance of gravity load at these floor levels (section 3.3). The design capacity at roof section 1 is greater than the elastic value $\left|M_1^{-UE}\right|_{roof}$, because the lower bound constraint was defined by $M_{\rho_{min}}$ (289 KN-m) which was greater than $\left|M_1^{-UE}\right|_{roof}$.

The large moment redistribution in both designs (44 percent) at floor level 10 is a cause of concern. As discussed previously, the optimization solution tends to minimize $\left|M_1^-\right|_{10}$ because of the contribution of the exterior column steel. Consequently, $\left|M_1^-\right|_{10}$ tends toward its lower bound. Since the service lateral load (due to wind) considered here is approximately one-fifth the seismic design forces, the lower bound on $\left|M_1^-\right|_{10}$ is defined by $M_{\rho_{min}}$ which is significantly smaller than $\left|M_1^{-UE}\right|_{10}$.

Excessive redistribution can be eliminated by imposing a new lower bound constraint which would ensure that

$$\left|M_i^-\right| \geq (1 - MRR) \left|M_i^{-UE}\right| \tag{3.22}$$

where MRR is the maximum desired moment redistribution. However, since required inelastic deformation demands in the upper stories are typically small [section 4.3.3(ii)], it is felt that a 44 percent redistribution in these stories should be acceptable. This conclusion should be confirmed by evaluating the nonlinear static and dynamic response of designs A and B.

On the basis of the above comparison of moment redistribution in designs A and B, it may be concluded that design B is preferable to design A. The real test of any design, however, is how well it performs in response to earthquake ground motion excitations. A comparison of designs A and B, with respect to nonlinear seismic response, is planned in a future study.

4. DESIGN RESULTS AND ANALYSIS OF PRELIMINARY DESIGNS

4.1 Member Design

Once the required optimum beam design moment capacities have been obtained, member design is found employing computer design aids developed by the authors [6]. Beam sizes and reinforcement are found first. Actual design moment capacities are found from the required optimum design capacities by considering slenderness amplification and capacity reduction factors. Both beam and column design are based on the ACI strength method. Beam design is based on the equation

$$\frac{M_u}{\phi} = \rho b d^2 f_y \left(1 - .59 \frac{\rho f_y}{f'_c}\right). \tag{4.1}$$

The beam size is assumed constant at a given floor and is found on the basis of the largest required negative design capacity at the floor under consideration, assuming that ρ is equal to ρ_{max}. Once the beam size has been determined, the required reinforcement for all critical sections in that floor is found by solving equation (4.1) for ρ. In the beam size selection, a width-to-depth ratio of one half was used. In the design of positive moment steel areas, the effective compression flange width defined by ACI was considered.

In column design, the capacity-reduction factor of 0.7 for tied columns was used and specified mimimum eccentricities were checked.* Column design moments were obtained on the basis of the weak-girder, strong-column design criterion by considering beam-column joint equilibrium under all possible beam plastic-hinge combinations. The as-designed beam moment capacities were amplified by a factor of 1.2 to account for the uncertainties in beam capacity computations, in particular, the variation in steel yield stress

*Design program based on ACI (318-71) [15].

and the effect of strain hardening. The design axial forces were determined by considering various combinations of gravity loading and gravity plus lateral seismic loading. A bound on the axial force due to overturning effects for an exterior column at story i is easily established by summing the maximum beam shears for stories i to NS where NS is the total number of stories in the structure. However, such a bound cannot be obtained as easily for an interior column. Therefore, overturning moment axial forces obtained in the ultimate-load elastic analysis used to formulate the optimum design problem were considered in the interior column design.

One factor which is not accounted for in column design is the effect of inelastic beam behavior and/or higher mode dynamic response on the distribution of beam moments to the columns at a given joint. The benefits of using an additional design factor, such as the dynamic magnification factor suggested by Paulay [16], to incorporate this aspect of seismic-resistant design in the procedure should be investigated.

In addition to the inelastic designs described in Chapter 3, two designs based on UBC seismic design story shears were obtained. The designs differed in the value of ρ_{max} assumed in beam sizing--values of $0.75\rho_b$ and $0.50\rho_b$ being used. The beam design moment capacities were obtained from the results of elastic analysis by considering code-allowed moment redistribution. The magnitude of moment redistribution, MR, was controlled by the ACI expression

$$MR = 20\left(1 - \frac{\rho - \rho'}{\rho_b}\right) \tag{4.2}$$

where

ρ = Tension reinforcement ratio A_s/bd

ρ' = Compression reinforcement ratio A'_s/bd

and

ρ_b = Balanced reinforcement ratio [9].

The moment redistribution defined by equation (4.2) was applied independently to each span of the design subassemblage in Fig. 4. Equation (4.2) is applicable to the design examples presented here because $\rho - \rho' \leq 0.5\rho_b$.*

Strictly speaking, the redistribution allowed by ACI is intended for the case of gravity loading in which negative moment redistribution is accompanied by changes in span design moments. Its application to lateral load combined with gravity load is considered appropriate, however, for seismic-resistant design in which a weak-girder, strong-column design criterion is followed.

The relationship between moment distribution and steel content is incorporated to ensure that member critical regions (plastic-hinge zones) possess sufficient inelastic rotation capacity to attain the assumed redistributions. In the case of seismic-resistant reinforced concrete frames, such a limitation on the magnitude of moment redistribution is believed to be conservative. Design in accordance with present seismic code requirements results in plastic-hinge zones characterized by relatively low steel percentages, by the presence of significant compression reinforcement, and by close spacing of transverse reinforcement. As a result, such structures should possess sufficient ductility to accommodate the moment redistributions necessary to form a mechanism. In seismic-resistant design, however, the inelastic deformation capacity must be adequate not only to allow a mechanism to form, but also to allow the displacement ductility (as a mechanism) assumed in design to be attained. In view of this, an upper bound on the magnitude of moment redistribution may be necessary. Paulay has suggested an upper bound of 30 percent [16].

Member design for UBC designs followed the same procedure outlined above for the inelastic designs. The UBC designs, following the convention

* A design constraint is $\left|M_i^+\right| \geq .5\left|M_i^-\right|$.

established in Chapter 3, are designated UBC-1.4 and UBC-2.1, corresponding to beam flexural steel percentages of 1.4 and 2.1, respectively.

4.2 Member Design Results

Preliminary design results obtained after two iterations of the preliminary design phase are summarized in Tables 5 and 6. Member design for inelastic design IV-1.4 was not obtained. It was felt that the essential features of design IV-1.4--in particular, its nonlinear response--would be bounded by the features of design I-1.4, II-1.4, and III-1.4. On the basis of previous results and, in view of the apparent bound on response, it was concluded that the design and analysis of design IV-1.4 would yield little additional information.

4.2.1 Member Sizes

Beam and column sizes are presented in Table 5. In determining member sizes, the following design constraints were imposed:

(a) Beam and column sizes (except for the first-story columns) were constrained to be the same for at least two stories.

(b) In order to achieve a smooth transition in stiffness through the frame height, the increment in beam and column depth was set at 40 mm.

(c) Selection of column size was constrained by the criterion that the axial load be less than the balanced ultimate axial load.

The above set of design constraints, in combination with the fact that design gravity loads were essentially the same in all designs, resulted in one set of column sizes (Table 5).

Four sets of beam sizes were obtained. The smaller beams obtained for the UBC designs are attributed to the magnitude of seismic design forces. Seismic design story shears for the various designs are presented in Fig. 9.

A comparison of designs UBC-1.4 and I-2.1* indicates that inelastic spectral design forces based on a displacement ductility of six exceed the UBC seismic design forces factored for strength design by more than 50 percent.

As expected, increasing ρ_{max} from $0.5\rho_b$ to $0.75\rho_b$ results in a reduction in beam size. A comparison of seismic story shears for designs I-1.4 and I-2.1 indicates that the resulting increase in frame flexibility leads to a reduction in seismic design forces (Fig. 9).

The smaller beam sizes for design II-1.4 (as compared to design I-1.4) are attributed primarily to the different nature of moment redistribution in these two designs. In design II-1.4, there was a reduction in required negative design capacities while, in design I-1.4, redistribution generally occurred at positive moment sections (Table 1 and 2). Since beam size was controlled by negative design capacities, the smaller negative capacities in design II-1.4 caused a reduction in required beam size.

4.2.2 Material Volume

Required concrete and flexural (longitudinal) steel volumes for the various designs are summarized in Table 6. The steel volumes presented were computed on the basis of equation (3.11) and provide only a qualitative measure of the required longitudinal steel.

A comparison of the material volume data for designs I-1.4, II-1.4, and III-1.4 indicates that moment redistribution has a minor effect on required volumes of concrete and steel--the variation in material volume being less than 5 percent. The relatively small variations in required steel volume indicates that the volume of flexural reinforcement is not the best choice for an optimization objective in reinforced concrete design. This conclusion is confirmed by a comparison of the value of the objective function, $C(M_i)$, corresponding to the optimum solution in designs I-1.4, III-1.4, and IV-1.4 (Table 7).

---

* These designs are compared because they have the same member sizes and are dynamically equivalent if gross section properties are used.

The data presented in Table 7 has been normalized with respect to $C(M_i)$ for design I-1.4. Except at story levels 9 and 10 in design IV-1.4, the difference in $C(M_i)$ among the various designs is less than 4 percent and gradually decreases to less than 1 percent in the lower stories. The relatively large values of $C(M_i)/C(M_i)_{I-1.4}$ for design IV-1.4 in the upper stories is attributed to the design constraint $\left|M_i^+\right| \geq \rho\left|M_i^-\right|$. In design IV-1.4, ρ was 0.75 and, in designs I-1.4 and III-1.4, ρ was 0.5.

Based on the above observations, it is apparent that the volume of flexural reinforcement is insensitive to the final distribution of beam design capacities. Consequently, if an optimum solution is desired, further study is required to formulate a new objective function which is based on a more sensitive design parameter.

As expected, the increase in the upper bound on the percentage of beam flexural reinforcement from 1.4 percent to 2.1 percent causes an increase in required steel volume and a corresponding decrease in concrete volume (Table 6). In the UBC designs, the increase in steel volume was approximately 10 percent, and the decrease in concrete volume was approximately 7 percent. In the inelastic design procedure, the increase in steel volume was approximately 3 percent, and the decrease in concrete volume was approximately 12 percent. The relatively small increase in steel volume in design I-2.1 is attributed, in part, to minimum reinforcement requirements. The design constraint, $\left|M_i\right| \geq M_{\rho_{min}}$, controlled design at more locations in design I-1.4 than it did in design I-2.1 (Tables 1 and 2). In addition, $M_{\rho_{min}}$ required more steel in design I-1.4 than in design I-2.1 because of the larger beam sizes in design I-1.4.

A comparison of material requirements for designs I-1.4 and UBC-1.4 indicates that, although seismic design forces determined on the basis of a spectral analysis technique exceed those specified by UBC by more than 80 percent (Fig. 9), the increase in steel volume is less than 20 percent and the increase

in concrete volume less than 15 percent. The effect of these increases in material volume on design performance will be discussed later.

4.3 Analysis of Preliminary Design

The final step of the preliminary design phase is to carry out a series of elastic and nonlinear structural analyses in order to evaluate the acceptability of the latest preliminary design with respect to established design criteria and with respect to the assumptions made in formulating the design problem.

Three separate computer programs are used to carry out the complete series of analyses, ETABS* [17] for elastic analysis, a modified version of ULARC [6] for nonlinear static analysis and SERF [18] for the nonlinear dynamic analysis. All three programs employ the same basic analytical model. The floor slab is modeled as a rigid diaphragm which constrains all the lateral displacements in a given story to be equal. A structural frame is modeled by a series of beam elements which span longitudinally between vertical column elements. It is also possible to model elements spanning diagonally between stories.

The axial stiffness of a beam element is assumed infinite to impose the rigid diaphragm constraint. However, axial deformations are allowed in column elements. In all analyses, gravity loads as well as rigid joint areas defined by actual member dimensions are considered. In addition, the slab contribution to the frame stiffness is approximated following a procedure suggested by Malik and Bertero [19].

---

*ETABS is used because of its eigenvalue analysis capabilities. If only static load analyses were required, either ULARC or SERF could have been used.

Inelastic member behavior is idealized by the two-component model. Basically, a flexural element is idealized as a perfectly elastic component with stiffness $\underline{K}_p$ acting in parallel with an elasto-plastic element with stiffness $\underline{K}_q$. In the elastic range the combined stiffness of the two components is identical to that of the actual member.

$$\underline{K} = \underline{K}_q + \underline{K}_p \tag{4.3}$$

In the inelastic range, yielding is idealized as concentrated plastic hinges at the ends of the elasto-plastic component and $\underline{K}_p$ is the desired rate of strain hardening.

In the analysis conducted in this study, strain hardening was taken as zero in the nonlinear static analyses (a program limitation) and was taken as 3 percent in the nonlinear dynamic analyses. The advantages and disadvantages of such an inelastic beam model are discussed in Ref. 20.

Both nonlinear analysis programs employ a simplified geometric stiffness based on axial loads due to gravity effects [18]. In this formulation, only the column translational degrees of freedom are affected by second-order effects.

In both programs, the effect of axial force level on reinforced concrete yield moments is considered. However, both programs ignore the effect of inelastic behavior on column axial stiffness. In the dynamic analysis program, Rayleigh-type damping with a 5 percent damping ratio in the first two modes is used.

The results of the analysis indicated above for the designs defined in Table 5 are summarized in the following paragraphs.

4.3.1 Elastic Analysis

The effect of the different beam sizes on the dynamic characteristics of the various designs is illustrated in Table 8. The first mode period, T_1, varies from 1.39 sec. in design UBC-2.1 to 1.08 sec. in design I-1.4.

Although, as noted previously, the increase in frame flexibility (which is associated with larger reinforcement ratios) decreases seismic design forces, the increased flexibility leads to larger service-level deformations. For example, a comparison of story drift indices, R_i, due to service-level wind loads, are presented in Fig. 10.

$$R_i = \frac{\Delta_i - \Delta_{i-1}}{h_i} \tag{4.4}$$

where

Δ_i = Lateral displacement at floor level i

Δ_{i-1} = Lateral displacement at floor level i-1

and

h_i = story height

The smaller beam sizes associated with larger values of ρ_{max} can increase service-level deformations by as much as 40 percent. Although the drift indices indicated in Fig. 10 are well within acceptable values (.002 is generally considered acceptable), the increased flexibility may be detrimental for more severe service conditions such as a minor or moderate, but frequent, earthquake ground motion.

4.3.2 Nonlinear Static Analysis

The results of the nonlinear static analyses for the various designs is summarized in Fig. 11. The behavior of design III-1.4 has been omitted since it is essentially the same as that indicated for design I-1.4. In the analysis, the frame was subjected to design gravity loads and a monotonically increasing base shear--which was distributed through the height of the frame according to the UBC force distribution in designs UBC-1.4 and UBC-2.1 and according to

lateral force pattern obtained from the spectral modal analysis in designs I-1.4, I.2.1, and II-1.4.

It is evident from Fig. 11 that all frames have significant overstrength ranging from 45 percent for design I-1.4 to 106 percent for design UBC-2.1. The overstrength is attributed in part to the fact that the beams were overdesigned with respect to design capacities required to resist the selected design loads. As noted previously, optimum beam design capacities were modified by slenderness amplification and capacity reduction factors prior to member design. In addition, the frame was transformed into a mechanism gradually, not instantaneously, as assumed in design. The significantly larger overstrength in the UBC designs is attributed, in part, to larger slenderness amplification factors. In addition, UBC seismic design forces were significantly smaller than spectral design forces (by as much as 55 percent). The smaller design base shear combined with the fact that the design gravity load moments were essentially the same in all designs caused additional overdesign of positive design sections in the UBC designs because of the design requirement

$$|M_i^+| \geq 0.5 \ |M_i^-|. \tag{4.5}$$

This was particularly true in the upper stories.

A comparison of base shear at initial hinge formation for the various designs indicates that the design base shear was exceeded prior to initial hinge formation in the UBC designs (by 65 percent in design UBC-2.1 and 33 percent in design UBC-1.4). In the optimum inelastic designs, however, initiation of inelastic behavior occurred prior to reaching the design base shear. For example, in design I-1.4, the first beam plastic hinge formed at a base shear of 34 percent of the design value.

The relatively early yielding in the optimum inelastic designs does not indicate an unserviceable structure. First, it should be noted that the seismic force level considered in these designs corresponds to an extreme event. In addition, a serviceable structure is ensured within the context of proposed inelastic design procedure by imposing serviceability design constraints. Although the service level lateral load considered in the examples presented in this report was due to relatively small wind forces, a more severe service lateral load (for example, one corresponding to a minor earthquake) could easily be considered.

The relatively early yielding in design I-1.4 requires additional comment. Initial yielding occurred in the interior roof beam at the right end. The next hinge to form was at a base shear equal to 55 percent of the design value and the third hinge did not form until a base shear equal to 86 percent of the design value. The effect of the first two hinge formations on the lateral stiffness is small as is evidenced by how closely the base-shear, roof-displacement relationship follows the elastic slope. In addition, the plastic rotation at the section of first yielding remains small (less than 0.005 radians) because a plastic hinge never forms on the left side of the roof beam.

On the basis of the data in Table 1, it would appear that first yielding should occur at essentially the same load in designs I-2.1 and II-1.4 as it does in design I-1.4 because negative moment redistribution is essentially the same in all three designs. Different slenderness amplification factors and the discrete nature of member design can alter the trends expected from examination of this data alone. For example, the as-designed negative design capacity for the roof interior beam was 447 kN-m in design I-1.4 and 520 kN-m in design I-2.1. Although the values differ by less than 20 percent, gravity load causes a negative moment of approximately 360 kN-m in both designs,

and the flexure strength remaining to resist lateral load in design I-2.1 is approximately twice that in design I-1.4.

Another factor which contributes to the larger beam overstrength in designs UBC-1.4 and UBC-2.1 is the nature of the inelastic design procedure used to obtain the beam design moment capacities. In designs UBC-1.4 and UBC-2.1, moment redistribution was based on the ACI recommendations. In implementing the code recommendations, elastic moment envelopes are first constructed considering the effects of partial and/or pattern loading. The redistribution defined by equation (4.2) is then applied to each span separately, after which practical code requirements that

$$\left|M_i^+\right| \geq 0.5 \left|M_i^-\right|$$
$$\left|M_i^-\right| \geq M_{\delta\ \min} \qquad (4.6)$$

are imposed.

This is in contrast to the proposed inelastic design procedure which was used to obtain the beam design capacities in designs I-1.4, II-1.4, III-1.4, and I-2.1. In this procedure, moment redistribution is based on an optimization technique in which the volume of flexural reinforcement is minimized. Member flexural strength is based on equilibrium constraints which are found by considering all possible failure mechanisms of the selected design subassemblage. As a result, all beam design capacities in a given story are coupled.

In addition to equilibrium constraints, the optimum beam-moment capacities must satisfy a set of practical constraints, two of which are defined by equation (4.6) and a set of serviceability constraints.

It is felt that because of the coupling of strength and practical design requirements, and the interdependence of all design capacities in a given

story, the proposed inelastic design procedure yields a more efficient moment redistribution than the ACI procedure. In other words, the ACI inelastic design procedure, at least as it was applied in this study, typically results in larger beam overstrength than the optimum inelastic design procedure described in this report.

A comparison of designs I-1.4 and II-1.4 indicates that there is a more gradual departure from the elastic loading curve in design II-1.4 than in design I-1.4. This is attributed to the reduction in negative design capacities associated with inelastic moment redistribution which occured in design II-1.4. Although initial yielding occurred much earlier in design I-1.4 than it did in design II-1.4, the yielding was isolated and had little effect on behavior. The reduced negative design capacities in design II-1.4 caused early yielding (as compared to design I-1.4) at negative sections over a relatively large region of the frame. Consequently, a gradual reduction in the frame lateral stiffness occurred.

4.3.3 Time History Analysis

The nonlinear dynamic response of the designed frames to the El Centro N-S (EC) component and the Derived Pacoima Dam (DPD) ground motions was assessed using SERF, a program developed by Mahin and Bertero [18]. The accelerations of both ground motions were scaled to have a peak value of 0.4 g. The behavior of the various designs are discussed and compared below.

(i) Global response

Examination of story displacement envelopes in response to the EC ground motion for designs UBC-2.1, UBC-1.4, I-1.4, and I-2.1 (Fig. 12[b]) indicates

that response is proportional to the initial frame flexibility. Maximum roof displacements increase from 109 mm in design I-1.4--which has an initial first-mode period, T_1, of 1.08 sec.--to 180 mm in design UBC-2.1 which has an initial T_1 of 1.39 sec.

A comparison of UBC-1.4 and I-2.1 indicates that frame strength also affects global response. Although these two designs have the same initial stiffness characteristics, the maximum roof displacements are 145 mm and 129 mm in designs UBC-1.4 and I-2.1, respectively. The smaller displacement in design I-2.1 is attributed to the fact that this design is approximately 133 percent as strong as design UBC-1.4 (Fig. 11).

The displacement envelopes for the DPD ground motion indicates that response to this particular accelerogram is primarily a function of strength. For example, designs UBC-2.1 and UBC-1.4--which have essentially the same static strength (1851 kN vs. 1931 kN)--have essentially the same displacement response in spite of the fact that design UBC-2.1 is 12 percent more flexible than design UBC-1.4*.

Observations similar to those made above concerning the effect of initial flexibility and strength on global response may be made by analyzing the story drift index envelopes in Fig. 13.

It should be emphasized that the above discussion is based on initial dynamic characteristics. During the response, however, inelastic member behavior (plastic-hinge formation at member ends)--which is a function of strength and the forces generated by the ground motion--increases the frame flexibiltiy which, in turn, affects the magnitude of earthquake-induced

---

* As measured by the first-mode period.

forces and the level of response. Member inelastic behavior is discussed in a subsequent presentation of beam inelastic rotation demands.

A comparison of the displacement and story drift index envelopes for the DPD and EC ground motions indicates a significant difference in response in spite of the fact that the maximum acceleration was the same for both ground motion records. Story displacements and story drifts for the DPD ground motion are approximately three times those for the EC motion. This demonstrates the need to consider all possible ground motions at a given site and also all characteristics of these ground motions (not just the peak ground acceleration) when selecting a design earthquake [21].

The magnitude of the story drift indices recorded during the DPD ground motion (as high as 0.021) indicates the possibility of significant non-structural damage. A comparison of designs UBC-1.4 and I-1.4 demonstrates one advantage of using spectral design forces in seismic design for severe earthquake ground motions. Although spectral design forces were about 80 percent larger than the UBC forces, the required steel and concrete volume increased by less than 20 percent and 15 percent, respectively. These increases must be weighed against the resulting reduction in response (maximum story drift indices for design I-1.4 are approximately 25 percent smaller than those for design UBC-1.4) which can lead to significant savings in repair costs for nonstructural damage suffered during moderate and major earthquake ground motion.

A comparison of designs I-2.1 and I-1.4 indicates that the increase in frame stiffness and also strength associated with smaller steel content reduces drift indices and consequently nonstructural damage.

The story displacement and story drift index envelopes for designs

I-1.4, II-1.4, and III-1.4 are presented in Figs. 14 and 15. A comparison of responses for designs I-1.4 and III-1.4, which have the same beam sizes* but different beam design capacities at the interior beam-column joint (Tables 1 and 2), indicates that local variations in beam design capacities have little effect on global response parameters such as story displacement and story drift.

On the basis of the global response for designs I-1.4 and II-1.4, which have essentially the same static strength (Fig. 11) but different initial flexibilities, and in view of the previous discussion of behavior of designs UBC-2.1, UBC-1.4, I-1.4, and I-2.1, it may be concluded that initial frame flexibility (at least within the range considered here) has a significant influence on response to ground motions with characterisitics similar to the EC ground motion and that strength has a significant influence on response to ground motions with characteristics similar to the DPD ground motion. For example, consider the maximum roof displacement recorded for designs I-1.4 and II-1.4. In response to the EC ground motion, the roof displacement was 109 mm for design I-1.4 and 129 mm for design II-1.4, an increase of approximately 18 percent. In response to the DPD ground motion, the roof displacements were 369 mm for design I-1.4 and 379 mm for design II-1.4, an increase of less than 3 percent. This conclusion appears consistent with the different characteristics of the two ground motions (Fig. 16), in particular the long duration acceleration pulses contained in the initial phase of the DPD motion. The response of a structure to this type of ground motion is like the response to impulsive loading, at least with respect to maximum response quantities. In such a situation, and in case of nonlinear behavior, strength is a

* The beam size was controlled by the negative capacity at Section 1, which was the same in both designs.

more important parameter than flexibility. Furthermore, damping will have little effect on maximum response.

(ii) Local inelastic behavior, beams

Accumulated beam plastic rotation, θ_p^{acc}, defined by the expression

$$\theta_p^{acc} = \sum_{i-1}^{NIN} |\theta_p|_i \qquad (4.7)$$

where NIN is the total number of inelastic excursions at the beam end and $|\theta_p|_i$ is the absolute value of the plastic rotation in excursion i, is used as a measure of cyclic inelastic deformation demand. Values of θ_p^{acc} for the various designs in both the exterior and interior spans are summarized in Figs. 17-20. A comparison of response to the two ground motions indicates, as expected from the global response, that inelastic rotation demands increase significantly in response to the DPD ground motion.

A comparison of behavior for designs UBC-1.4, UBC-2.1, I-1.4, and I-2.1 (Figs. 17 and 18) indicates the following:

a. Inelastic rotation demands for the UBC designs are typically smaller in the upper stories than those corresponding to designs I-1.4 and I-2.1. This is attributed primarily to the larger overdesign of positive moment sections in the UBC designs discussed in Section 4.3.2.

b. A comparison of inelastic deformation demands for designs I-1.4 and I-2.1 indicate that demands in the exterior span are typically larger for design I-2.1 than for design I-1.4 and that the deformation demands reflect the opposite trend in the interior spans. This is attributed to the different nature of moment redistribution in the two designs. As noted previously

(Section 3.3), redistribution caused a reduction in negative design capacities in the exterior span in design I-2.1 and in the interior span in design I-1.4. This concentration of negative moment redistribution at a single section tends to amplify the inelastic rotation demands at that section. This is particularly evident in design I-2.1. In the interior span, where the negative design capacity is equal to the elastic value, the maximum θ_p^{acc} was 0.020 radians during the EC ground motion and 0.040 during the DPD ground motion. The respective values for the exterior span (where the redistribution was concentrated) were 0.030 and 0.055. This observation indicates that an optimum moment redistribution should attempt to balance the reduction in elastic design moments in order to prevent excessive deformation demands at a particular region (critical section).

c. The maximum inelastic deformation demands in response to the El Centro ground motion occurred in designs based on spectral design forces. For example, the maximum value of θ_p^{acc} for design I-2.1 in the exterior span was 0.030 radians while the corresponding value for design UBC-1.4 was 0.022 radians. This again reflects the effect of concentrating the negative moment redistribution at a particular section.

The inelastic deformation behavior observed for designs I-1.4, II-1.4, and III-1.4 (Figs. 19 and 20) indicate the following:

a. The moment redistribution associated with elimination of bar curtailment at the interior beam-column joint has only a minor effect on inelastic rotation demands except at floor level 7. A peak in

the θ_p^{acc} envelope is evident at this level in design III-1.4 and is attributed to the reduction of the positive moment capacity at section 3 from a value of 581 kN-m in design I-1.4 to 401 kN-m in design III-1.4.

b. Inelastic deformation demands in the exterior span for design II-1.4 are significantly larger than those for design I-1.4. Maximum θ_p^{acc} values are more than 70 percent larger in response to the EC ground motion and more than 20 percent larger in response to the DPD motion. The larger deformation demands in design II-1.4 is attributed to the degree of negative moment redistribution associated with this design (Table 1).

c. The relatively larger increase in inelastic deformation demand for design II-1.4 in response to the EC ground motion corresponds to the observed increase in global response parameters discussed earlier [Section 4.3.3(i)].

An important consideration in evaluating seismic inelastic deformations is whether or not the indicated demands are compatible with expected capacities of reinforced concrete beams. Based on the experimental results of several investigators [22,23], the required inelastic deformations in response to the EC ground motion are compatible with expected capacities. However, the magnitude of deformations recorded in response to the DPD ground motion may lead to severe structural damage and may result in structural failure if high nominal shear stresses ($V_u/b_w d$) are also present unless the transverse reinforcement is specifically designed and detailed to develop these deformations. This is especially true for UBC designs in which maximum plastic rotations of 0.02 radians and θ_p^{acc} values larger than 0.06 radians are required.

(iii) Local inelastic behavior, columns.

A final concern in evaluating nonlinear dynamic response is the adequacy of the imposed weak girder-strong column design criterion. The analytical results indicate that column yielding does not occur during response to the EC ground motion. However, the column curvature ductility data presented in Figs. 21-24 illustrates that column yielding (indicated by a curvature ductility larger than one) does occur at various locations through the height of the frame and at the foundation during response to the DPD motion. Column yielding is attributed in part to the increase in beam capacities due to strain hardening (a post yield slope of 3 percent was assumed in the moment-curvature relationship.) In addition, the distribution of beam moments between the column sections above and below a given joint was typically different from that assumed in design.

In design, the beam moments at a given joint were distributed to the columns at the joint on the basis of an elastic stiffness distribution factor [6]. However, higher mode response and formation of beam plastic hinges can alter the moment distribution at a joint to the extent that the sum of the beam capacities is resisted by only one of the columns at the joint.

Column ductilities presented in Fig. 21-24 indicate that column yielding occurs primarily at the top of interior columns. In most cases, columns experienced only one yield excursion and the maximum θ_p^{acc} values, excluding the column sections at the foundation level, varied from 0.001 radians in design ULC-2.1 to 0.003 radians in design III-1.4. At no time during the response of any design did the same column yield simultaneously at top and bottom. The recorded inelastic deformation demands are well within expected deformation capacities of ductile R/C columns [24].

Significant inelastic column response does occur in the column sections at the foundation level in all designs. Values of θ_p^{acc} varied from 0.004 radians in design I-2.1 to 0.017 radians in design UBC-1.4. These values reflect one major inelastic excursion and, at most, four minor excursions. For example, in design UBC-1.4, the maximum plastic rotation due to a positive excursion was 0.013 radians, and the θ_p^{acc} value of 0.017 radians was due to two negative excursions and one additional positive excursion. On the basis of recent experimental results [24], the indicated inelastic rotation demands may be attained if proper reinforcement details are provided.

4.4 Concluding Remarks

The nonlinear dynamic results discussed above do not include the effect of cyclic stiffness degradation--a common characteristic of the inelastic cyclic behavior of reinforced concrete members. It is hoped that the future development of accurate and relatively simple analytical models will enable the effect of this phenomenon on inelastic rotation demands and global-response parameters to be evaluated.

5. CONCLUSIONS AND RECOMMENDATIONS

In this chapter, conclusions are drawn from results presented in the body of the report. Recommendations are made for future investigations designed to clarify some of the questions raised by this study.

The inelastic seismic design procedure which formed the basis of this report enables the designer to consider essential features of the comprehensive design philosophy in a consistent manner. The design idealizations used to evaluate performance at serviceability, damageability, and ultimate limit design states reflect the expected behavior at these respective limit states.

For example, it is generally accepted that design for a severe earthquake ground motion is controlled by the ultimate limit state and significant inelastic behavior is expected. Current design practice, however, is typically based on minimum seismic design forces and the results of linear elastic analysis. Consequently, actual behavior and the behavior assumed in design are inconsistent.

In the proposed design procedure, actual and assumed behavior are based on the same limit state. Member design forces are determined by an inelastic design procedure which includes moment redistribution and which consequently takes advantage of the structure's capacity to dissipate energy through controlled inelastic deformations.

Some beam moment redistribution is possible following current ACI [9] and UBC [4] stipulations. Code-allowed redistribution is strictly intended for gravity load acting alone. It is felt, however, that its use is appropriate for seismic-resistant design in which a weak girder-strong column philosophy is followed.

It is felt that the inelastic design method proposed in this report provides a more realistic approach to moment redistribution in seismic-resistant design than the method defined in ACI. The coupling of practical and strength design requirements and the fact that all design capacities in a given story depend on each other--characteristics of the proposed method--typically result in a more efficient moment redistribution than that obtained employing the ACI method.

Previously it was concluded that the ACI limitation on magnitude of moment redistribution (MR) is conservative. The intent of this conclusion requires an explanation. The feature thought conservative is the dependency of MR on steel content. The reason for the dependency is to ensure sufficient inelastic deformation capacity to attain the expected redistribution. However, design of ductile moment resisting frames in accordance with present seismic code requirements should result in plastic hinge zones with sufficient deformation capacity to obtain most practical moment redistributions. Consequently, it is felt that in seismic-resistant design, MR need not depend on steel content.

It should be emphasized, however, that the upper bound of 20 percent imposed by ACI may not be conservative. The required deformation capacities for design II-1.4, in which MR values of 35 percent were typical, were significantly larger than those for design I-1.4 in which MR was typically less than 20 percent (except in the upper stories). A study is required to evaluate a practical upper bound on MR. Based on preliminary results for design B, it appears that because of the upper bound constraint

imposed on the positive capacity at a given section

$$M_i^+ \leq M_i^-$$

a moment redistribution greater than 20 percent (the maximum allowed by ACI) may result in an impractical design, particularly in the lower stories.

Although the current automated features of the proposed design procedure relieve the designer of a time consuming computational chore, further program development is warranted. The central feature of this development would be a design/analysis control language which would interface a series of design and analysis operations. The overall structure of the proposed program would maximize interaction between the designer and computer and minimize the data preparation necessary for this interaction.

The inelastic design results (designs II-1.4 through IV-1.4, and I-2.1) clearly demonstrate that consideration of realistic steel detailing results in an objective function which tends to maximize negative design capacities and minimize positive capacities. The resulting distribution of design capacities is contrary to what may be considered an optimum. Typically, in seismic-resistant design, it is desirable to reduce negative capacities in order to alleviate congestion of reinforcement at beam-column joints.

The results for design II-1.4 illustrate that by imposing proper design constraints a reduction in negative capacities can be achieved within the context of the proposed design procedure. Although significant negative moment redistribution was achieved in design II-1.4, the fact that the redistribution was concentrated at the interior beam-column joint resulted in relatively large inelastic deformation demands. This is undesirable.

An important conclusion with respect to the proposed optimum design model is that minimizing the volume of flexural reinforcement is not the

best criterion for selecting flexural steel distribution in a seismic-resistant reinforced concrete frame. The results for the various designs obtained in this study indicate that the volume of reinforcement is insensitive to variations in the distribution of beam design capacities. The design solution (required beam capacities) is bounded by equilibrium requirements and serviceability and practical constraints. Consequently, if one design capacity changes, an opposing change typically occurs at another section. The net result is that the total volume of reinforcement remains essentially the same.

In view of the above conclusions, it is apparent that the optimum design problem should be modified. As suggested earlier, one possible modification is to force a reduction in negative design capacities by decreasing the upper bound constraint on negative capacities to a value less than M_i^{-UE}. Except in the upper stories, such a constraint results in a uniform moment redistribution at each floor and throughout the height of the structure (Table 4). The consequence of this design modification on nonlinear dynamic response--in particular, on inelastic deformation demands--should be evaluated in the future.

Another possible modification is to formulate a new objective function. The results obtained in this study indicate that, although material quantities are relatively insensitive to beam design moment capacities, response parameters such as local inelastic deformation are sensitive to these capacities. However, it is difficult to formulate a function which relates inelastic rotations to beam design capacities.

One possibility is to formulate an objective function which would assign an equal weight to each beam design capacity. The appropriate form of the design solution would be achieved by imposing proper design constraints. Such a formulation has two advantages over the current

objective function. First, it would result in a linear programming problem. Consequently, the computational effort (by the computer) required to obtain beam design capacities would be reduced. In addition, the characteristics of the resulting design will be those which the designer deems appropriate for the given situation.

Another possible form for a new objective function is to assume that the positive and negative steel in a given span is constant. This assumption reduces the number of required beam design capacities (for the three-bay frame considered here from 8 to 4) and, also, results in a linear objective function which is easily evaluated. Consequently, the computational effort required to solve the optimization problem is reduced. With respect to practicality, this design assumption simplifies beam construction by eliminating bar curtailment.

One shortcoming of the constant steel assumption is that the required volume of flexural reinforcement increases. However, this increase must be weighed against the resulting benefits. Elimination of bar curtailment will reduce fabrication costs which may offset the increase in volume. In addition, as discussed in Ref. 25, inelastic deformation demands during severe earthquake excitations are reduced in a design found by assuming constant positive and negative beam steel.

A future study is required to investigate the relative merits of the objective functions described above with respect to required material volumes and inelastic behavior during earthquake excitation.

A comparison of the designs based on different seismic-force levels indicated that, although UBC design forces were approximately 50 percent smaller than the spectral design forces, the required material volumes differ by less than 20 percent. The increased material volumes for designs

based on spectral design forces must be weighed against the resulting benefits. Larger seismic design forces increase strength and stiffness. The increased stiffness will reduce response under both service and ultimate-load conditions. The increase in strength will provide greater safety and also reduce nonlinear response during extreme events such as severe earthquake ground shaking.

A comparison of global and local behavior in response to the two ground motions considered in this study demonstrates the difficult task confronting the structural engineer in selecting design earthquakes. The significantly larger response to the DPD ground motion indicates that all characteristics of possible ground motions at a given site must be defined, not just the peak ground acceleration.

A comparison of the behavior of the various designs considered here indicates that frame flexibility is an important system parameter affecting response to earthquake ground motions with characteristics similar to the EC motion. Frame strength, however, has a significant effect on response to ground motions with characteristics similar to the DPD (in particular, long-duration acceleration pulses). On the basis of this observation, it is evident that selection of appropriate seismic design criteria depends on proper characterization of possible ground motion excitations at the selected building site.

A comparison of designs I-1.4 and I-2.1 and designs UBC-1.4 and UBC-2.1 indicates that changes in required concrete and steel volume--which occur as a result of decreasing ρ_{max} from 2.1 percent to 1.4 percent--offset each other. However, the resulting increase in stiffness improves performance under service load conditions (by as much as 40 percent) as well as under severe seismic excitations with characteristics similar to the EC ground

motion. In addition, the larger seismic design forces associated with the stiffer frames increase strength and, consequently, improve response to ground motions with characteristics similar to the DPD motion.

The various design criteria imposed during member sizing caused the column sizes to be the same in all designs considered in this study. Basically, in order to satisfy the criterion that the design axial load be less than the balanced failure axial load, relatively large columns were required at ground level. In subsequent column sizing, this fact, in conjunction with the constraint on the increment in column depth (40 mm) and the constraint that the column size be the same for at least two stories, resulted in oversized columns. In other words, the column size was controlled by the design constraints enumerated above, and minimum steel requirements typically controlled reinforcement selection. Consequently, a factor of safety against column yielding (column overstrength factor) is built into the design.

This overstrength is in addition to an imposed factor of 1.2 and the fact that a capacity reduction factor of 0.7 is used in column design. Since unfactored beam and column capacities were used in subsequent nonlinear analyses, the columns have been overdesigned with respect to the beams by a factor of at least 1.7. This factor is typically larger because of oversized columns.

The results of nonlinear dynamic analysis indicate that the column overdesign discussed above may be excessive. Column yielding did not occur during response to the EC ground motion, and yielding in response to the DPD motion was limited.

It is felt that the current column design operation should be re-evaluated with the intent of optimizing column overstrength. In particular,

the current limitation on the level of axial force may be too stringent, and the consequences of relaxing this limitation should be explored. Park [26] has indicated that significant inelastic deformation can be developed in tied columns with axial force levels as high as $0.6\ f'_c\ A_g$ provided that the column transverse reinforcement is sufficient and properly detailed.

REFERENCES

[1] Bertero, V. V., and Bresler, B. "Failure Criteria (Limit States)," Panel Position Paper on Design and Engineering Decisions, preprint from the Sixth World Conference on Earthquake Engineering (6WCEE), New Delhi, India, January, 1977.

[2] Gasparini, D. A., and Vanmarcke, E. H. "Simulated Earthquake Motions Compatible with Prescribed Response Spectra," Department of Civil Engineering, Publication No. R76-4, Massachusetts Institute of Technology, Cambridge, January, 1976.

[3] Jennings, P. C., Housner, G. W., and Tsai, N. C. "Simulated Earthquake Motions," Earthquake Engineering Research Laboratory, California Institute of Technology, Pasadena, April, 1968.

[4] Uniform Building Code Standards (1976 Edition), International Conference of Building Officials, Whittier, California.

[5] Tentative Provisions for the Development of Seismic Regulations for Buildings, Applied Technology Council, Publication No. ATC-3-06, Palo Alto, California, 1978.

[6] Zagajeski, S. W., and Bertero, V. V. "Computer Aided Seismic-Resistant Design of Ductile Reinforced Concrete Frames," Earthquake Engineering Research Center, Report No. UCB/EERC-77/16, University of California, Berkeley, December, 1977.

[7] Kelley, J. E., "The Cutting Plane Method for Solving Convex Programs," Journal of the Society of Industrial Applied Mathematics, Vol. 8 (1960), pp. 703-712.

[8] Wolfe, P. "Accelerating the Cutting Plane Method for Nonlinear Programming," Journal of the Society of Industrial Applied Mathematics, Vol. 9 (September, 1961), pp. 481-488.

[9] Building Code Requirements for Reinforced Concrete, American Concrete Institute, ACI-318-77, Detroit, Michigan.

[10] Newmark, N. M. "Seismic Design Criteria for Structures and Facilities, Trans-Alaska Pipeline System," U. S. Conference on Earthquake Engineering, Ann Arbor, Michigan (1976), pp. 95-103.

[11] Zagajeski, S. W. and Bertero, V. V. "Application of Optimization Technique in Seismic-Resistant Design of Reinforced Concrete Multistory Frames," Journal of Structural Division, American Society of Civil Engineers, Vol. 105 (May, 1979), pp. 829-845.

[12] Skinner, A. J. Handbook for Earthquake-Generated Forces and Moments in Tall Buildings, Dominion Physics Laboratory, New Zealand, 1960.

[13] Applied Technology Council, "An Evaluation of a Response Spectrum Approach to Seismic Design of Buildings," A Study Report for the Center for Building Technology, Institute of Applied Technology, National Bureau of Standards, Washington, D. C., September, 1974.

[14] Pasta, E. "Sensitivity of Optimal Weight Design with Respect to Ways of Formulating the Objective Function," Division of Structural Engineering and Structural Mechanics, Graduate Student Report No. 697, University of California, Berkeley, June, 1978.

[15] Building Code Requirements for Reinforced Concrete, American Concrete Institute, ACI-318-71, Detroit, Michigan, 1971.

[16] Paulay, T. "Capacity Design of Reinforced Concrete Ductile Frames," Proceedings of Earthquake Resistant Reinforced Concrete Building Construction Workshop, Vol. III, Berkeley, California (July, 1977), pp. 1043-1075.

[17] Wilson, E. L., Hollings, J. P., and Dovey, H. H. "Three-Dimensional Analysis of Building Systems (Extended Version)," Earthquake Engineering Research Center, Report No. EERC 75-13, University of California, Berkeley, April, 1975.

[18] Mahin, S. A., and Bertero, V. V. "An Evaluation of Some Methods for Predicting Seismic Behavior of Reinforced Concrete Buildings," Earthquake Engineering Research Center, Report No. EERC 75-5, University of California, Berkeley, February, 1975

[19] Malik, L. E., and Bertero, V. V. "Contribution of a Floor System to the Dynamic Characteristics of Reinforced Concrete Buildings," Earthquake Engineering Research Center, Report No. EERC 76-30, University of California, Berkeley, December, 1976.

[20] Mahin, S. A., and Bertero, V. V. "Problems in Establishing and Predicting Ductility in Aseismic Design," Proceedings: International Symposium on Earthquake Structural Engineering, St. Louis, Missouri (August, 1976), pp. 613-628.

[21] Bertero, V. V. "Establishment of Design Earthquakes--Evaluation of Present Methods," Proceedings: International Symposium on Earthquake Structural Engineering, St. Louis, Missouri (August, 1976), pp. 551-580.

[22] Ma, S. M., Bertero, V. V., and Popov, E. P. "Experimental and Analytical Studies on the Hysteretic Behavior of Reinforced Concrete Rectangular and T-Beams," Earthquake Engineering Research Center, Report No. EERC 76-2, University of California, Berkeley, May, 1976.

[23] Bertero, V. V., Popov, E. P., and Wang, T. Y. "Hysteretic Behavior of Reinforced Concrete Members with Special Web Reinforcement," Earthquake Engineering Research Center, Report No. EERC 74-9, University of California, Berkeley, 1974.

[24] Zagajeski, S. W., Bertero, V. V., and Bouwkamp, J. G. "Hysteretic Behavior of Reinforced Concrete Columns Subjected to High Axial and Cyclic Shear Forces," Earthquake Engineering Research Center, Report No. UCB/EERC 78/05, University of California, Berkeley, April, 1978.

[25] Bertero, V. V., and Zagajeski, S. W., "Computer Aided Seismic-Resistant Design of Reinforced Concrete Multistory Frames," Proceedings of Sixth European Conference on Earthquake Engineering, Vol. II, Dubrovik, Yugoslavia (September, 1978), pp. 289-296.

[26] Park, R. "Columns Subjected to Flexure and Axial Load," New Zealand National Society for Earthquake Engineering, Bulletin No. 2 (June, 1977), pp. 95-101.

T A B L E S

TABLE 1 NEGATIVE BEAM DESIGN CAPACITIES

Floor Level	Section	Design Capacity/Results of Elastic Analysis				
		Design I-1.4	Design I-2.1	Design II-1.4	Design III-1.4	Design IV-1.4
Roof	1	1.10*	0.78	0.91	1.10*	1.10*
	3	0.81	0.68	0.68	1.05*	0.81
	4	0.63	0.68	0.65	0.63	0.63
10	1	1.00	0.78	0.90	1.00	1.00
	3	0.82	0.68	0.68	1.00	0.82
	4	0.63	0.68	0.65	0.64	0.63
9	1	1.00	0.79	0.91	1.00	1.00
	3	0.83	1.00	0.68	1.00	0.82
	4	0.74	0.68	0.65	0.70	0.63
8	1	1.00	0.79	0.91	1.00	1.00
	3	1.00	1.00	0.68	1.00	0.82
	4	0.74	0.87	0.65	0.73	0.63
7	1	1.00	0.78	0.91	1.00	1.00
	3	1.00	1.00	0.68	1.00	0.83
	4	0.74	0.90	0.65	0.74	0.63
6	1	1.00	0.79	0.91	1.00	1.00
	3	1.00	1.00	0.68	1.00	0.96
	4	0.84	1.00	0.65	0.77	0.63
5	1	1.00	0.86	0.91	1.00	1.00
	3	1.00	1.00	0.68	1.00	0.96
	4	0.84	1.00	0.65	0.79	0.63
4	1	1.00	0.87	0.91	1.00	1.00
	3	1.00	1.00	0.74	1.00	1.00
	4	0.87	1.00	0.65	0.83	0.63
3	1	1.00	0.87	0.91	1.00	1.00
	3	1.00	1.00	0.74	1.00	1.00
	4	0.87	1.00	0.65	0.87	0.63
2	1	1.00	0.95	0.91	1.00	1.00
	3	1.00	1.00	0.80	1.00	1.00
	4	0.94	1.00	0.65	0.95	0.75

*Design capacity controlled by ρ_{min}.

TABLE 2 POSITIVE BEAM DESIGN CAPACITIES

Floor Level	Section	Design Capacity/Results of Elastic Analysis				
		Design I-1.4	Design I-2.1	Design II-1.4	Design III-1.4	Design IV-1.4
Roof	1	7.22*	8.28*	6.15*	7.22*	7.22*
	3	-	-	-	-	-
	4	-	-	-	-	-
10	1	1.83*	1.77*	3.02*	1.83*	2.46*
	3	1.48*	1.40*	1.73	1.48*	1.51*
	4	1.61**	2.38**	3.06	1.61*	1.88
9	1	1.09*	1.00	1.96	1.09*	1.60*
	3	.98	1.04**	1.29	.98	1.13
	4	1.00**	1.20**	1.87	1.00**	1.28
8	1	0.97	0.84**	1.79	0.97	1.46
	3	1.21	0.91	1.16	1.01	1.01
	4	0.89**	1.31**	1.67	1.07**	1.14
7	1	0.89	0.74	1.65	1.27	1.34
	3	1.11	0.82	1.07	0.77	0.96
	4	0.79**	1.12**	1.47	0.79**	1.02
6	1	0.86	0.71	1.59	0.96	1.29
	3	1.11	0.79	1.04	0.99	1.07
	4	0.88**	1.18**	1.43	1.07**	0.99
5	1	0.81	0.74	1.49	0.86	1.21
	3	1.06	0.94	1.00	0.93	1.03
	4	0.82	1.14**	1.32	1.00	0.92
4	1	0.77	0.68	1.42	0.92	1.15
	3	1.25	0.79	1.08	0.96	1.23
	4	0.84	1.03**	1.29	1.08	0.91
3	1	0.78	0.77	1.34	0.84	1.09
	3	1.09	0.96	1.04	0.87	1.11
	4	0.80	1.02**	1.22	0.99	0.86
2	1	0.65	0.66	1.21	0.79	0.98
	3	1.26	1.03	1.17	0.91	1.07
	4	0.83	1.01**	1.19	1.07	1.00

*Design capacity controlled by ρ_{min}.

**Elastic moment is less than one-half the negative moment at that section.

TABLE 3 RATIO OF POSITIVE-TO-NEGATIVE DESIGN CAPACITY

Floor Level	Section	$\lvert M^+\rvert / \lvert M^-\rvert$				
		Design I-1.4	Design I-2.1	Design II-1.4	Design III-1.4	Design IV-1.4
Roof	1	1.00*	1.00*	1.00*	1.00*	1.00*
	3	1.00*	0.87*	1.00*	0.78*	1.00*
	4	0.78*	0.56*	1.00	-	0.78*
10	1	0.56*	0.56*	1.00	0.56*	0.75
	3	0.74*	0.69*	1.00	0.60	0.75
	4	0.60*	0.50	1.00	-	0.75
9	1	0.51*	0.53*	1.00	0.51*	0.75
	3	0.64*	0.50	1.00	0.53*	0.75
	4	0.50	0.50	1.00	-	0.75
8	1	0.50	0.50	1.00	0.50	0.75
	3	0.76	0.50	1.00	0.61	0.75
	4	0.50	0.50	1.00	-	0.75
7	1	0.50	0.50	1.00	0.71	0.75
	3	0.72	0.50	1.00	0.50	0.75
	4	0.50	0.50	1.00	-	0.75
6	1	0.50	0.50	1.00	0.56	0.75
	3	0.75	0.50	1.00	0.66	0.75
	4	0.50	0.50	1.00	-	0.75
5	1	0.50	0.50	1.00	0.54	0.75
	3	0.74	0.60	1.00	0.65	0.75
	4	0.50	0.50	1.00	-	0.75
4	1	0.50	0.50	1.00	0.60	0.75
	3	0.88	0.54	1.00	0.68	0.87
	4	0.50	0.50	1.00	-	0.75
3	1	0.54	0.58	1.00	0.58	0.75
	3	0.79	0.66	1.00	0.63	0.80
	4	0.50	0.50	1.00	-	0.75
2	1	0.50	0.50	1.00	0.61	0.75
	3	0.88	0.68	1.00	0.64	0.75
	4	0.50	0.50	1.00	-	0.75

*Positive design capacity controlled by ρ_{min}.

TABLE 4 COMPARISON OF NORMALIZED BEAM DESIGN CAPACITIES FOR DESIGNS BASED ON DIFFERENT UPPER BOUND CONSTRAINTS ON NEGATIVE DESIGN CAPACITIES

Floor Level	Design	Negative Section			Positive Section		
		1	2	3	1	2	3
Roof	A	1.10	.81	.63	7.22	-	-
	B	1.10	.81	.63	7.22	-	-
10	A	.56	.62	.76	1.83	1.48	1.61
	B	.56	.79	.66	1.83	1.48	1.61
9	A	.75	1.00	.78	1.09	.98	1.05
	B	.80	.80	.80	1.09	1.16	1.08
8	A	.74	1.00	1.00	.87	.82	1.21
	B	.80	.80	.80	1.15	1.32	1.14
7	A	.67	1.00	1.00	.89	.81	1.03
	B	.80	.80	.80	1.03	1.22	1.05
6	A	.81	1.00	1.00	.85	.95	1.05
	B	.80	.80	.80	1.13	1.19	1.27
5	A	.71	1.00	1.00	.73	1.09	.97
	B	.80	.80	.80	1.06	1.14	1.14
4	A	.87	1.00	1.00	.75	1.13	.96
	B	.80	.80	.80	1.14	1.13	1.36
3	A	.67	1.00	1.00	.64	1.36	.91
	B	.80	.80	.80	1.07	1.11	1.19
2	A	.96	1.00	1.00	.76	1.06	.88
	B	.80	.80	.80	1.05	1.14	1.39

TABLE 5 MEMBER SIZES

Floor Level	Columns*		Beams			
			Design			
	Exterior	Interior	UBC-2.1	UBC-1.4, I-2.1	II-1.4	I-1.4, III-1.4
	millimeters		millimeters			
Roof	520	680	320 × 640	360 × 720	380 × 760	400 × 800
10	560	720	340 × 680	360 × 720	380 × 760	400 × 800
9	560	720	340 × 680	380 × 760	400 × 800	420 × 840
8	600	760	360 × 720	380 × 760	400 × 800	420 × 840
7	600	760	360 × 720	400 × 800	420 × 840	440 × 880
6	640	800	380 × 760	400 × 800	420 × 840	440 × 880
5	640	800	380 × 760	400 × 800	440 × 880	460 × 920
4	680	840	380 × 760	420 × 840	440 × 880	460 × 920
3	680	840	380 × 760	420 × 840	460 × 920	480 × 960
2	720	880	380 × 760	420 × 840	460 × 920	480 × 960

*Columns are square.

TABLE 6 MATERIAL VOLUMES, m^3

Design	Flexural Steel	Concrete
UBC-2.1	2.09	126
UBC-1.4	1.91	136
I-2.1	2.31	136
I-1.4	2.26	153
II-1.4	2.31	146
III-1.4	2.27	153

TABLE 7 COMPARISON OF OBJECTIVE FUNCTION VALUES

Floor Level	$C(M_i)\ /C(M_i)_{I-1.4}$		
	Design I-1.4	Design III-1.4	Design IV-1.4
Roof	1.000	1.022	1.000
10	1.000	1.018	1.080
9	1.000	1.020	1.092
8	1.000	1.013	1.033
7	1.000	1.012	1.039
6	1.000	1.008	1.021
5	1.000	1.007	1.020
4	1.000	1.008	1.015
3	1.000	1.005	1.015
2	1.000	1.003	1.007

TABLE 8 FRAME PERIODS FOR FIRST FIVE MODES (IN SECONDS)

Design	Mode				
	1	2	3	4	5
UBC-2.1	1.386	.492	.276	.184	.132
UBC-1.4*	1.241	.441	.252	.170	.123
I-2.1*	1.241	.441	.252	.170	.123
I-1.4**	1.076	.385	.222	.152	.112
II-1.4	1.134	.406	.234	.159	.117
III-1.4**	1.076	.385	.222	.152	.112

*These designs have the same beam-column sizes.
**These designs have the same beam-column sizes.

F I G U R E S

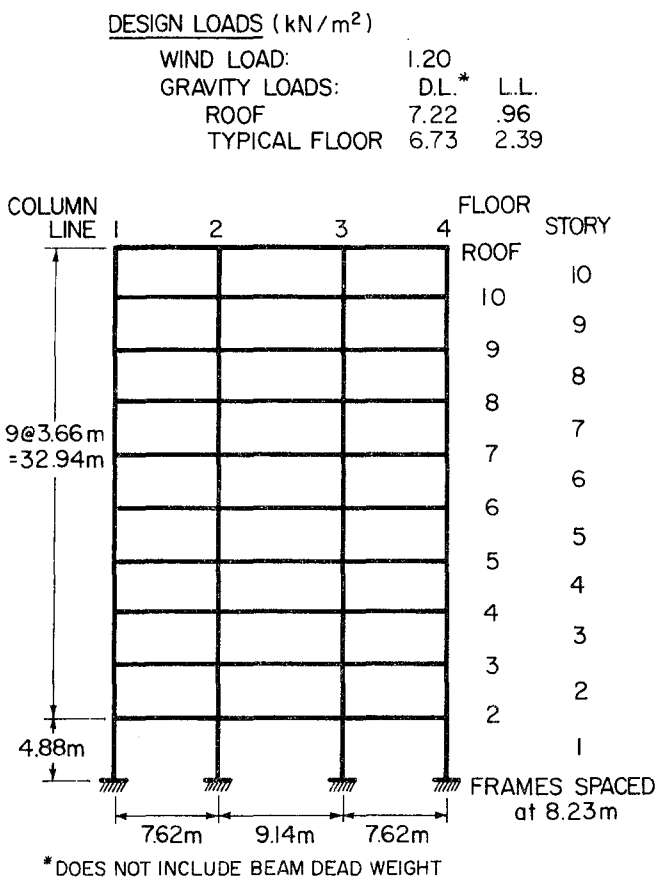

FIG. 1 DESIGN EXAMPLE

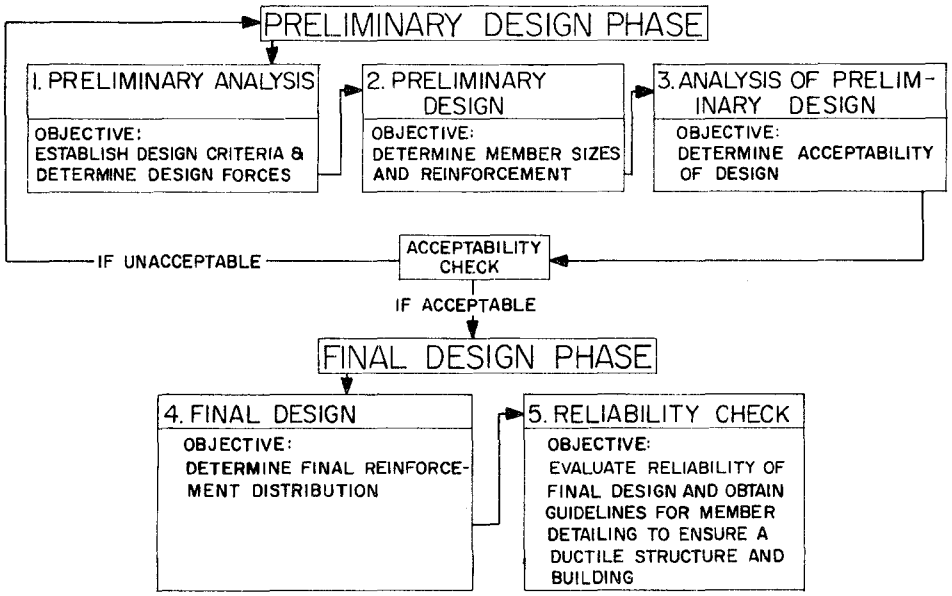

FIG. 2 FLOW CHART OF DESIGN PROCEDURE

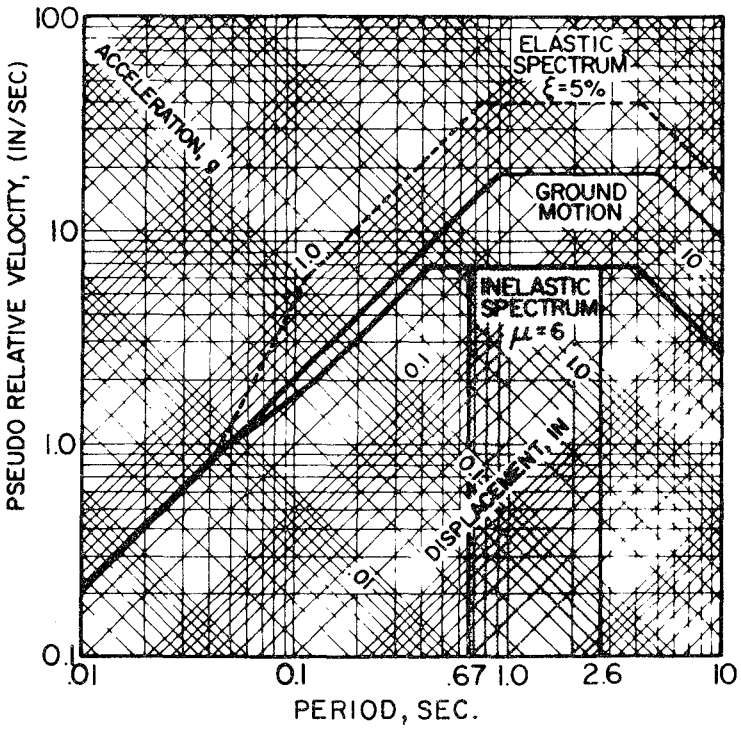

FIG. 3 DESIGN SPECTRA

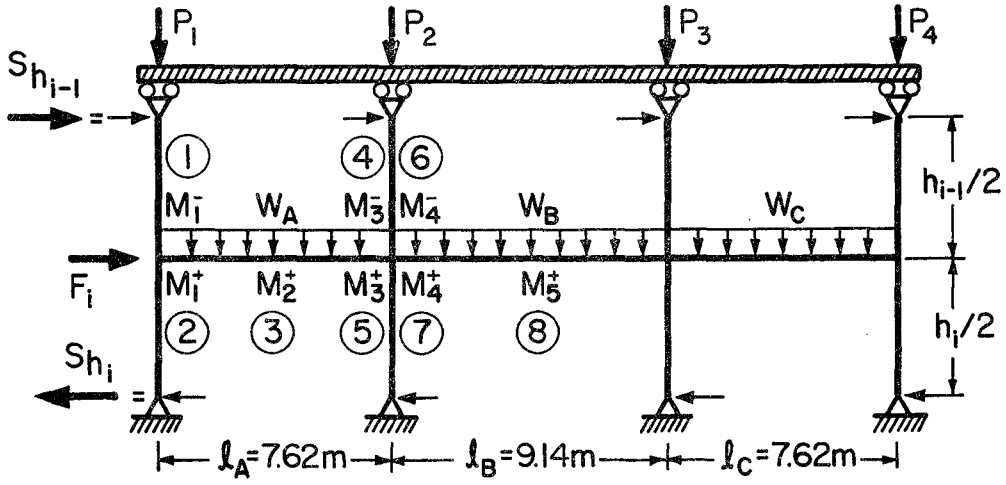

FIG. 4 SUBASSEMBLAGE FOR PRELIMINARY DESIGN

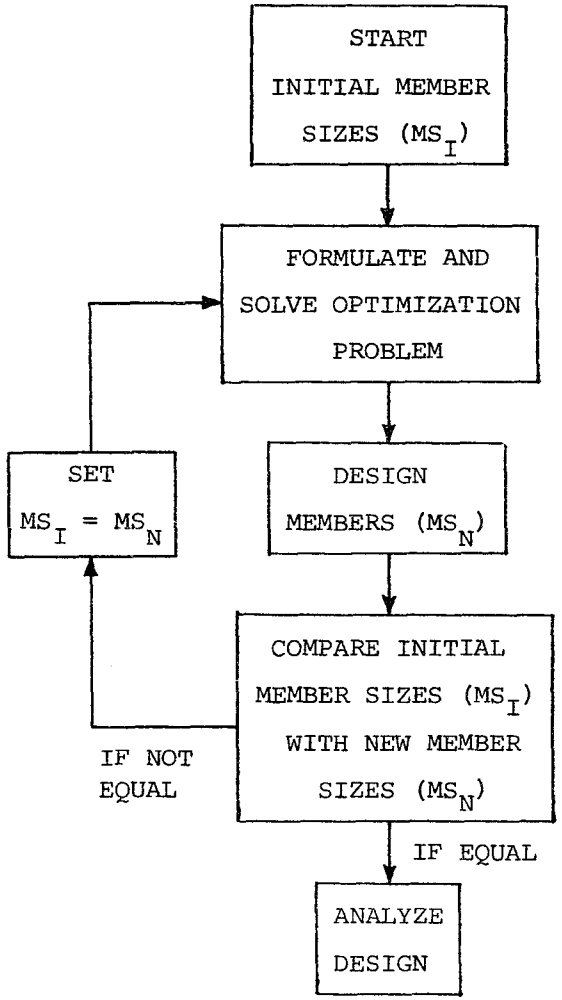

FIG. 5 ITERATIVE LOOP IN PRELIMINARY DESIGN STEP

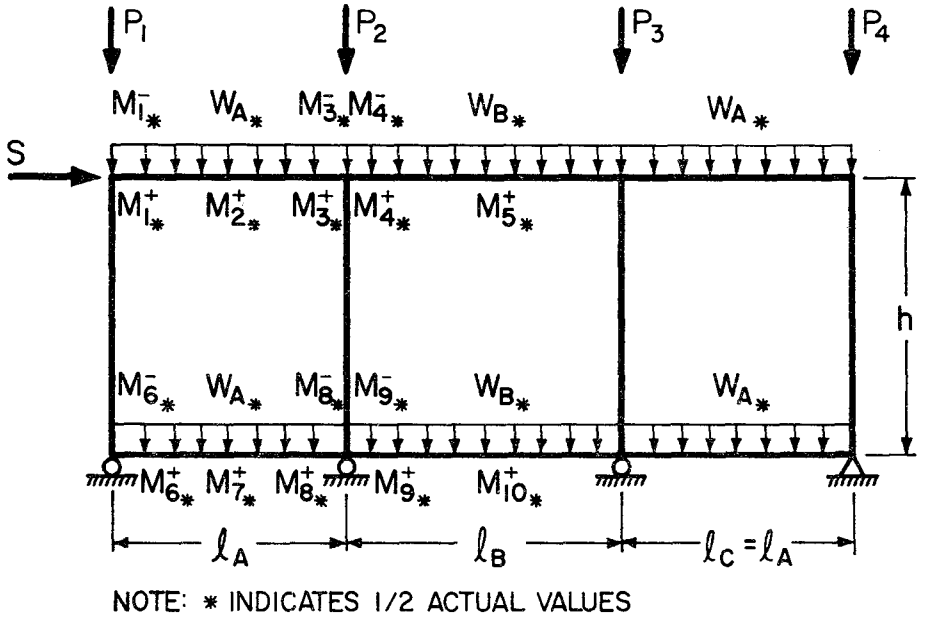

FIG. 6 FINAL DESIGN SUBASSEMBLAGE

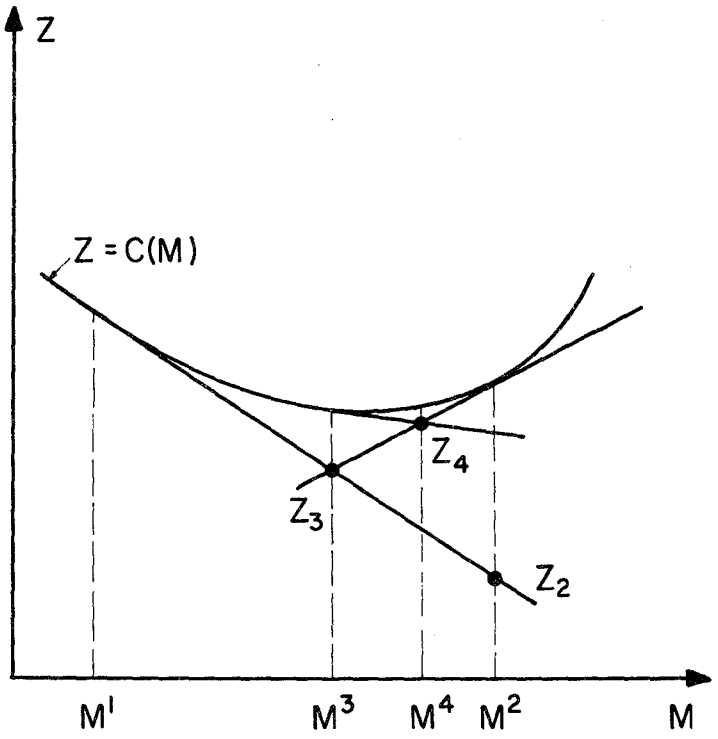

FIG. 7 EXAMPLE OF CUTTING PLANE METHOD

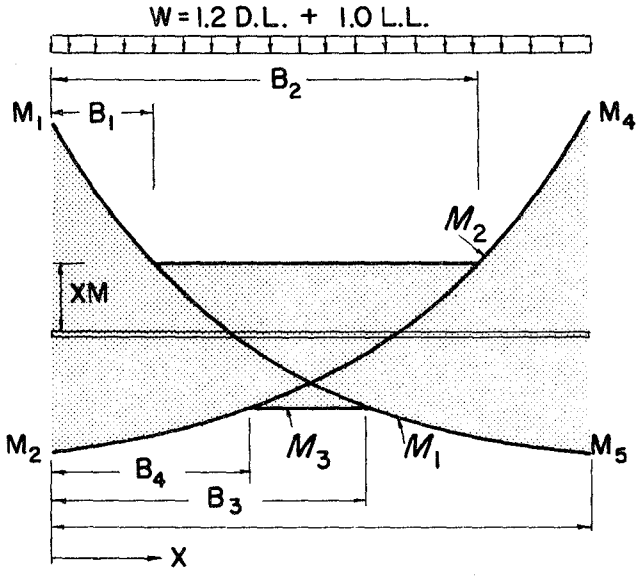

FIG. 8 TYPICAL DESIGN MOMENT ENVELOPE

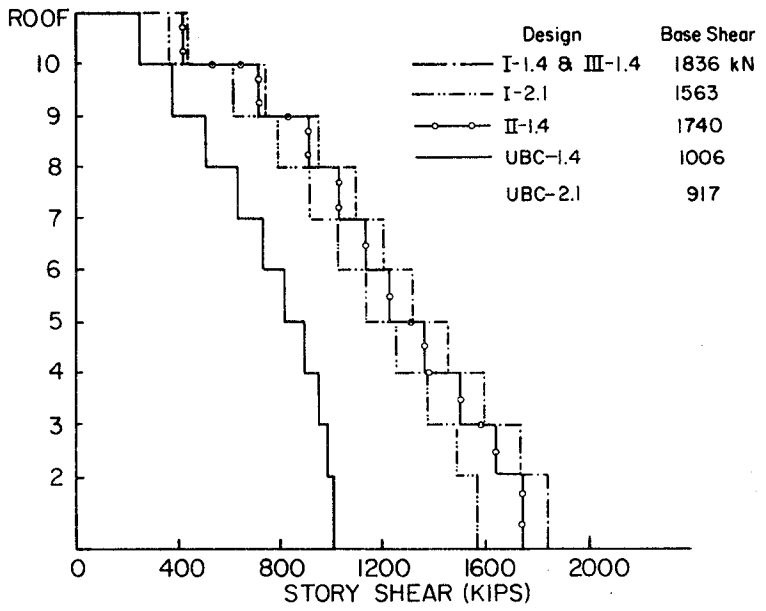

FIG. 9 COMPARISON OF SEISMIC DESIGN STORY SHEARS

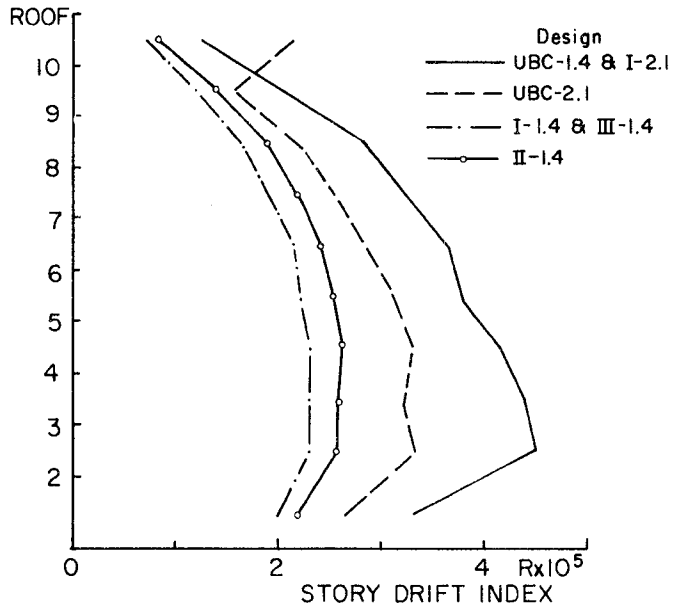

FIG. 10 STORY DRIFT INDEX DUE TO SERVICE LEVEL WIND LOAD

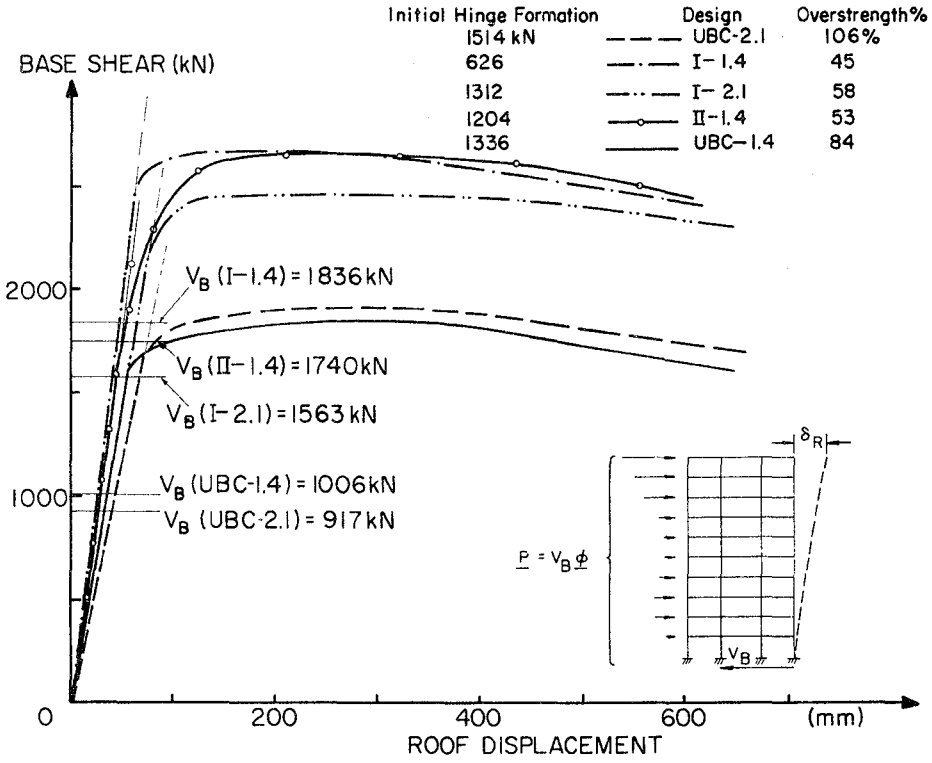

FIG. 11 COMPARISON OF NONLINEAR STATIC BEHAVIOR

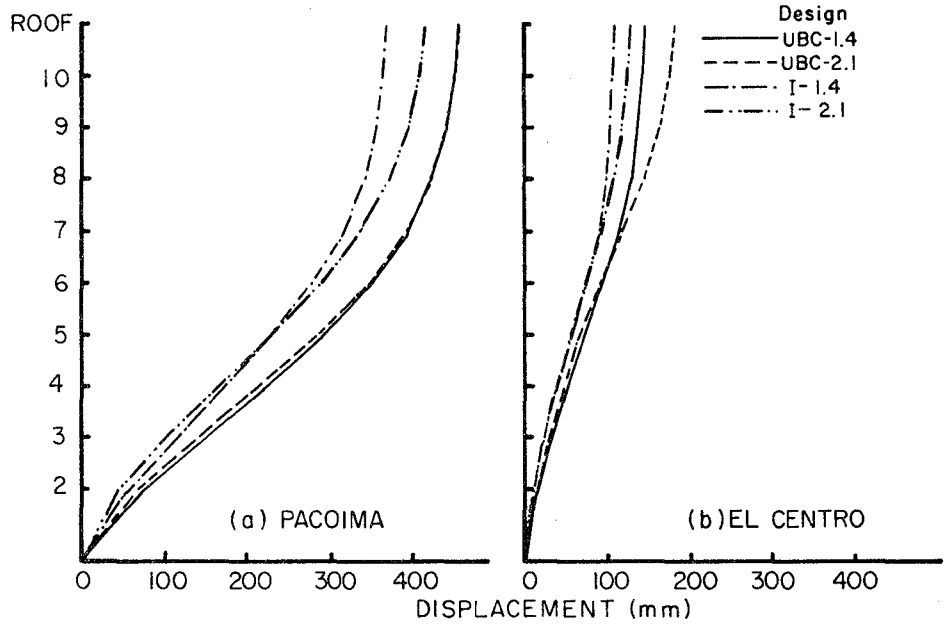

FIG. 12 STORY DISPLACEMENT ENVELOPES FOR DESIGNS UBC-1.4, UBC-2.1, I-1.4 AND I-2.1

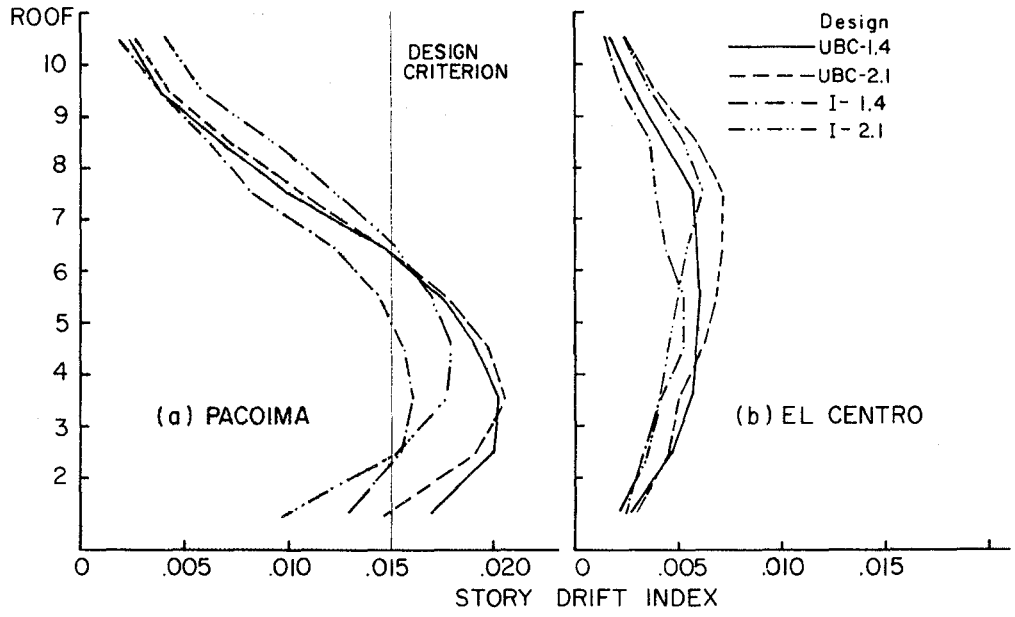

FIG. 13 STORY DRIFT ENVELOPES FOR DESIGNS UBC-1.4, UBC-2.1, I-1.4 AND I-2.1

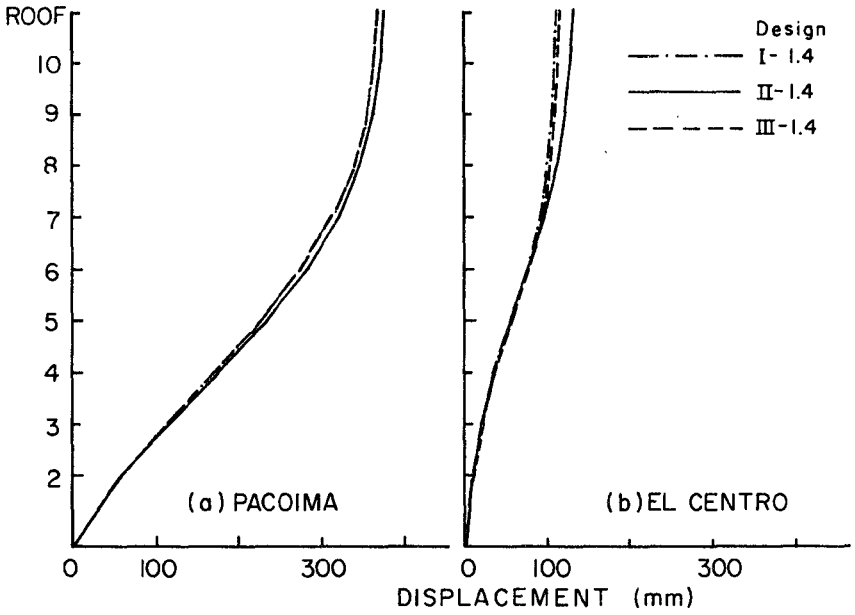

FIG. 14 STORY DISPLACEMENT ENVELOPES FOR DESIGNS I-1.4, II-1.4 AND III-1.4

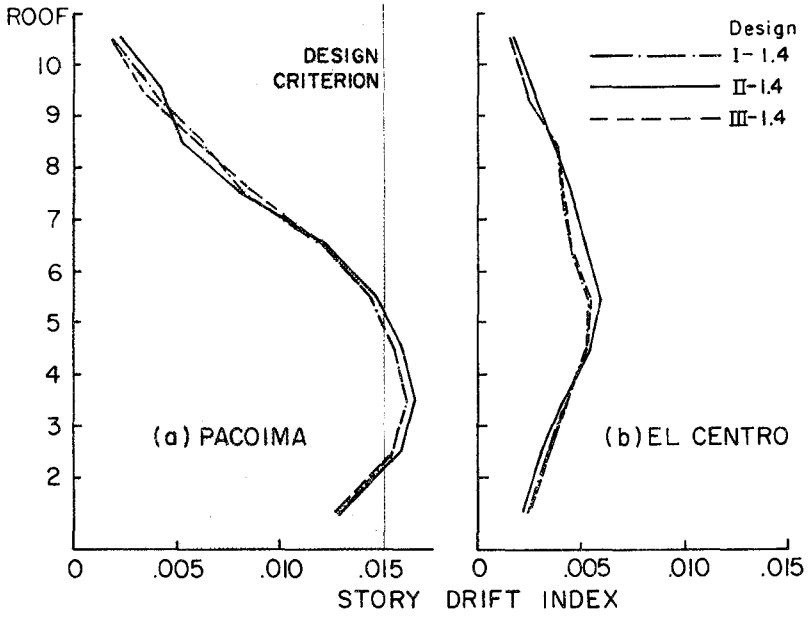

FIG. 15 STORY DRIFT ENVELOPES FOR DESIGNS I-1.4, II-1.4 AND III-1.4

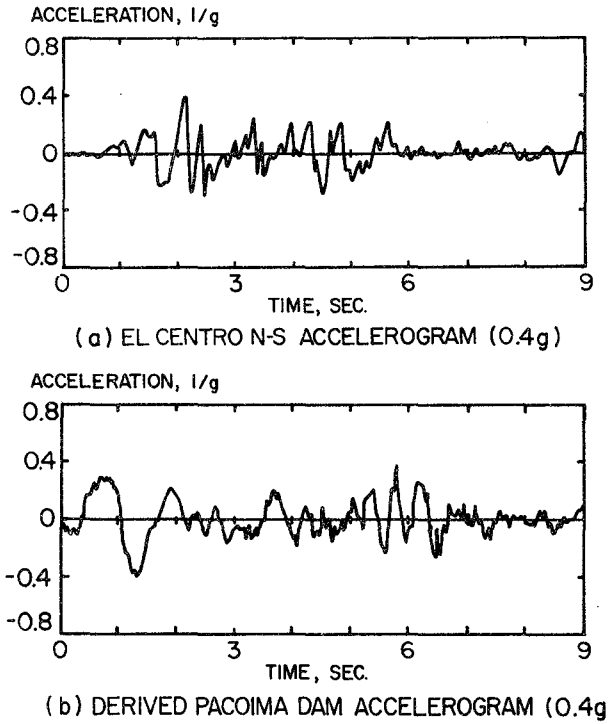

FIG. 16 COMPARISON OF EL CENTRO AND DERIVED PACOIMA DAM ACCELEROGRAMS

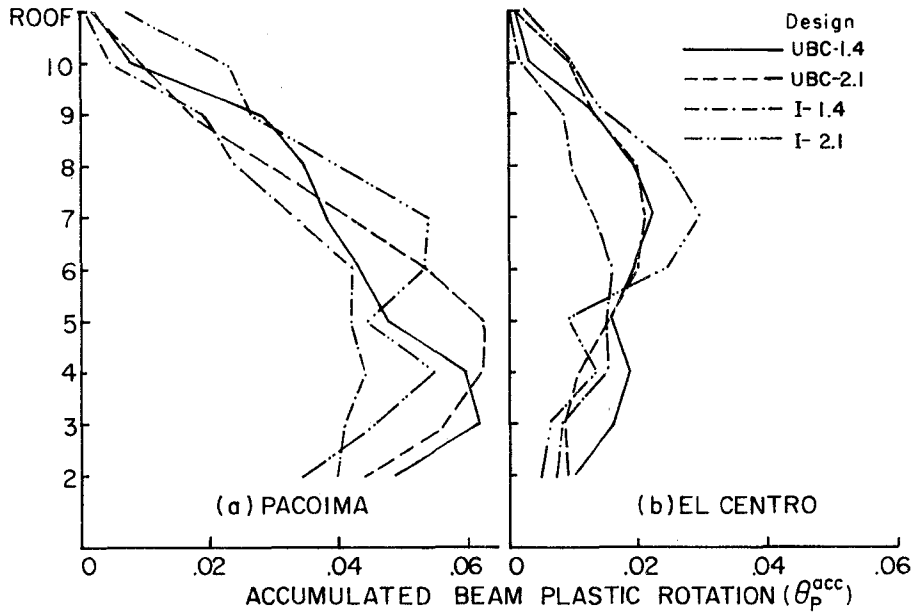

FIG. 17 ACCUMULATED BEAM PLASTIC ROTATIONS IN EXTERIOR SPAN FOR DESIGNS UBC-1.4, UBC-2.1, I-1.4 AND I-2.1

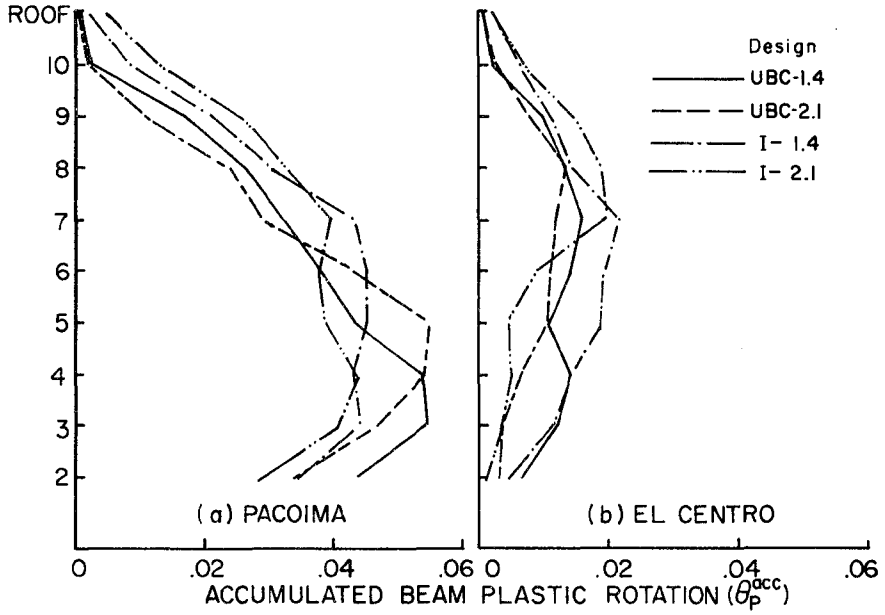

FIG. 18 ACCUMULATED BEAM PLASTIC ROTATIONS IN INTERIOR SPAN FOR DESIGNS UBC-1.4, UBC-2.1, I-1.4 AND I-2.1

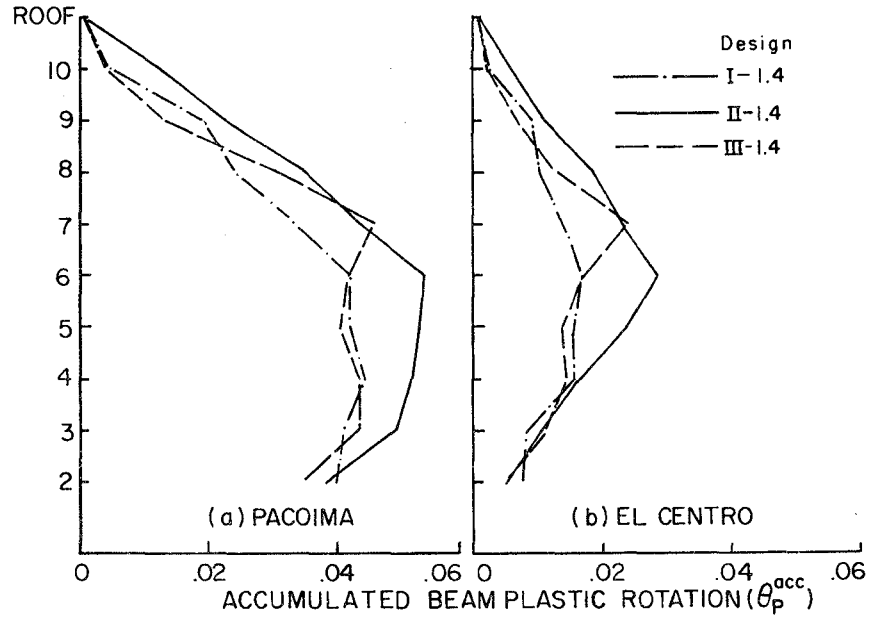

FIG. 19 ACCUMULATED BEAM PLASTIC ROTATIONS IN EXTERIOR SPAN FOR DESIGNS I-1.4, II-1.4 AND III-1.4

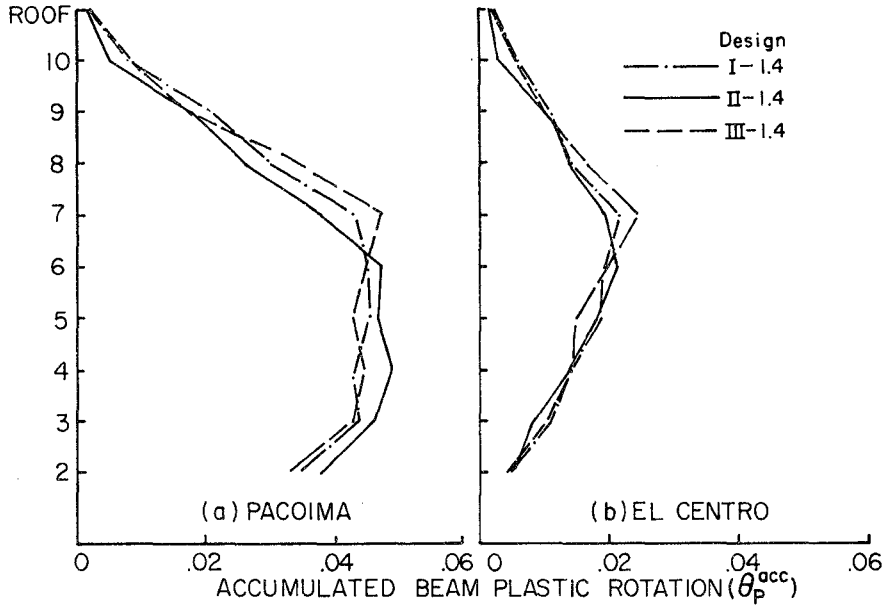

FIG. 20 ACCUMULATED BEAM PLASTIC ROTATIONS IN INTERIOR SPAN FOR DESIGNS I-1.4, II-1.4 AND III-1.4

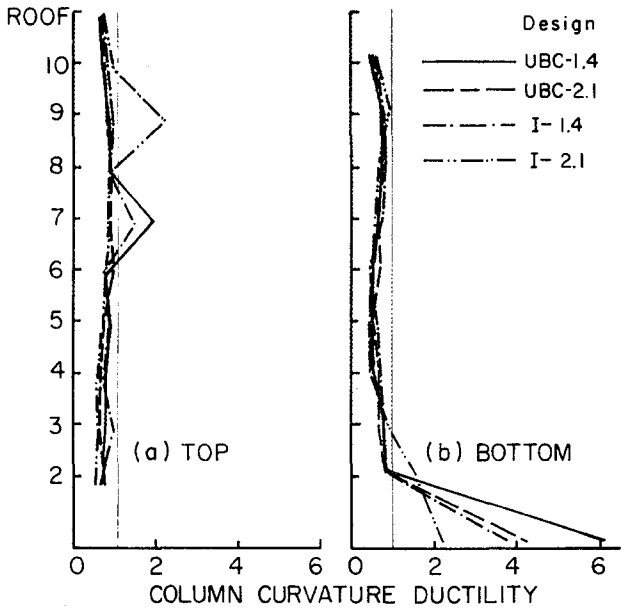

FIG. 21 EXTERIOR COLUMN CURVATURE DUCTILITIES DURING RESPONSE TO THE DERIVED PACOIMA DAM GROUND MOTION FOR DESIGNS UBC-1.4, UBC-2.1, I-1.4 AND I-2.1

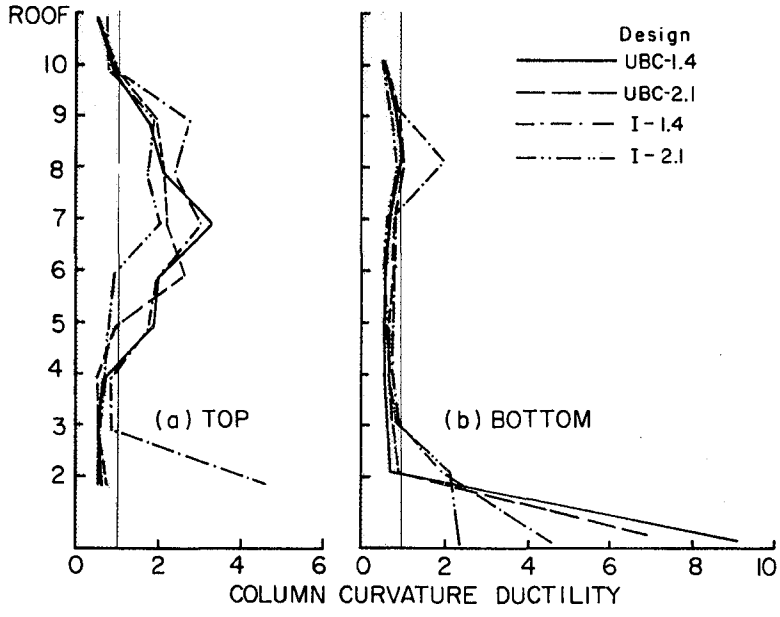

FIG. 22 INTERIOR COLUMN CURVATURE DUCTILITIES DURING RESPONSE TO THE DERIVED PACOIMA DAM GROUND MOTION FOR DESIGNS UBC-1.4, UBC-2.1, I-1.4 AND I-2.1

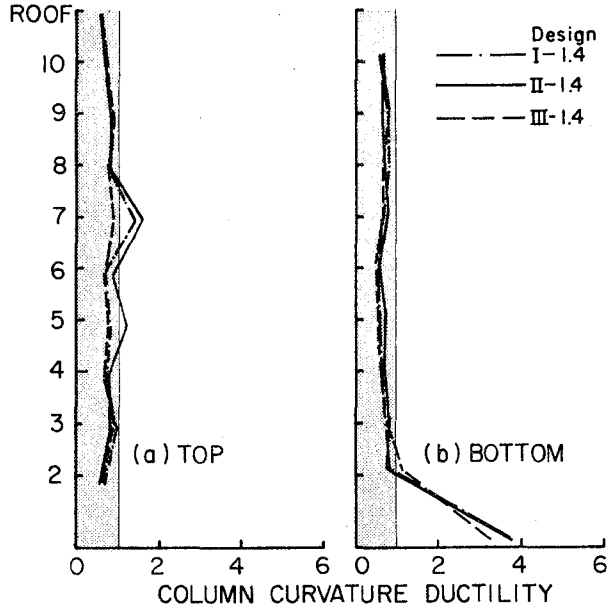

FIG. 23 EXTERIOR COLUMN CURVATURE DUCTILITIES DURING RESPONSE TO THE DERIVED PACOIMA DAM GROUND MOTION FOR DESIGNS I-1.4, II-1.4 AND III-1.4

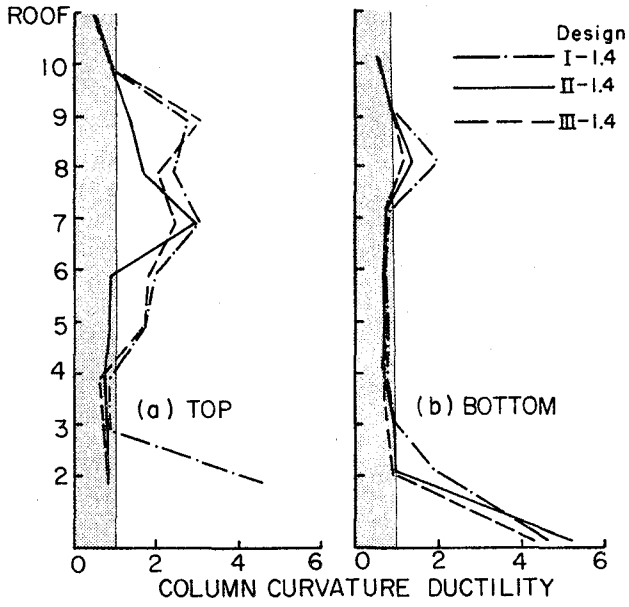

FIG. 24 INTERIOR COLUMN CURVATURE DUCTILITIES DURING RESPONSE TO THE DERIVED PACOIMA DAM GROUND MOTION FOR DESIGNS I-1.4, II-1.4 AND III-1.4

APPENDIX A

A.1 Numerical Example of Cutting Plane Algorithm

In order to illustrate the cutting plane algorithm described in Section 3.2, the following problem is solved here in detail.

Find $M_1, M_2 \geq 0$

which minimize $C(M_i) = 4M_1^2 + 3M_2^2$

and which satisfy the constraints

$$\begin{aligned} M_1 + 3M_2 &\geq 5 \\ 2M_1 + 0.5M_2 &\geq 2 \end{aligned} \tag{A.1}$$

In terms of the notation in equation (3.7):

$g_{11} = 1.0$ $\quad g_{12} = 3.0$ $\quad b_1 = 5.0$

$g_{21} = 2.0$ $\quad g_{22} = 0.5$ $\quad b_2 = 2.0$

$\nabla C_1(M_k^1) = 8M_1^1$ $\quad \nabla C_2(M_k^1) = 6M_2^1$

Assuming an initial solution, $M_i^1 = [3.0, 4.0]$,*
the constraint

$$Z - \nabla C_i(M_k^1) \geq C_1 \tag{A.2}$$

can be evaluated. First

$$C_1(M_k^1) = 8(3) = 24$$

and

$$C_2(M_k^1) = 6(4) = 24$$

Then

$$C_1 = C(M_k^1) - \nabla C_i(M_k^1)M_i^1 = 4(3)^2 + 3(4)^2 - 24(3) - 24(4)$$
$$= -84$$

The constraints for the first iteration (step 1) are:

$$\begin{bmatrix} 1.0 & 3.0 & 0 \\ 2.0 & 0.5 & 0 \\ -24. & -24. & 1.0 \end{bmatrix} \begin{Bmatrix} M_1 \\ M_2 \\ Z \end{Bmatrix} \geq \begin{Bmatrix} 5 \\ 2 \\ -84 \end{Bmatrix} \tag{A.3}$$

*This is an arbitrary choice. However, it does satisfy the constraints.

By employing a standard simplex algorithm, the solution to this linear problem is found to be

$$M_1^2 = 2.75 \qquad M_2^2 = 0.75 \qquad Z = 0$$

Evaluating a new inequality constraint based on the latest solution, M_i^2, we have

$$\nabla C_1(M_k^2) = 8(2.75) = 22$$

and

$$\nabla C_2(M_k^2) = 6(0.75) = 4.5$$

$$C_2 = 4(2.75)^2 + 3(.75)^2 - 22(2.75) - 4.5(.75)$$

$$= -31.94$$

and

$$-22M_1 - 4.5M_2 + Z \geq -31.94$$

This constraint is added to the three constraints defined by equation (A.3) and the resulting linear programming problem is solved. The solution is

$$M_1^3 = 1.192 \qquad M_2^3 = 1.269 \qquad Z = 0$$

The process described above is repeated for the new solution (M_i^3) and the following constraint is added:

$$-9.54M_1 - 7.61M_2 + Z \geq -10.52$$

The solution of the resulting linear programming problem is

$$M_1^4 = 0.636 \qquad M_2^4 = 1.45 \qquad Z = 6.63$$

After forming a new constraint, the solution of the resulting linear programming problem is the same as in the previous iteration, except that Z becomes 7.97, the minimum value of $C(M_i)$. Therefore, the optimum solution is:

$$M_1 = 0.636$$

$$M_2 = 1.45$$

A.2 Evaluation of the Gradient of $C(M_i)$

The cutting plane method is employed to solve the nonlinear optimization problem described in this report. In this method, the original problem of finding a vector of beam design capacities, M_i (i = 1, N) which minimizes

$$C(M_i) > 0 \qquad (A.4)$$

and which satisfies the linear constraints

$$g_{ji} M_i \geq b_j \quad (j = 1, NC) \tag{A.5}$$

is replaced by the equivalent problem of minimizing a new variable, Z, such that

$$\begin{aligned} Z &\geq C(M_i) \\ g_{ji} M_i &\geq b_j \end{aligned} \tag{A.6}$$

The nonlinear constraint in equation (A.6) is linearized by the Taylor series approximation

$$Z \geq C(M_k^t) + \nabla C(M_k^t)(M_i - M_i^t) \tag{A.7}$$

where $M_i^t(M_k^t)$ is the current solution. In order to evaluate this constraint, the gradient of the objective function, $C(M_i)$ is required.

The objective function can be separated into two parts:

$$C(M_i) = C_C(M_i) + C_B(M_i) \tag{A.8}$$

The term, $C_C(M_i)$, accounts for the column reinforcement. Since it is a linear function in M_i [6], a typical $\nabla C_{C_i}(M_k)$ is a constant equal to the coefficient of M_i in $C_C(M_i)$. The term, $C_B(M_i)$ accounts for the beam reinforcement. For the k*th* span, $C_B(M_i)$ is given by

$$\begin{aligned} [C_B(M_i)]_k = &-\int_0^{B_1} M_1(x, M_i)\,dx - \int_{B_2}^{L} M_2(x, M_i)\,dx + \int_{B_3}^{L} M_1(x, M_i)\,dx \\ &+\int_0^{B_4} M_2(x, M_i)\,dx + \int_{B_4}^{B_3} M_3\,dx + XM \cdot (B_2 - B_1) + F_A(M_i) \end{aligned} \tag{A.9}$$

where

$$M_i > 0 \qquad i = 1,5$$

$$M_1 = -M_1 + \frac{WLx}{2} + \frac{(M_1 + M_5)x}{L} - \frac{Wx^2}{2}$$

$$M_2 = M_2 + \frac{WLx}{2} - \frac{(M_2 + M_4)x}{L} - \frac{Wx^2}{2}$$

$$M_3 = M_3$$

$$W = 1.2 \text{ D.L.} + 1.0 \text{ L.L.}$$

$$XM = 1/4 \text{ MAX}(|M_1|, |M_4|)$$

$$B_1 = x \ @ \ M_1(x, M_i) = -XM$$

$$B_2 = x \ @ \ M_2(x, M_i) = -XM$$

$$B_3 = x \ @ \ M_1(x, M_i) = M_3$$

$$B_4 = x \ @ \ M_2(x, M_i) = M_3$$

and

$F_A(M_i)$ = A linear function in M_i which depends on the development length and column width.

As noted the function, $F_A(M_i)$, in equation (A.9) is linear in M_i. Consequently, as for $C_C(M_i)$, the gradient of $F_A(M_i)$ is a vector of constants and is ignored in the subsequent discussion. In addition, the function XM is considered a constant in order to prevent possible solution oscillation.*

*The function, XM, may be written as $1/4\ (|M_1|\delta_{1j} + |M_4|\delta_{4j})$ where

$\delta_{ij} = 1$ if $i = j$, and

$= 0$ if $i \neq j$.

If $|M_1| \geq |M_4|$, $j = 1$; if not, $j = 4$. In this form, XM is obviously discontinuous.

In expressing B_1 through B_4 in terms of M_i, it is convenient to define

$$\beta_1 = \frac{WL}{2} + \frac{(M_1 + M_5)}{L} \quad \text{and} \quad \beta_2 = \frac{WL}{2} - \frac{(M_2 + M_4)}{L} \tag{A.10}$$

Then

$$\begin{aligned} WB_1 &= -\beta_1 \pm \sqrt{\beta_1^2 + 2W(XM - M_1)} \\ WB_2 &= -\beta_2 \pm \sqrt{\beta_2^2 + 2W(M_2 + XM)} \\ WB_3 &= -\beta_1 \pm \sqrt{\beta_1^2 - 2W(M_1 + M_3)} \end{aligned} \tag{A.11}$$

and

$$WB_4 = -\beta_2 \pm \sqrt{\beta_2^2 + 2W(M_2 - M_3)}.$$

To facilitate differentiation of the integral terms of $C_B(M_i)$, Leibnitz's rule for differentiating a definite integral is employed. If

$$I(M,x) = \int_{L_1(M)}^{L_2(M)} F(M,x)dx \tag{A.12}$$

then

$$\frac{dI(M,x)}{dM} = \int_{L_1(M)}^{L_2(M)} \frac{\partial F(M,x)}{\partial x}\, dx + F(M,L_2)\, \frac{\partial L_2}{\partial M} - F(M,L_1)\, \frac{\partial L_1}{\partial M} \tag{A.13}$$

For a typical span, five coefficients are required to define the gradient vector

$$\nabla C_{B_i} = \frac{\partial C_B(M_k)}{\partial M_i} \qquad i = 1,5. \tag{A.14}$$

Applying Leibnitz's rule to the first six terms in equation (A.9), the following coefficients result:

$$\nabla C_{B_1} = \frac{\partial C_B(M_i)}{\partial M_1} = -\int_0^{B_1} \frac{\partial M_1}{\partial M_1}\,dx - M_1(B_1)\frac{\partial B_1}{\partial M_1} + \int_{B_3}^{L} \frac{\partial M_1}{\partial M_1}\,dx$$

$$- M_1(B_3)\frac{\partial B_3}{\partial M_1} - XM\frac{\partial B_1}{\partial M_1}$$

$$\nabla C_{B_2} = \frac{\partial C_B(M_i)}{\partial M_2} = \int_0^{B_4} \frac{\partial M_2}{\partial M_2}\,dx + M_2(B_4)\frac{\partial B_4}{\partial M_2} - \int_{B_2}^{L} \frac{\partial M_2}{\partial M_2}\,dx$$

$$+ M_2(B_2)\frac{\partial B_2}{\partial M_2} + XM\frac{\partial B_2}{\partial M_2}$$

$$\nabla C_{B_3} = \frac{\partial C_B(M_i)}{\partial M_3} = M_2(B_4)\frac{\partial B_4}{\partial M_3} - M_1(B_3)\frac{\partial B_3}{\partial M_3} + (B_3 - B_4) - M_3(B_4)\frac{\partial B_4}{\partial M_3}$$

$$+ M_3(B_3)\frac{\partial B_3}{\partial M_3}.$$

Since, by definition

$$M_2(B_4) = M_3(B_4)$$

$$M_1(B_3) = M_3(B_3)$$

$$\nabla C_{B_3} = B_3 - B_4$$

$$\nabla C_{B_4} = \frac{\partial C_B(M_i)}{\partial M_4} = \int_0^{B_4} \frac{\partial M_2}{\partial M_4}\,dx + M_2(B_4)\frac{\partial B_4}{\partial M_4} - \int_{B_2}^{L} \frac{\partial M_2}{\partial M_4}\,dx + M_2(B_2)\frac{\partial B_2}{\partial M_4} + XM\frac{\partial B_2}{\partial M_4}$$

(A.15)

$$\nabla C_{B_5} = \frac{\partial C_B(M_i)}{\partial M_5} = -\int_0^{B_1} \frac{\partial M_1}{\partial M_5}\, dx + M_1(B_1)\frac{\partial B_1}{\partial M_5} + \int_{B_3}^{L} \frac{\partial M_1}{\partial M_5}\, dx - M_1(B_3)\frac{\partial B_3}{\partial M_5} + XM\frac{\partial B_1}{\partial M_5}$$

The differentiation and integration indicated in equation (A.15) have been carried out explicitly prior to coding. For example,

$$\frac{\partial M_1(x,M_i)}{\partial M_1} = -1 + \frac{x}{L}$$

and

$$\int_0^{B_1} \left(\frac{x}{L} - 1\right) dx = \frac{B_1^2}{L} - B_1$$

The value of B_1 is that found for the current solution, M_k^t. In evaluating $\partial B_i/\partial M_k$ ($i = 1, 4$; $k = 1, 5$), the sign of the radical in equation (A.11) is taken to be the same as that used to find the values of B_1 through B_4 corresponding to the current solution M_k^t.

EARTHQUAKE ENGINEERING RESEARCH CENTER REPORTS

NOTE: Numbers in parenthesis are Accession Numbers assigned by the National Technical Information Service; these are followed by a price code. Copies of the reports may be ordered from the National Technical Information Service, 5285 Port Royal Road, Springfield, Virginia, 22161. Accession Numbers should be quoted on orders for reports (PB --- ---) and remittance must accompany each order. Reports without this information were not available at time of printing. Upon request, EERC will mail inquirers this information when it becomes available.

EERC 67-1 "Feasibility Study Large-Scale Earthquake Simulator Facility," by J. Penzien, J.G. Bouwkamp, R.W. Clough and D. Rea - 1967 (PB 187 905)A07

EERC 68-1 Unassigned

EERC 68-2 "Inelastic Behavior of Beam-to-Column Subassemblages Under Repeated Loading," by V.V. Bertero - 1968 (PB 184 888)A05

EERC 68-3 "A Graphical Method for Solving the Wave Reflection-Refraction Problem," by H.D. McNiven and Y. Mengi - 1968 (PB 187 943)A03

EERC 68-4 "Dynamic Properties of McKinley School Buildings," by D. Rea, J.G. Bouwkamp and R.W. Clough - 1968 (PB 187 902)A07

EERC 68-5 "Characteristics of Rock Motions During Earthquakes," by H.B. Seed, I.M. Idriss and F.W. Kiefer - 1968 (PB 188 338)A03

EERC 69-1 "Earthquake Engineering Research at Berkeley," - 1969 (PB 187 906)A11

EERC 69-2 "Nonlinear Seismic Response of Earth Structures," by M. Dibaj and J. Penzien - 1969 (PB 187 904)A08

EERC 69-3 "Probabilistic Study of the Behavior of Structures During Earthquakes," by R. Ruiz and J. Penzien - 1969 (PB 187 886)A06

EERC 69-4 "Numerical Solution of Boundary Value Problems in Structural Mechanics by Reduction to an Initial Value Formulation," by N. Distefano and J. Schujman - 1969 (PB 187 942)A02

EERC 69-5 "Dynamic Programming and the Solution of the Biharmonic Equation," by N. Distefano - 1969 (PB 187 941)A03

EERC 69-6 "Stochastic Analysis of Offshore Tower Structures," by A.K. Malhotra and J. Penzien - 1969 (PB 187 903)A09

EERC 69-7 "Rock Motion Accelerograms for High Magnitude Earthquakes," by H.B. Seed and I.M. Idriss - 1969 (PB 187 940)A02

EERC 69-8 "Structural Dynamics Testing Facilities at the University of California, Berkeley," by R.M. Stephen, J.G. Bouwkamp, R.W. Clough and J. Penzien - 1969 (PB 189 111)A04

EERC 69-9 "Seismic Response of Soil Deposits Underlain by Sloping Rock Boundaries," by H. Dezfulian and H.B. Seed 1969 (PB 189 114)A03

EERC 69-10 "Dynamic Stress Analysis of Axisymmetric Structures Under Arbitrary Loading," by S. Ghosh and E.L. Wilson 1969 (PB 189 026)A10

EERC 69-11 "Seismic Behavior of Multistory Frames Designed by Different Philosophies," by J.C. Anderson and V. V. Bertero - 1969 (PB 190 662)A10

EERC 69-12 "Stiffness Degradation of Reinforcing Concrete Members Subjected to Cyclic Flexural Moments," by V.V. Bertero, B. Bresler and H. Ming Liao - 1969 (PB 202 942)A07

EERC 69-13 "Response of Non-Uniform Soil Deposits to Travelling Seismic Waves," by H. Dezfulian and H.B. Seed - 1969 (PB 191 023)A03

EERC 69-14 "Damping Capacity of a Model Steel Structure," by D. Rea, R.W. Clough and J.G. Bouwkamp - 1969 (PB 190 663)A06

EERC 69-15 "Influence of Local Soil Conditions on Building Damage Potential during Earthquakes," by H.B. Seed and I.M. Idriss - 1969 (PB 191 036)A03

EERC 69-16 "The Behavior of Sands Under Seismic Loading Conditions," by M.L. Silver and H.B. Seed - 1969 (AD 714 982)A07

EERC 70-1 "Earthquake Response of Gravity Dams," by A.K. Chopra - 1970 (AD 709 640)A03

EERC 70-2 "Relationships between Soil Conditions and Building Damage in the Caracas Earthquake of July 29, 1967," by H.B. Seed, I.M. Idriss and H. Dezfulian - 1970 (PB 195 762)A05

EERC 70-3 "Cyclic Loading of Full Size Steel Connections," by E.P. Popov and R.M. Stephen - 1970 (PB 213 545)A04

EERC 70-4 "Seismic Analysis of the Charaima Building, Caraballeda, Venezuela," by Subcommittee of the SEAONC Research Committee: V.V. Bertero, P.F. Fratessa, S.A. Mahin, J.H. Sexton, A.C. Scordelis, E.L. Wilson, L.A. Wyllie, H.B. Seed and J. Penzien, Chairman - 1970 (PB 201 455)A06

EERC 70-5 "A Computer Program for Earthquake Analysis of Dams," by A.K. Chopra and P. Chakrabarti - 1970 (AD 723 994)A05

EERC 70-6 "The Propagation of Love Waves Across Non-Horizontally Layered Structures," by J. Lysmer and L.A. Drake 1970 (PB 197 896)A03

EERC 70-7 "Influence of Base Rock Characteristics on Ground Response," by J. Lysmer, H.B. Seed and P.B. Schnabel 1970 (PB 197 897)A03

EERC 70-8 "Applicability of Laboratory Test Procedures for Measuring Soil Liquefaction Characteristics under Cyclic Loading," by H.B. Seed and W.H. Peacock - 1970 (PB 198 016)A03

EERC 70-9 "A Simplified Procedure for Evaluating Soil Liquefaction Potential," by H.B. Seed and I.M. Idriss - 1970 (PB 198 009)A03

EERC 70-10 "Soil Moduli and Damping Factors for Dynamic Response Analysis," by H.B. Seed and I.M. Idriss - 1970 (PB 197 869)A03

EERC 71-1 "Koyna Earthquake of December 11, 1967 and the Performance of Koyna Dam," by A.K. Chopra and P. Chakrabarti 1971 (AD 731 496)A06

EERC 71-2 "Preliminary In-Situ Measurements of Anelastic Absorption in Soils Using a Prototype Earthquake Simulator," by R.D. Borcherdt and P.W. Rodgers - 1971 (PB 201 454)A03

EERC 71-3 "Static and Dynamic Analysis of Inelastic Frame Structures," by F.L. Porter and G.H. Powell - 1971 (PB 210 135)A06

EERC 71-4 "Research Needs in Limit Design of Reinforced Concrete Structures," by V.V. Bertero - 1971 (PB 202 943)A04

EERC 71-5 "Dynamic Behavior of a High-Rise Diagonally Braced Steel Building," by D. Rea, A.A. Shah and J.G. Bouwkamp 1971 (PB 203 584)A06

EERC 71-6 "Dynamic Stress Analysis of Porous Elastic Solids Saturated with Compressible Fluids," by J. Ghaboussi and E. L. Wilson - 1971 (PB 211 396)A06

EERC 71-7 "Inelastic Behavior of Steel Beam-to-Column Subassemblages," by H. Krawinkler, V.V. Bertero and E.P. Popov 1971 (PB 211 335)A14

EERC 71-8 "Modification of Seismograph Records for Effects of Local Soil Conditions," by P. Schnabel, H.B. Seed and J. Lysmer - 1971 (PB 214 450)A03

EERC 72-1 "Static and Earthquake Analysis of Three Dimensional Frame and Shear Wall Buildings," by E.L. Wilson and H.H. Dovey - 1972 (PB 212 904)A05

EERC 72-2 "Accelerations in Rock for Earthquakes in the Western United States," by P.B. Schnabel and H.B. Seed - 1972 (PB 213 100)A03

EERC 72-3 "Elastic-Plastic Earthquake Response of Soil-Building Systems," by T. Minami - 1972 (PB 214 868)A08

EERC 72-4 "Stochastic Inelastic Response of Offshore Towers to Strong Motion Earthquakes," by M.K. Kaul - 1972 (PB 215 713)A05

EERC 72-5 "Cyclic Behavior of Three Reinforced Concrete Flexural Members with High Shear," by E.P. Popov, V.V. Bertero and H. Krawinkler - 1972 (PB 214 555)A05

EERC 72-6 "Earthquake Response of Gravity Dams Including Reservoir Interaction Effects," by P. Chakrabarti and A.K. Chopra - 1972 (AD 762 330)A08

EERC 72-7 "Dynamic Properties of Pine Flat Dam," by D. Rea, C.Y. Liaw and A.K. Chopra - 1972 (AD 763 928)A05

EERC 72-8 "Three Dimensional Analysis of Building Systems," by E.L. Wilson and H.H. Dovey - 1972 (PB 222 438)A06

EERC 72-9 "Rate of Loading Effects on Uncracked and Repaired Reinforced Concrete Members," by S. Mahin, V.V. Bertero, D. Rea and M. Atalay - 1972 (PB 224 520)A08

EERC 72-10 "Computer Program for Static and Dynamic Analysis of Linear Structural Systems," by E.L. Wilson, K.-J. Bathe, J.E. Peterson and H.H.Dovey - 1972 (PB 220 437)A04

EERC 72-11 "Literature Survey - Seismic Effects on Highway Bridges," by T. Iwasaki, J. Penzien and R.W. Clough - 1972 (PB 215 613)A19

EERC 72-12 "SHAKE-A Computer Program for Earthquake Response Analysis of Horizontally Layered Sites," by P.B. Schnabel and J. Lysmer - 1972 (PB 220 207)A06

EERC 73-1 "Optimal Seismic Design of Multistory Frames," by V.V. Bertero and H. Kamil - 1973

EERC 73-2 "Analysis of the Slides in the San Fernando Dams During the Earthquake of February 9, 1971," by H.B. Seed, K.L. Lee, I.M. Idriss and F. Makdisi - 1973 (PB 223 402)A14

EERC 73-3 "Computer Aided Ultimate Load Design of Unbraced Multistory Steel Frames," by M.B. El-Hafez and G.H. Powell 1973 (PB 248 315)A09

EERC 73-4 "Experimental Investigation into the Seismic Behavior of Critical Regions of Reinforced Concrete Components as Influenced by Moment and Shear," by M. Celebi and J. Penzien - 1973 (PB 215 884)A09

EERC 73-5 "Hysteretic Behavior of Epoxy-Repaired Reinforced Concrete Beams," by M. Celebi and J. Penzien - 1973 (PB 239 568)A03

EERC 73-6 "General Purpose Computer Program for Inelastic Dynamic Response of Plane Structures," by A. Kanaan and G.H. Powell - 1973 (PB 221 260)A08

EERC 73-7 "A Computer Program for Earthquake Analysis of Gravity Dams Including Reservoir Interaction," by P. Chakrabarti and A.K. Chopra - 1973 (AD 766 271)A04

EERC 73-8 "Behavior of Reinforced Concrete Deep Beam-Column Subassemblages Under Cyclic Loads," by O. Küstü and J.G. Bouwkamp - 1973 (PB 246 117)A12

EERC 73-9 "Earthquake Analysis of Structure-Foundation Systems," by A.K. Vaish and A.K. Chopra - 1973 (AD 766 272)A07

EERC 73-10 "Deconvolution of Seismic Response for Linear Systems," by R.B. Reimer - 1973 (PB 227 179)A08

EERC 73-11 "SAP IV: A Structural Analysis Program for Static and Dynamic Response of Linear Systems," by K.-J. Bathe, E.L. Wilson and F.E. Peterson - 1973 (PB 221 967)A09

EERC 73-12 "Analytical Investigations of the Seismic Response of Long, Multiple Span Highway Bridges," by W.S. Tseng and J. Penzien - 1973 (PB 227 816)A10

EERC 73-13 "Earthquake Analysis of Multi-Story Buildings Including Foundation Interaction," by A.K. Chopra and J.A. Gutierrez - 1973 (PB 222 970)A03

EERC 73-14 "ADAP: A Computer Program for Static and Dynamic Analysis of Arch Dams," by R.W. Clough, J.M. Raphael and S. Mojtahedi - 1973 (PB 223 763)A09

EERC 73-15 "Cyclic Plastic Analysis of Structural Steel Joints," by R.B. Pinkney and R.W. Clough - 1973 (PB 226 843)A08

EERC 73-16 "QUAD-4: A Computer Program for Evaluating the Seismic Response of Soil Structures by Variable Damping Finite Element Procedures," by I.M. Idriss, J. Lysmer, R. Hwang and H.B. Seed - 1973 (PB 229 424)A05

EERC 73-17 "Dynamic Behavior of a Multi-Story Pyramid Shaped Building," by R.M. Stephen, J.P. Hollings and J.G. Bouwkamp - 1973 (PB 240 718)A06

EERC 73-18 "Effect of Different Types of Reinforcing on Seismic Behavior of Short Concrete Columns," by V.V. Bertero, J. Hollings, O. Küstü, R.M. Stephen and J.G. Bouwkamp - 1973

EERC 73-19 "Olive View Medical Center Materials Studies, Phase I," by B. Bresler and V.V. Bertero - 1973 (PB 235 986)A06

EERC 73-20 "Linear and Nonlinear Seismic Analysis Computer Programs for Long Multiple-Span Highway Bridges," by W.S. Tseng and J. Penzien - 1973

EERC 73-21 "Constitutive Models for Cyclic Plastic Deformation of Engineering Materials," by J.M. Kelly and P.P. Gillis 1973 (PB 226 024)A03

EERC 73-22 "DRAIN - 2D User's Guide," by G.H. Powell - 1973 (PB 227 016)A05

EERC 73-23 "Earthquake Engineering at Berkeley - 1973," (PB 226 033)A11

EERC 73-24 Unassigned

EERC 73-25 "Earthquake Response of Axisymmetric Tower Structures Surrounded by Water," by C.Y. Liaw and A.K. Chopra 1973 (AD 773 052)A09

EERC 73-26 "Investigation of the Failures of the Olive View Stairtowers During the San Fernando Earthquake and Their Implications on Seismic Design," by V.V. Bertero and R.G. Collins - 1973 (PB 235 106)A13

EERC 73-27 "Further Studies on Seismic Behavior of Steel Beam-Column Subassemblages," by V.V. Bertero, H. Krawinkler and E.P. Popov - 1973 (PB 234 172)A06

EERC 74-1 "Seismic Risk Analysis," by C.S. Oliveira - 1974 (PB 235 920)A06

EERC 74-2 "Settlement and Liquefaction of Sands Under Multi-Directional Shaking," by R. Pyke, C.K. Chan and H.B. Seed 1974

EERC 74-3 "Optimum Design of Earthquake Resistant Shear Buildings," by D. Ray, K.S. Pister and A.K. Chopra - 1974 (PB 231 172)A06

EERC 74-4 "LUSH - A Computer Program for Complex Response Analysis of Soil-Structure Systems," by J. Lysmer, T. Udaka, H.B. Seed and R. Hwang - 1974 (PB 236 796)A05

EERC 74-5 "Sensitivity Analysis for Hysteretic Dynamic Systems: Applications to Earthquake Engineering," by D. Ray 1974 (PB 233 213)A06

EERC 74-6 "Soil Structure Interaction Analyses for Evaluating Seismic Response," by H.B. Seed, J. Lysmer and R. Hwang 1974 (PB 236 519)A04

EERC 74-7 Unassigned

EERC 74-8 "Shaking Table Tests of a Steel Frame - A Progress Report," by R.W. Clough and D. Tang - 1974 (PB 240 869)A03

EERC 74-9 "Hysteretic Behavior of Reinforced Concrete Flexural Members with Special Web Reinforcement," by V.V. Bertero, E.P. Popov and T.Y. Wang - 1974 (PB 236 797)A07

EERC 74-10 "Applications of Reliability-Based, Global Cost Optimization to Design of Earthquake Resistant Structures," by E. Vitiello and K.S. Pister - 1974 (PB 237 231)A06

EERC 74-11 "Liquefaction of Gravelly Soils Under Cyclic Loading Conditions," by R.T. Wong, H.B. Seed and C.K. Chan 1974 (PB 242 042)A03

EERC 74-12 "Site-Dependent Spectra for Earthquake-Resistant Design," by H.B. Seed, C. Ugas and J. Lysmer - 1974 (PB 240 953)A03

EERC 74-13 "Earthquake Simulator Study of a Reinforced Concrete Frame," by P. Hidalgo and R.W. Clough - 1974 (PB 241 944)A13

EERC 74-14 "Nonlinear Earthquake Response of Concrete Gravity Dams," by N. Pal - 1974 (AD/A 006 583)A06

EERC 74-15 "Modeling and Identification in Nonlinear Structural Dynamics - I. One Degree of Freedom Models," by N. Distefano and A. Rath - 1974 (PB 241 548)A06

EERC 75-1 "Determination of Seismic Design Criteria for the Dumbarton Bridge Replacement Structure, Vol. I: Description, Theory and Analytical Modeling of Bridge and Parameters," by F. Baron and S.-H. Pang - 1975 (PB 259 407)A15

EERC 75-2 "Determination of Seismic Design Criteria for the Dumbarton Bridge Replacement Structure, Vol. II: Numerical Studies and Establishment of Seismic Design Criteria," by F. Baron and S.-H. Pang - 1975 (PB 259 408)A11 (For set of EERC 75-1 and 75-2 (PB 259 406))

EERC 75-3 "Seismic Risk Analysis for a Site and a Metropolitan Area," by C.S. Oliveira - 1975 (PB 248 134)A09

EERC 75-4 "Analytical Investigations of Seismic Response of Short, Single or Multiple-Span Highway Bridges," by M.-C. Chen and J. Penzien - 1975 (PB 241 454)A09

EERC 75-5 "An Evaluation of Some Methods for Predicting Seismic Behavior of Reinforced Concrete Buildings," by S.A. Mahin and V.V. Bertero - 1975 (PB 246 306)A16

EERC 75-6 "Earthquake Simulator Study of a Steel Frame Structure, Vol. I: Experimental Results," by R.W. Clough and D.T. Tang - 1975 (PB 243 981)A13

EERC 75-7 "Dynamic Properties of San Bernardino Intake Tower," by D. Rea, C.-Y. Liaw and A.K. Chopra - 1975 (AD/A008 406) A05

EERC 75-8 "Seismic Studies of the Articulation for the Dumbarton Bridge Replacement Structure, Vol. I: Description, Theory and Analytical Modeling of Bridge Components," by F. Baron and R.E. Hamati - 1975 (PB 251 539)A07

EERC 75-9 "Seismic Studies of the Articulation for the Dumbarton Bridge Replacement Structure, Vol. 2: Numerical Studies of Steel and Concrete Girder Alternates," by F. Baron and R.E. Hamati - 1975 (PB 251 540)A10

EERC 75-10 "Static and Dynamic Analysis of Nonlinear Structures," by D.P. Mondkar and G.H. Powell - 1975 (PB 242 434)A08

EERC 75-11 "Hysteretic Behavior of Steel Columns," by E.P. Popov, V.V. Bertero and S. Chandramouli - 1975 (PB 252 365)A11

EERC 75-12 "Earthquake Engineering Research Center Library Printed Catalog," - 1975 (PB 243 711)A26

EERC 75-13 "Three Dimensional Analysis of Building Systems (Extended Version)," by E.L. Wilson, J.P. Hollings and H.H. Dovey - 1975 (PB 243 989)A07

EERC 75-14 "Determination of Soil Liquefaction Characteristics by Large-Scale Laboratory Tests," by P. De Alba, C.K. Chan and H.B. Seed - 1975 (NUREG 0027)A08

EERC 75-15 "A Literature Survey - Compressive, Tensile, Bond and Shear Strength of Masonry," by R.L. Mayes and R.W. Clough - 1975 (PB 246 292)A10

EERC 75-16 "Hysteretic Behavior of Ductile Moment Resisting Reinforced Concrete Frame Components," by V.V. Bertero and E.P. Popov - 1975 (PB 246 388)A05

EERC 75-17 "Relationships Between Maximum Acceleration, Maximum Velocity, Distance from Source, Local Site Conditions for Moderately Strong Earthquakes," by H.B. Seed, R. Murarka, J. Lysmer and I.M. Idriss - 1975 (PB 248 172)A03

EERC 75-18 "The Effects of Method of Sample Preparation on the Cyclic Stress-Strain Behavior of Sands," by J. Mulilis, C.K. Chan and H.B. Seed - 1975 (Summarized in EERC 75-28)

EERC 75-19 "The Seismic Behavior of Critical Regions of Reinforced Concrete Components as Influenced by Moment, Shear and Axial Force," by M.B. Atalay and J. Penzien - 1975 (PB 258 842)A11

EERC 75-20 "Dynamic Properties of an Eleven Story Masonry Building," by R.M. Stephen, J.P. Hollings, J.G. Bouwkamp and D. Jurukovski - 1975 (PB 246 945)A04

EERC 75-21 "State-of-the-Art in Seismic Strength of Masonry - An Evaluation and Review," by R.L. Mayes and R.W. Clough 1975 (PB 249 040)A07

EERC 75-22 "Frequency Dependent Stiffness Matrices for Viscoelastic Half-Plane Foundations," by A.K. Chopra, P. Chakrabarti and G. Dasgupta - 1975 (PB 248 121)A07

EERC 75-23 "Hysteretic Behavior of Reinforced Concrete Framed Walls," by T.Y. Wong, V.V. Bertero and E.P. Popov - 1975

EERC 75-24 "Testing Facility for Subassemblages of Frame-Wall Structural Systems," by V.V. Bertero, E.P. Popov and T. Endo - 1975

EERC 75-25 "Influence of Seismic History on the Liquefaction Characteristics of Sands," by H.B. Seed, K. Mori and C.K. Chan - 1975 (Summarized in EERC 75-28)

EERC 75-26 "The Generation and Dissipation of Pore Water Pressures during Soil Liquefaction," by H.B. Seed, P.P. Martin and J. Lysmer - 1975 (PB 252 648)A03

EERC 75-27 "Identification of Research Needs for Improving Aseismic Design of Building Structures," by V.V. Bertero 1975 (PB 248 136)A05

EERC 75-28 "Evaluation of Soil Liquefaction Potential during Earthquakes," by H.B. Seed, I. Arango and C.K. Chan - 1975 (NUREG 0026)A13

EERC 75-29 "Representation of Irregular Stress Time Histories by Equivalent Uniform Stress Series in Liquefaction Analyses," by H.B. Seed, I.M. Idriss, F. Makdisi and N. Banerjee - 1975 (PB 252 635)A03

EERC 75-30 "FLUSH - A Computer Program for Approximate 3-D Analysis of Soil-Structure Interaction Problems," by J. Lysmer, T. Udaka, C.-F. Tsai and H.B. Seed - 1975 (PB 259 332)A07

EERC 75-31 "ALUSH - A Computer Program for Seismic Response Analysis of Axisymmetric Soil-Structure Systems," by E. Berger, J. Lysmer and H.B. Seed - 1975

EERC 75-32 "TRIP and TRAVEL - Computer Programs for Soil-Structure Interaction Analysis with Horizontally Travelling Waves," by T. Udaka, J. Lysmer and H.B. Seed - 1975

EERC 75-33 "Predicting the Performance of Structures in Regions of High Seismicity," by J. Penzien - 1975 (PB 248 130)A03

EERC 75-34 "Efficient Finite Element Analysis of Seismic Structure - Soil - Direction," by J. Lysmer, H.B. Seed, T. Udaka, R.N. Hwang and C.-F. Tsai - 1975 (PB 253 570)A03

EERC 75-35 "The Dynamic Behavior of a First Story Girder of a Three-Story Steel Frame Subjected to Earthquake Loading," by R.W. Clough and L.-Y. Li - 1975 (PB 248 841)A05

EERC 75-36 "Earthquake Simulator Study of a Steel Frame Structure, Volume II - Analytical Results," by D.T. Tang - 1975 (PB 252 926)A10

EERC 75-37 "ANSR-I General Purpose Computer Program for Analysis of Non-Linear Structural Response," by D.P. Mondkar and G.H. Powell - 1975 (PB 252 386)A08

EERC 75-38 "Nonlinear Response Spectra for Probabilistic Seismic Design and Damage Assessment of Reinforced Concrete Structures," by M. Murakami and J. Penzien - 1975 (PB 259 530)A05

EERC 75-39 "Study of a Method of Feasible Directions for Optimal Elastic Design of Frame Structures Subjected to Earthquake Loading," by N.D. Walker and K.S. Pister - 1975 (PB 257 761)A06

EERC 75-40 "An Alternative Representation of the Elastic-Viscoelastic Analogy," by G. Dasgupta and J.L. Sackman - 1975 (PB 252 173)A03

EERC 75-41 "Effect of Multi-Directional Shaking on Liquefaction of Sands," by H.B. Seed, R. Pyke and G.R. Martin - 1975 (PB 258 781)A03

EERC 76-1 "Strength and Ductility Evaluation of Existing Low-Rise Reinforced Concrete Buildings - Screening Method," by T. Okada and B. Bresler - 1976 (PB 257 906)A11

EERC 76-2 "Experimental and Analytical Studies on the Hysteretic Behavior of Reinforced Concrete Rectangular and T-Beams," by S.-Y.M. Ma, E.P. Popov and V.V. Bertero - 1976 (PB 260 843)A12

EERC 76-3 "Dynamic Behavior of a Multistory Triangular-Shaped Building," by J. Petrovski, R.M. Stephen, E. Gartenbaum and J.G. Bouwkamp - 1976 (PB 273 279)A07

EERC 76-4 "Earthquake Induced Deformations of Earth Dams," by N. Serff, H.B. Seed, F.I. Makdisi & C.-Y. Chang - 1976 (PB 292 065)A08

EERC 76-5 "Analysis and Design of Tube-Type Tall Building Structures," by H. de Clercq and G.H. Powell - 1976 (PB 252 220) A10

EERC 76-6 "Time and Frequency Domain Analysis of Three-Dimensional Ground Motions, San Fernando Earthquake," by T. Kubo and J. Penzien (PB 260 556)A11

EERC 76-7 "Expected Performance of Uniform Building Code Design Masonry Structures," by R.L. Mayes, Y. Omote, S.W. Chen and R.W. Clough - 1976 (PB 270 098)A05

EERC 76-8 "Cyclic Shear Tests of Masonry Piers, Volume 1 - Test Results," by R.L. Mayes, Y. Omote, R.W. Clough - 1976 (PB 264 424)A06

EERC 76-9 "A Substructure Method for Earthquake Analysis of Structure - Soil Interaction," by J.A. Gutierrez and A.K. Chopra - 1976 (PB 257 783)A08

EERC 76-10 "Stabilization of Potentially Liquefiable Sand Deposits using Gravel Drain Systems," by H.B. Seed and J.R. Booker - 1976 (PB 258 820)A04

EERC 76-11 "Influence of Design and Analysis Assumptions on Computed Inelastic Response of Moderately Tall Frames," by G.H. Powell and D.G. Row - 1976 (PB 271 409)A06

EERC 76-12 "Sensitivity Analysis for Hysteretic Dynamic Systems: Theory and Applications," by D. Ray, K.S. Pister and E. Polak - 1976 (PB 262 859)A04

EERC 76-13 "Coupled Lateral Torsional Response of Buildings to Ground Shaking," by C.L. Kan and A.K. Chopra - 1976 (PB 257 907)A09

EERC 76-14 "Seismic Analyses of the Banco de America," by V.V. Bertero, S.A. Mahin and J.A. Hollings - 1976

EERC 76-15 "Reinforced Concrete Frame 2: Seismic Testing and Analytical Correlation," by R.W. Clough and J. Gidwani - 1976 (PB 261 323)A08

EERC 76-16 "Cyclic Shear Tests of Masonry Piers, Volume 2 - Analysis of Test Results," by R.L. Mayes, Y. Omote and R.W. Clough - 1976

EERC 76-17 "Structural Steel Bracing Systems: Behavior Under Cyclic Loading," by E.P. Popov, K. Takanashi and C.W. Roeder - 1976 (PB 260 715)A05

EERC 76-18 "Experimental Model Studies on Seismic Response of High Curved Overcrossings," by D. Williams and W.G. Godden - 1976 (PB 269 548)A08

EERC 76-19 "Effects of Non-Uniform Seismic Disturbances on the Dumbarton Bridge Replacement Structure," by F. Baron and R.E. Hamati - 1976 (PB 282 981)A16

EERC 76-20 "Investigation of the Inelastic Characteristics of a Single Story Steel Structure Using System Identification and Shaking Table Experiments," by V.C. Matzen and H.D. McNiven - 1976 (PB 258 453)A07

EERC 76-21 "Capacity of Columns with Splice Imperfections," by E.P. Popov, R.M. Stephen and R. Philbrick - 1976 (PB 260 378)A04

EERC 76-22 "Response of the Olive View Hospital Main Building during the San Fernando Earthquake," by S. A. Mahin, V.V. Bertero, A.K. Chopra and R. Collins - 1976 (PB 271 425)A14

EERC 76-23 "A Study on the Major Factors Influencing the Strength of Masonry Prisms," by N.M. Mostaghel, R.L. Mayes, R. W. Clough and S.W. Chen - 1976 (Not published)

EERC 76-24 "GADFLEA - A Computer Program for the Analysis of Pore Pressure Generation and Dissipation during Cyclic or Earthquake Loading," by J.R. Booker, M.S. Rahman and H.B. Seed - 1976 (PB 263 947)A04

EERC 76-25 "Seismic Safety Evaluation of a R/C School Building," by B. Bresler and J. Axley - 1976

EERC 76-26 "Correlative Investigations on Theoretical and Experimental Dynamic Behavior of a Model Bridge Structure," by K. Kawashima and J. Penzien - 1976 (PB 263 388)A11

EERC 76-27 "Earthquake Response of Coupled Shear Wall Buildings," by T. Srichatrapimuk - 1976 (PB 265 157)A07

EERC 76-28 "Tensile Capacity of Partial Penetration Welds," by E.P. Popov and R.M. Stephen - 1976 (PB 262 899)A03

EERC 76-29 "Analysis and Design of Numerical Integration Methods in Structural Dynamics," by H.M. Hilber - 1976 (PB 264 410)A06

EERC 76-30 "Contribution of a Floor System to the Dynamic Characteristics of Reinforced Concrete Buildings," by L.E. Malik and V.V. Bertero - 1976 (PB 272 247)A13

EERC 76-31 "The Effects of Seismic Disturbances on the Golden Gate Bridge," by F. Baron, M. Arikan and R.E. Hamati - 1976 (PB 272 279)A09

EERC 76-32 "Infilled Frames in Earthquake Resistant Construction," by R.E. Klingner and V.V. Bertero - 1976 (PB 265 892)A13

UCB/EERC-77/01 "PLUSH - A Computer Program for Probabilistic Finite Element Analysis of Seismic Soil-Structure Interaction," by M.P. Romo Organista, J. Lysmer and H.B. Seed - 1977

UCB/EERC-77/02 "Soil-Structure Interaction Effects at the Humboldt Bay Power Plant in the Ferndale Earthquake of June 7, 1975," by J.E. Valera, H.B. Seed, C.F. Tsai and J. Lysmer - 1977 (PB 265 795)A04

UCB/EERC-77/03 "Influence of Sample Disturbance on Sand Response to Cyclic Loading," by K. Mori, H.B. Seed and C.K. Chan - 1977 (PB 267 352)A04

UCB/EERC-77/04 "Seismological Studies of Strong Motion Records," by J. Shoja-Taheri - 1977 (PB 269 655)A10

UCB/EERC-77/05 "Testing Facility for Coupled-Shear Walls," by L. Li-Hyung, V.V. Bertero and E.P. Popov - 1977

UCB/EERC-77/06 "Developing Methodologies for Evaluating the Earthquake Safety of Existing Buildings," by No. 1 - B. Bresler; No. 2 - B. Bresler, T. Okada and D. Zisling; No. 3 - T. Okada and B. Bresler; No. 4 - V.V. Bertero and B. Bresler - 1977 (PB 267 354)A08

UCB/EERC-77/07 "A Literature Survey - Transverse Strength of Masonry Walls," by Y. Omote, R.L. Mayes, S.W. Chen and R.W. Clough - 1977 (PB 277 933)A07

UCB/EERC-77/08 "DRAIN-TABS: A Computer Program for Inelastic Earthquake Response of Three Dimensional Buildings," by R. Guendelman-Israel and G.H. Powell - 1977 (PB 270 693)A07

UCB/EERC-77/09 "SUBWALL: A Special Purpose Finite Element Computer Program for Practical Elastic Analysis and Design of Structural Walls with Substructure Option," by D.Q. Le, H. Peterson and E.P. Popov - 1977 (PB 270 567)A05

UCB/EERC-77/10 "Experimental Evaluation of Seismic Design Methods for Broad Cylindrical Tanks," by D.P. Clough (PB 272 280)A13

UCB/EERC-77/11 "Earthquake Engineering Research at Berkeley - 1976," - 1977 (PB 273 507)A09

UCB/EERC-77/12 "Automated Design of Earthquake Resistant Multistory Steel Building Frames," by N.D. Walker, Jr. - 1977 (PB 276 526)A09

UCB/EERC-77/13 "Concrete Confined by Rectangular Hoops Subjected to Axial Loads," by J. Vallenas, V.V. Bertero and E.P. Popov - 1977 (PB 275 165)A06

UCB/EERC-77/14 "Seismic Strain Induced in the Ground During Earthquakes," by Y. Sugimura - 1977 (PB 284 201)A04

UCB/EERC-77/15 "Bond Deterioration under Generalized Loading," by V.V. Bertero, E.P. Popov and S. Viwathanatepa - 1977

UCB/EERC-77/16 "Computer Aided Optimum Design of Ductile Reinforced Concrete Moment Resisting Frames," by S.W. Zagajeski and V.V. Bertero - 1977 (PB 280 137)A07

UCB/EERC-77/17 "Earthquake Simulation Testing of a Stepping Frame with Energy-Absorbing Devices," by J.M. Kelly and D.F. Tsztoo - 1977 (PB 273 506)A04

UCB/EERC-77/18 "Inelastic Behavior of Eccentrically Braced Steel Frames under Cyclic Loadings," by C.W. Roeder and E.P. Popov - 1977 (PB 275 526)A15

UCB/EERC-77/19 "A Simplified Procedure for Estimating Earthquake-Induced Deformations in Dams and Embankments," by F.I. Makdisi and H.B. Seed - 1977 (PB 276 820)A04

UCB/EERC-77/20 "The Performance of Earth Dams during Earthquakes," by H.B. Seed, F.I. Makdisi and P. de Alba - 1977 (PB 276 821)A04

UCB/EERC-77/21 "Dynamic Plastic Analysis Using Stress Resultant Finite Element Formulation," by P. Lukkunapvasit and J.M. Kelly - 1977 (PB 275 453)A04

UCB/EERC-77/22 "Preliminary Experimental Study of Seismic Uplift of a Steel Frame," by R.W. Clough and A.A. Huckelbridge 1977 (PB 278 769)A08

UCB/EERC-77/23 "Earthquake Simulator Tests of a Nine-Story Steel Frame with Columns Allowed to Uplift," by A.A. Huckelbridge - 1977 (PB 277 944)A09

UCB/EERC-77/24 "Nonlinear Soil-Structure Interaction of Skew Highway Bridges," by M.-C. Chen and J. Penzien - 1977 (PB 276 176)A07

UCB/EERC-77/25 "Seismic Analysis of an Offshore Structure Supported on Pile Foundations," by D.D.-N. Liou and J. Penzien 1977 (PB 283 180)A06

UCB/EERC-77/26 "Dynamic Stiffness Matrices for Homogeneous Viscoelastic Half-Planes," by G. Dasgupta and A.K. Chopra - 1977 (PB 279 654)A06

UCB/EERC-77/27 "A Practical Soft Story Earthquake Isolation System," by J.M. Kelly, J.M. Eidinger and C.J. Derham - 1977 (PB 276 814)A07

UCB/EERC-77/28 "Seismic Safety of Existing Buildings and Incentives for Hazard Mitigation in San Francisco: An Exploratory Study," by A.J. Meltsner - 1977 (PB 281 970)A05

UCB/EERC-77/29 "Dynamic Analysis of Electrohydraulic Shaking Tables," by D. Rea, S. Abedi-Hayati and Y. Takahashi 1977 (PB 282 569)A04

UCB/EERC-77/30 "An Approach for Improving Seismic - Resistant Behavior of Reinforced Concrete Interior Joints," by B. Galunic, V.V. Bertero and E.P. Popov - 1977 (PB 290 870)A06

UCB/EERC-78/01 "The Development of Energy-Absorbing Devices for Aseismic Base Isolation Systems," by J.M. Kelly and D.F. Tsztoo - 1978 (PB 284 978)A04

UCB/EERC-78/02 "Effect of Tensile Prestrain on the Cyclic Response of Structural Steel Connections, by J.G. Bouwkamp and A. Mukhopadhyay - 1978

UCB/EERC-78/03 "Experimental Results of an Earthquake Isolation System using Natural Rubber Bearings," by J.M. Eidinger and J.M. Kelly - 1978 (PB 281 686)A04

UCB/EERC-78/04 "Seismic Behavior of Tall Liquid Storage Tanks," by A. Niwa - 1978 (PB 284 017)A14

UCB/EERC-78/05 "Hysteretic Behavior of Reinforced Concrete Columns Subjected to High Axial and Cyclic Shear Forces," by S.W. Zagajeski, V.V. Bertero and J.G. Bouwkamp - 1978 (PB 283 858)A13

UCB/EERC-78/06 "Inelastic Beam-Column Elements for the ANSR-I Program," by A. Riahi, D.G. Row and G.H. Powell - 1978

UCB/EERC-78/07 "Studies of Structural Response to Earthquake Ground Motion," by O.A. Lopez and A.K. Chopra - 1978 (PB 282 790)A05

UCB/EERC-78/08 "A Laboratory Study of the Fluid-Structure Interaction of Submerged Tanks and Caissons in Earthquakes," by R.C. Byrd - 1978 (PB 284 957)A08

UCB/EERC-78/09 "Model for Evaluating Damageability of Structures," by I. Sakamoto and B. Bresler - 1978

UCB/EERC-78/10 "Seismic Performance of Nonstructural and Secondary Structural Elements," by I. Sakamoto - 1978

UCB/EERC-78/11 "Mathematical Modelling of Hysteresis Loops for Reinforced Concrete Columns," by S. Nakata, T. Sproul and J. Penzien - 1978

UCB/EERC-78/12 "Damageability in Existing Buildings," by T. Blejwas and B. Bresler - 1978

UCB/EERC-78/13 "Dynamic Behavior of a Pedestal Base Multistory Building," by R.M. Stephen, E.L. Wilson, J.G. Bouwkamp and M. Button - 1978 (PB 286 650)A08

UCB/EERC-78/14 "Seismic Response of Bridges - Case Studies," by R.A. Imbsen, V. Nutt and J. Penzien - 1978 (PB 286 503)A10

UCB/EERC-78/15 "A Substructure Technique for Nonlinear Static and Dynamic Analysis," by D.G. Row and G.H. Powell - 1978 (PB 288 077)A10

UCB/EERC-78/16 "Seismic Risk Studies for San Francisco and for the Greater San Francisco Bay Area," by C.S. Oliveira - 1978

UCB/EERC-78/17 "Strength of Timber Roof Connections Subjected to Cyclic Loads," by P. Gülkan, R.L. Mayes and R.W. Clough - 1978

UCB/EERC-78/18 "Response of K-Braced Steel Frame Models to Lateral Loads," by J.G. Bouwkamp, R.M. Stephen and E.P. Popov - 1978

UCB/EERC-78/19 "Rational Design Methods for Light Equipment in Structures Subjected to Ground Motion," by J.L. Sackman and J.M. Kelly - 1978 (PB 292 357)A04

UCB/EERC-78/20 "Testing of a Wind Restraint for Aseismic Base Isolation," by J.M. Kelly and D.E. Chitty - 1978 (PB 292 833)A03

UCB/EERC-78/21 "APOLLO - A Computer Program for the Analysis of Pore Pressure Generation and Dissipation in Horizontal Sand Layers During Cyclic or Earthquake Loading," by P.P. Martin and H.B. Seed - 1978 (PB 292 835)A04

UCB/EERC-78/22 "Optimal Design of an Earthquake Isolation System," by M.A. Bhatti, K.S. Pister and E. Polak - 1978 (PB 294 735)A06

UCB/EERC-78/23 "MASH - A Computer Program for the Non-Linear Analysis of Vertically Propagating Shear Waves in Horizontally Layered Deposits," by P.P. Martin and H.B. Seed - 1978 (PB 293 101)A05

UCB/EERC-78/24 "Investigation of the Elastic Characteristics of a Three Story Steel Frame Using System Identification," by I. Kaya and H.D. McNiven - 1978

UCB/EERC-78/25 "Investigation of the Nonlinear Characteristics of a Three-Story Steel Frame Using System Identification," by I. Kaya and H.D. McNiven - 1978

UCB/EERC-78/26 "Studies of Strong Ground Motion in Taiwan," by Y.M. Hsiung, B.A. Bolt and J. Penzien - 1978

UCB/EERC-78/27 "Cyclic Loading Tests of Masonry Single Piers: Volume 1 - Height to Width Ratio of 2," by P.A. Hidalgo, R.L. Mayes, H.D. McNiven and R.W. Clough - 1978

UCB/EERC-78/28 "Cyclic Loading Tests of Masonry Single Piers: Volume 2 - Height to Width Ratio of 1," by S.-W.J. Chen, P.A. Hidalgo, R.L. Mayes, R.W. Clough and H.D. McNiven - 1978

UCB/EERC-78/29 "Analytical Procedures in Soil Dynamics," by J. Lysmer - 1978

UCB/EERC-79/01 "Hysteretic Behavior of Lightweight Reinforced Concrete Beam-Column Subassemblages," by B. Forzani, E.P. Popov, and V.V. Bertero - 1979

UCB/EERC-79/02 "The Development of a Mathematical Model to Predict the Flexural Response of Reinforced Concrete Beams to Cyclic Loads, Using System Identification," by J.F. Stanton and H.D. McNiven - 1979

UCB/EERC-79/03 "Linear and Nonlinear Earthquake Response of Simple Torsionally Coupled Systems," by C.L. Kan and A.K. Chopra - 1979

UCB/EERC-79/04 "A Mathematical Model of Masonry for Predicting Its Linear Seismic Response Characteristics," by Y. Mengi and H.D. McNiven - 1979

UCB/EERC-79/05 "Mechanical Behavior of Light Weight Concrete Confined by Different Types of Lateral Reinforcement," by M.A. Manrique and V.V. Bertero - 1979

UCB/EERC-79/06 "Static Tilt Tests of a Tall Cylindrical Liquid Storage Tank," by R.W. Clough and A. Niwa - 1979

UCB/EERC-79/07 "The Design of Steel Energy Absorbing Restrainers and Their Incorporation Into Nuclear Power Plants for Enhanced Safety: Volume 1 - Summary Report," by P.N. Spencer, V.F. Zackay, and E.R. Parker - 1979

UCB/EERC-79/08 "The Design of Steel Energy Absorbing Restrainers and Their Incorporation Into Nuclear Power Plants for Enhanced Safety: Volume 2 - The Development of Analyses for Reactor System Piping," "Simple Systems" by M.C. Lee, J. Penzien, A.K. Chopra, and K. Suzuki "Complex Systems" by G.H. Powell, E.L. Wilson, R.W. Clough and D.G. Row - 1979

UCB/EERC-79/09 "The Design of Steel Energy Absorbing Restrainers and Their Incorporation Into Nuclear Power Plants for Enhanced Safety: Volume 3 - Evaluation of Commerical Steels," by W.S. Owen, R.M.N. Pelloux, R.O. Ritchie, M. Faral, T. Ohhashi, J. Toplosky, S.J. Hartman, V.F. Zackay, and E.R. Parker - 1979

UCB/EERC-79/10 "The Design of Steel Energy Absorbing Restrainers and Their Incorporation Into Nuclear Power Plants for Enhanced Safety: Volume 4 - A Review of Energy-Absorbing Devices," by J.M. Kelly and M.S. Skinner - 1979

UCB/EERC-79/11 "Conservatism In Summation Rules for Closely Spaced Modes," by J.M. Kelly and J.L. Sackman - 1979

UCB/EERC-79/12 "Cyclic Loading Tests of Masonry Single Piers Volume 3 - Height to Width Ratio of 0.5," by P.A. Hidalgo, R.L. Mayes, H.D. McNiven and R.W. Clough - 1979

UCB/EERC-79/13 "Cyclic Behavior of Dense Coarse-Grain Materials in Relation to the Seismic Stability of Dams," by N.G. Banerjee, H.B. Seed and C.K. Chan - 1979

UCB/EERC-79/14 "Seismic Behavior of R/C Interior Beam Column Subassemblages," by S. Viwathanatepa, E.P. Popov and V.V. Bertero - 1979

UCB/EERC-79/15 "Optimal Design of Localized Nonlinear Systems with Dual Performance Criteria Under Earthquake Excitations," by M.A. Bhatti - 1979

UCB/EERC-79/16 "OPTDYN - A General Purpose Optimization Program for Problems with or without Dynamic Constraints," by M.A. Bhatti, E. Polak and K.S. Pister - 1979

UCB/EERC-79/17 "ANSR-II, Analysis of Nonlinear Structural Response, Users Manual," by D.P. Mondkar and G.H. Powell - 1979

UCB/EERC-79/18 "Soil Structure Interaction in Different Seismic Environments," A. Gomez-Masso, J. Lysmer, J.-C. Chen and H.B. Seed - 1979

UCB/EERC-79/19 "ARMA Models for Earthquake Ground Motions," by M.K. Chang, J.W. Kwiatkowski, R.F. Nau, R.M. Oliver and K.S. Pister - 1979

UCB/EERC-79/20 "Hysteretic Behavior of Reinforced Concrete Structural Walls," by J.M. Vallenas, V.V. Bertero and E.P. Popov - 1979

UCB/EERC-79/21 "Studies on High-Frequency Vibrations of Buildings I: The Column Effects," by J. Lubliner - 1979

UCB/EERC-79/22 "Bond Deterioration of Reinforcing Bars Embedded in Confined Concrete Blocks," by S. Viwathanatepa, E.P. Popov and V.V. Bertero - 1979

UCB/EERC-79/23 "Shaking Table Study of Single-Story Masonry Houses, Volume 1: Test Structures 1 and 2," by P. Gülkan, R.L. Mayes and R.W. Clough - 1979

UCB/EERC-79/24 "Shaking Table Study of Single-Story Masonry Houses, Volume 2: Test Structures 3 and 4," by P. Gülkan, R.L. Mayes and R.W. Clough - 1979

UCB/EERC-79/25 "Shaking Table Study of Single-Story Masonry Houses, Volume 3: Summary, Conclusions and Recommendations," by R.W. Clough, P. Gülkan and R.L. Mayes

UCB/EERC-79/26 "Recommendations for a U.S.-Japan Cooperative Research Program Utilizing Large-Scale Testing Facilities," by U.S.-Japan Planning Group - 1979

UCB/EERC-79/27 "Earthquake-Induced Liquefaction Near Lake Amatitlan, Guatemala," by H.B. Seed, I. Arango, C.K. Chan, A. Gomez-Masso, and R. Grant de Ascoli - 1979

UCB/EERC-79/28 "Infill Panels: Their Influence on Seismic Response of Buildings," by J.W. Axley and V.V. Bertero - 1979

UCB/EERC-79/29 "3D Truss Bar Element (Type 1) for the ANSR-II Program," by D.P. Mondkar and G.H. Powell - 1979

UCB/EERC-79/30 "2D Beam-Column Element (Type 5 - Parallel Element Theory) for the ANSR-II Program," by D.G. Row, G.H. Powell, and D.P. Mondkar

UCB/EERC-79/31 "3D Beam-Column Element (Type 2 - Parallel Element Theory) for the ANSR-II Program," by A. Riahi, G.H. Powell, and D.P. Mondkar - 1979

UCB/EERC-79/32 "On Response of Structures to Stationary Excitation," by A. Der Kiureghian - 1979

UCB/EERC-79/33 "Undisturbed Sampling and Cyclic Load Testing of Sands," by S. Singh, H.B. Seed, and C.K. Chan - 1979

UCB/EERC-79/34 "Interaction Effects of Simultaneous Torsional and Compressional Cyclic Loading of Sand," by P.M. Griffin and W.N. Houston - 1979

UCB/EERC-80/01 "Earthquake Response of Concrete Gravity Dams Including Hydrodynamic and Foundation Interaction Effects," by A.K. Chopra, P. Chakrabarti, and S. Gupta - 1980

UCB/EERC-80/02 "Rocking Response of Rigid Blocks to Earthquakes," by C.S. Yim, A.K. Chopra, and J. Penzien - 1980

UCB/EERC-80/03 "Optimum Inelastic Design of Seismic-Resistant Reinforced Concrete Frame Structures," by S. W. Zagajeski and V. V. Bertero - 1980

For sale by the National Technical Information Service, U. S. Department of Commerce, Springfield, Virginia 22161.

See back of report for up to date listing of EERC reports.